Thermal and Photochemical Reduction and Functionalization Chemistry of the Uranyl Dication, [U VI O2] 2+

CHEMICAL REVIEWS

Review

Cite This: Chem. Rev. XXXX, XXX, XXX−XXX

pubs.acs.org/CR

Thermal and Photochemical Reduction and Functionalization Chemistry of the Uranyl Dication, $[U^{VI}O_2]^{2+}$

Bradley E. Cowie,[†] Jamie M. Purkis,[†] Jonathan Austin,[‡] Jason B. Love,*[,†] and Polly L. Arnold*[,†]

[†]EaStCHEM School of Chemistry, The University of Edinburgh, Joseph Black Building, The King's Buildings, Edinburgh EH9 3FJ, U.K.

[‡]National Nuclear Laboratory, Chadwick House, Warrington Road, Birchwood Park, Warrington WA3 6AE, U.K.

ABSTRACT: The uranyl ion, $[U^{VI}O_2]^{2+}$, possesses rigorously *trans*, strongly covalent, and chemically robust U-oxo groups. However, through the use of anaerobic reaction techniques, both one- and two-electron reductive functionalization of the uranyl oxo groups has been discovered and developed. Prior to 2010, this unusual reactivity centered around the reductive silylation of the uranyl ion which entailed conversion of the oxo ligands into siloxy ligands and reductive metalation of the uranyl oxo with Group 1 and *f*-block metals. This review surveys the large number of new examples of reductive functionalization of the uranyl ion that have been reported since 2010, including reductive borylation and alumination, metalation with *d*- or *f*-block metals, and new examples of reductive silylation. Other examples of oxo-group functionalization of $[U^{VI}O_2]^{2+}$ that do not involve reduction, mainly with Group 1 cations, are also covered, along with new advances in the photochemistry of the uranyl(VI) ion that involve the transient formation of formally uranyl(V) $[U^{V}O_2]^{+}$ ion.

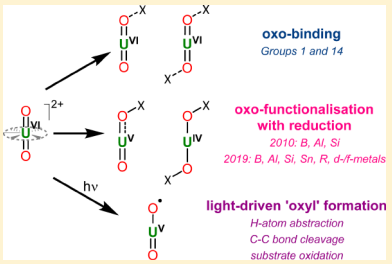

CONTENTS

1. INTRODUCTION

The uranyl(VI) ion, $[U^{VI}O_2]^{2+}$, is the dominant form of uranium in the environment. It is a linear cation which exhibits mutually *trans* and strongly covalent oxo groups, denoted here as $U{-}O_{yl}$. These $U{-}O_{yl}$ bonds are formally triple bonds, arising from one σ- and two π-bonds between 2*p* orbitals on the oxo-groups and hybrid orbitals (5*f* and 6*d*) on uranium.[1] The result is a gas-phase bond energy of 604 kJ mol^{-1} for the $[U^{VI}O_2]^{2+}$ ion, making it thermodynamically stable and generally inert to chemical functionalization in the laboratory. However, the one-electron reduction of $[U^{VI}O_2]^{2+}$ to $[U^{V}O_2]^{+}$ is readily achieved by minerals and microbes in the environment under anaerobic conditions;[2,3] under these conditions $[U^{V}O_2]^{+}$ disproportionates into $[U^{VI}O_2]^{2+}$ and $[U^{IV}O_2]$, of which the latter is insoluble in water.[4] In recent years, anaerobic reaction conditions have been deployed and proven effective for the isolation of both $[U^{V}O_2]^{+}$ (uranyl(V)) and $[U^{IV}O_2]$ (U(IV) dioxo) compounds through reductive functionalization processes (Scheme 1). There is significant interest in studying uranyl(V) complexes due to the more Lewis-basic oxo groups showing an increased propensity to bridge to other metals. These interactions are often referred to as cation−cation interactions, CCIs, but the use of this specific term is not warranted as metal oxo-group basicity is common in *d*-block chemistry. This phenomenon is very rare in uranyl(VI) chemistry but relatively common in heavier actinyl (i.e., neptunium and plutonium) chemistry. Through the formation of oxo-bridged complexes, U^{V} has the potential to disrupt nuclear waste separations such as in the PUREX process;[5] consequently, the study of oxo-functionalized U^{V} complexes is spurred by understanding these interactions. With an estimated two million tonnes of depleted uranium waste globally,[6] maximizing the efficiency of waste remediation processes is of paramount importance to the nuclear industry. While actinyl compounds require specialized containment procedures to handle, their chemistry can be modeled through the study of uranyl(V) compounds in a standard laboratory

Received: January 18, 2019

DOI: 10.1021/acs.chemrev.9b00048
Chem. Rev. XXXX, XXX, XXX−XXX

(and therefore more convenient and less costly) environment. Additionally, understanding the processes by which various elements reductively functionalize water-soluble uranyl ions to insoluble uranium(IV) oxides is also relevant to the mineral and microbial-initiated reductions that occur in the environment, for example in iron-containing strata such as goethite[7] or with *geobacter* microbes.[8] The chemistry of such a traditionally inert oxo group is also of great academic interest, since its lack of reactivity contrasts so strongly with the lighter Group 6 congeners such as the chromyl ion.

The uranyl(V) ion is also a key intermediate in photochemical processes involving the uranyl(VI) ion. Solutions containing $[U^{VI}O_2]^{2+}$ are photochemically active when exposed to ultraviolet (UV) and near-UV light sources (ca. 420 nm), generating $[{}^*UO_2]^{2+}$, a long-lived ($\leq\mu$s) and highly oxidizing (ca. +2.6 V, comparable to F_2) excited state of uranyl.[9,10] Subsequent ligand-to-metal charge transfer (LMCT) that arises from U(5*f*) ← O(2*p*) transitions generates the $[U^{V}O_2]^{+}$ $5f^1$ intermediate which contains an extremely reactive oxyl radical, O$^\bullet$ (Scheme 1b). This intermediate may generally be quenched by H atom abstraction (HAA) if the quencher is aliphatic (to give a functionalized $[O{=}U^{V}{-}OH]^{2+}$ motif)[11−13] or by electron transfer if the quencher is unsaturated.[14−19] The highly oxidizing nature of photoactivated $[U^{VI}O_2]^{2+}$ has previously been exploited in the degradation of volatile organic compounds, VOCs, such as methanol,[20] and many other applications, including in metal ion sensing and biochemistry, have been developed since the last reviews appeared in 2010 and 2013.[9,10,21,22]

Scheme 1. (a) Thermal and (b) Photochemical Reduction and Functionalization of the Uranyl Ion, $[U^{VI}O_2]^{2+}$

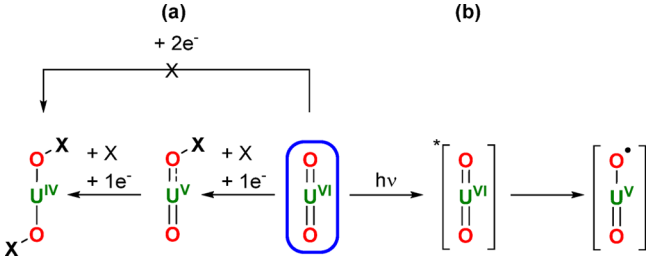

While several generalized reviews of the chemistry of the uranyl ion have been published in recent years, the last review dedicated to oxo-group reactivity of the uranyl cation was published in 2010.[10,22−24] This current review therefore focuses on the significant advances that have occurred in reductive functionalization of the uranyl ion since 2010, including reductive borylation and alumination, metalation with *d*-block and *f*-block metals, and substitution of the oxo-functionalized groups coordinated to uranyl(V) complexes by Group 1 and *d*-block metals and stannyl, silyl, and alkyl groups. Emphasis is placed on the synthesis and reactivity of these compounds. Discussions of the more complex physical properties of these compounds such as magnetism and gas-phase uranyl-oxo reactivity[25,26] are beyond the scope of this review. There have also been numerous reports of the coordination chemistry of newly designed ligands with the uranyl ion, and unless those complexes possess activated/functionalized U−O_{yl} groups, they are beyond the scope of this review. We also note recent developments in the computational chemistry of the actinides, which possess complex electronic structures and are difficult to model effectively; interested readers are referred to recent contributions from Dolg[27] and Kaltsoyannis,[28] and we will not cover these issues further in this review. For completeness we include a section on functionalized uranyl(VI) complexes for comparison, excluding hydrogen-bonded and halogen-bonded uranyl complexes. We use the term "thermal" to represent any nonphotochemical means of generating a uranyl(V) or U(IV) dioxo species. This review is therefore divided into sections that cover the following: oxo-functionalization reactions of uranyl(VI) complexes that occur without reduction; one-electron uranyl(VI) → uranyl(V) reduction reactions and further reactions of these that do not involve uranium redox; two-electron reduction and sequential uranyl(VI) → U(IV) dioxo processes; a survey of the solid-state structures and OUO vibrational stretching frequencies of $[U^{VI}O_2]^{2+}$, $[U^{V}O_2]^{+}$, and $[U^{IV}O_2]$ complexes reported since 2010; and photochemical reactions of uranyl(VI) complexes that involve uranyl(V) intermediates.

2. $[U^{VI}O_2]^{2+}$ OXO FUNCTIONALIZATION WITHOUT REDUCTION

The poor Lewis basicity of the uranyl(VI) oxo groups means that their functionalization is considerably rarer than that of the U^{V} or U^{IV} analogues. Current examples are limited to examples of Lewis adduct formation with the highly electropositive cations Li^+ or K^+ such as $U^{VI}{-}O_{yl}{-}Li^+$ adduct formation in $[Li(py)_2][U^{VI}O_2\{N(SiMe_3)_2\}_3]$ (**1**) from 1 equiv of $[U^{VI}O_2\{N(SiMe_3)_2\}_2(py)_2]$ (**2-py**) and $LiN(SiMe_3)_2$;[29] $[Li(dme)_{1.5}]_2[U^{VI}O_2(CH_2SiMe_3)_4]$ (**3**) from $[U^{VI}O_2Cl_2(THF)_2]$ (**4-THF**) and 4 equiv of $Li(CH_2SiMe_3)$ in the synthesis of a rare $U^{VI}O_2^{2+}$-alkyl "-ate" complex;[30] $[Li(THF)]_2[U^{VI}O_2\{N(SiMe_3)_2\}_2(tmtaa)]$ (**5**; tmtaa = dibenzotetramethyltetraaz[14]annulene) and $[Li(THF)_3][Li(THF)_2][(U^{VI}O_2Cl_2)_2(tmtaa)]$ (**6**) from $Li_2(tmtaa)$ and $[U^{VI}O_2\{N(SiMe_3)_2\}_2(THF)_2]$ (**2-THF**),[31] and $Li_2(tmtaa)$ and 2 equiv of **4-THF**,[32] respectively, to target the isolation of the as-yet unseen "*cis*-uranyl"; $[Li(THF)(TMEDA)][U^{VI}O_2(NC^tBu_2)_3]$ (**7**) and $[Li(THF)(OEt_2)]_2[U^{VI}O_2(NC^tBuPh)_4]$ (**8**) from **4-THF** and 6 equiv of $LiNC^tBu_2$ or 8 equiv of $LiNC^tBuPh$ in THF, respectively, as the first examples of uranyl ketimide complexes (Figure 1).[33] Further, Li^+-functionalization has also been seen in $[Li(THF)_3][U^{VI}O_2\{N(HSiMe_2)(^tBu)\}_3]$ (**9**);[34] in the uranyl(VI) Pacman complex, $[U^{VI}O_2(S)(HLiL^{Me})]$ (S = THF (**10-THF**), py (**10-py**)), formed by treating $[U^{VI}O_2(S)(H_2L^{Me})]$ (S = THF (**11-THF**), py (**11-py**)) with 1 equiv of LiR (R = H, NH_2, N^iPr_2, $N(SiMe_3)_2$, CPh_3, C_5H_5; H_4L^{Me} = a Pacman-shaped macrocyclic Schiff-base ligand with methyl substituents on the *meso*-carbon atoms and a dimethylphenylene hinge);[35] and in $[Li(MeIm)][U^{VI}O_2(Ar_2nacnac)(\kappa^1\text{-}C\text{-}C_4H_5N_2)_2]$ (**12**; MeIm = 1-methylimidazole, $Ar_2nacnac$ = $ArNC(Me)CHC(Me)NAr$, Ar = 2,6-$^iPr_2C_6H_3$), which was synthesized by treating 0.5 equiv of $[U^{VI}O_2Cl(Ar_2nacnac)]_2$ (**13**) with 2 equiv of 2-lithio-1-methylimidazole in toluene/THF. Compound **12** features imidazole coordination to the U^{VI} center through the central carbon atoms rather than the flanking nitrogen atoms (Figure 1); the donor atom can be switched from the imidazole carbon to the nitrogen atoms by treatment of **12** with MCl_2 (M = Fe, Co), affording $[MCl(MeIm)][U^{VI}O_2(Ar_2nacnac)(\kappa^1\text{-}N\text{-}C_4H_5N_2)_2]$ (M = Fe (**14**), Co (**15**)).[36]

Adducts between K^+ and uranyl(VI), i.e. $U^{VI}{-}O_{yl}{-}{-}K^+$ have also been reported in an effort to further manipulate the

DOI: 10.1021/acs.chemrev.9b00048
Chem. Rev. XXXX, XXX, XXX−XXX

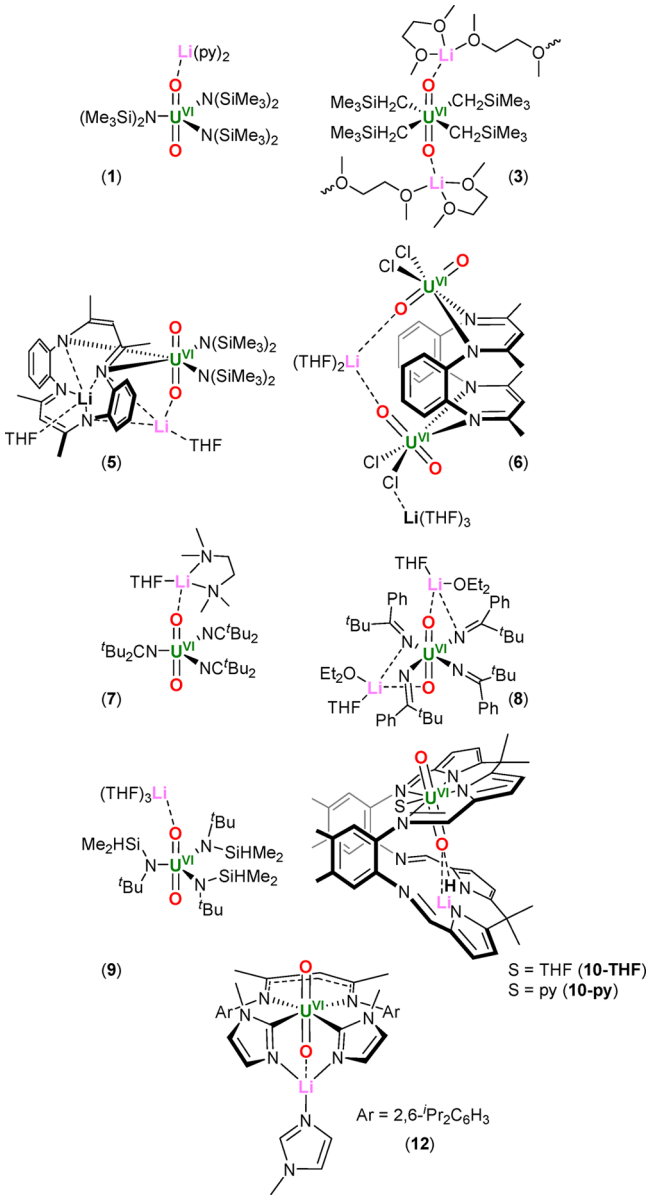

Figure 1. Examples of Li-functionalized $[U^{VI}O_2]^{2+}$ complexes.[29−36]

bonding and reactivity of the uranyl dication. Starting from **4-THF**, 6 equiv of the fluorinated diarylamide $KNPh^F(2\text{-py})$ ($Ph^F = C_6F_5$) or 8 equiv of $[KNAr^FPh(THF)_{0.5}]$ ($Ar^F = C_6H_3$-3,5-$(CF_3)_2$) reacts with **4** in THF to produce $[\{K(THF)_3\}\{U^{VI}O_2(NPh^Fpy)_3\}]_n$ (**16**) and $[K(\eta^6\text{-}C_6H_5CH_3)_2][U^{VI}O_2(NAr^FPh)_4]$ (**17**), respectively (Figure 2). These complexes possess noncovalent π−K^+ and F−K^+ interactions in their solid-state structures, in addition to U^{VI}−O_{yl}--K^+ interactions.[37]

Adduct formation between K^+ and uranyl(VI) has also been observed in a bis(uranyl(VI)) Pacman complex, $[K(py)_3]_2[K(py)]_2[(U^{VI}O_2)_2(\mu\text{-}O_2)(L^{Me})]_2$ (**18**), which is synthesized *via* oxidation of the bis(uranyl(V)) Pacman complex, $\{[K(py)_3][K(py)][(U^{V}O_2)_2(L^{Me})]\}_2$ (**19-py**; see Scheme 48 in Section 6 for the synthesis of **19-py**), using dry O_2 in pyridine; both uranyl(V) ions have been oxidized to uranyl(VI), and a peroxide ligand bridges the two U^{VI} centers (Scheme 2). Alternatively, **19-py** reacts with pyridine-*N*-oxide to form

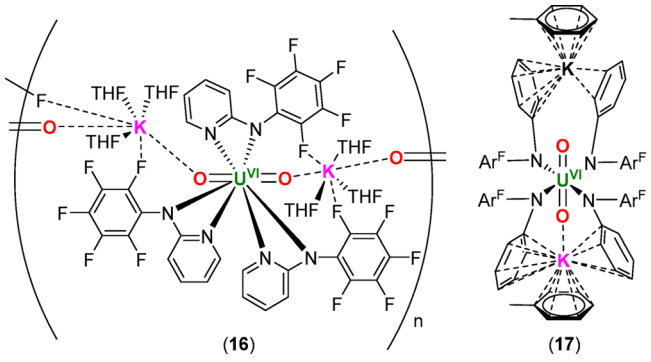

Figure 2. Examples of K^+-functionalized $[U^{VI}O_2]^{2+}$ complexes; $Ar^F = C_6H_3$-3,5-$(CF_3)_2$.[37]

$[K(py)_3]_2[K(py)]_2[(U^{VI}O_2)_2(\mu\text{-}O)(L^{Me})]_2$ (**20**), in which an oxo ligand bridges the two U^{VI} centers (Scheme 2).[38]

Scheme 2. Oxidation of $[K(py)_3]_2[K(py)]_2[(U^{V}O_2)_2(L^{Me})]_2$ (19-py) to $[K(py)_3]_2[K(py)]_2[(U^{VI}O_2)_2(\mu\text{-}O_2)(L^{Me})]_2$ (18) and $[K(py)_3]_2[K(py)]_2[(U^{VI}O_2)_2(\mu\text{-}O)(L^{Me})]_2$ (20) using dry O_2 and C_5H_5NO, respectively[a]

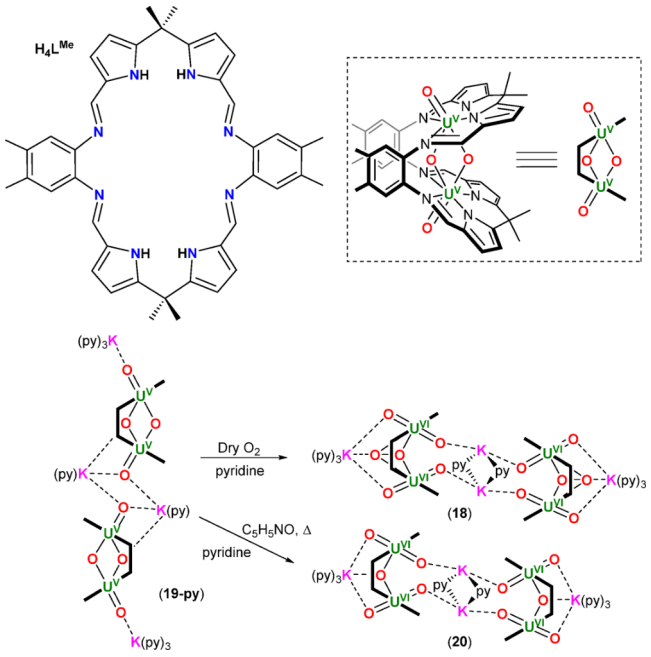

[a]The Pacman macrocycle, H_4L^{Me}, and an abbreviated depiction of the bis(uranyl(V)) Pacman complex are provided at the top of the scheme.[38].

Adduct formation between K^+ and uranyl(VI) has also been observed in $[\{U^{VI}O_2(OH)K(C_6H_6)(H_2L^{Me})\}_2]$ (**21**), which is formed by treating $[U^{VI}O_2(THF)(H_2L^{Me})]$ (**11-THF**) with KH in THF (Scheme 3). Complex **21** likely forms as a result of KOH impurities in the KH, or decomposition of $[U^{VI}O_2(THF)(K_2L^{Me})]$ (**22**) by reaction with adventitious H_2O. Compound **21** may also be formed directly by treating **11-THF** with dry KOH in THF (Scheme 3). Complex **21** is a uranyl(VI)/uranyl(VI) dimer formed via bridging $K^+\cdots[U^{VI}O_2]^{2+}$ interactions involving the exogeneous oxo ligand, referred to as O_{exo}. Dissolving **21** into a mixture of THF and benzene followed by crystallization results in the formation of $[U^{V}O_2(OH)K(THF)_2(H_2L^{Me})]$ (**23**; Scheme 3). In this case,

DOI: 10.1021/acs.chemrev.9b00048
Chem. Rev. XXXX, XXX, XXX−XXX

Scheme 3. Synthesis of $[\{U^{VI}O_2(OH)K(C_6H_6)(H_2L^{Me})\}_2]$ (21) by Treating $[U^{VI}O_2(THF)(H_2L^{Me})]$ (11-THF) Either with KH in THF or with dry KOH in THF[a]

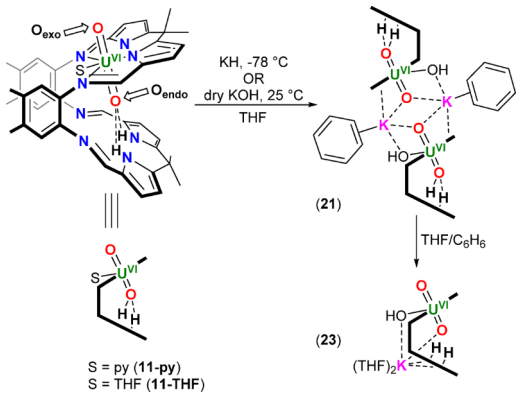

[a] $[U^{V}O_2(OH)K(THF)_2(H_2L^{Me})]$ (23) is formed by dissolving 21 in THF/benzene. A depiction of the uranyl(VI) Pacman complex 11 is given on the left of the Scheme, in which O_{exo} and O_{endo} have been labeled (S = coordinating solvent).[39].

the K^+ cation is coordinated to the endogenous oxo ligand of the uranyl(VI) ion, referred to as O_{endo}. Furthermore, coordination of K^+ to THF in **23** results in cleavage of the uranyl(VI)/uranyl(VI) dimer, yielding a monomeric uranyl-(VI) complex. The U−O bond lengths in **21** are nearly equal within s.u.s (1.796(2), 1.803(2) Å), whereas one of the U−O bond lengths in **23** is elongated relative to the other (1.788(6), 1.821(6) Å). In both cases, the elongated U−oxo bond corresponds to the oxo ligand coordinated to the K^+ cation. Furthermore, complexes **21** and **23** give rise to asymmetric OUO stretching frequencies of 894 and 895 cm^{-1},[39] respectively, which are at lower frequency relative to the unactivated uranyl(VI) analogue, **11-THF** (908 cm^{-1}),[40] indicating a decrease of electron density at the uranyl ion in these complexes.

Similarly to the tris- and tetrakis-ketimide complexes $[Li(THF)(TMEDA)][U^{VI}O_2(NC^tBu_2)_3]$ (**7**) and $[Li(THF)(OEt_2)]_2[U^{VI}O_2(NC^tBuPh)_4]$ (**8**; see Figure 1),[33] significant elongation of the U−O bond lengths is often observed on moving from neutral to "ate" U^{VI} complexes. For example, the U^{VI} $K^+\cdots[OU^{VI}O]^{2+}$-containing "ate" complex $K_2[K(OEt_2)_2]_2[U^{VI}O_2(^{dipp}AP)_2]_2$ (**24**; ^{dipp}AP = 4,6-di-*tert*-butyl-2-{(2,6-diisopropylphenyl)amido}phenolate) (prepared from $[U^{VI}O_2(^{dipp}ISQ)_2(THF)]$ (**25**; ^{dipp}ISQ = 4,6-di-*tert*-butyl-2-{(2,6-diisopropylphenyl)imino}semiquinone) by reduction with 2 equiv of KC_8 (Scheme 4)) has U−O bond lengths of 1.824(3) and 1.834(3) Å. These are significantly longer than in the neutral U^{VI} precursor **25** (1.762(4) and 1.786(3) Å) and likely arise from increased π-donation to the uranium center, as well as the electrostatic $K^+\cdots[OU^{VI}O]^{2+}$ adduct formation.[33,41] The role of increased ligand donor ability in U−O bond length elongation was highlighted by removal of the oxo-coordinated K^+ cations from **24** using 2 equiv of 18-crown-6 to make $[K(THF)_2(18\text{-c-}6)]_2[U^{VI}O_2(^{dipp}AP)_2(THF)]$ (**26**). The U−O bond lengths (1.812(2) and 1.814(2) Å) of the unfunctionalized uranyl(VI) unit in **26** are shorter than in the K-coordinated **24** but still longer than in the neutral **25**,[41] comparing well with those in the tris- and tetrakis-ketimide complexes **7** and **8**, respectively.[33]

Compound **25** also reacts either with 4 equiv of *B*-chlorocatecholborane (Cl-Bcat) in THF to afford $[U^{IV}Cl_4(^{dipp}IQ)(THF)_2]$ (**27**; ^{dipp}IQ = 4,6-di-*tert*-butyl-2-{(2,6-diisopropylphenyl)imino}quinone) and 2 equiv of O-$(Bcat)_2$ or with 4 equiv of pivaloyl chloride ($ClCO(^tBu)$) in benzene to yield $[U^{IV}Cl_4(^{dipp}IQ)_2]$ (**28**) and 2 equiv of $O(CO(^tBu))_2$.[41]

The contact- or separated-ion pairs, $[M][U^{VI}O_2\{N(SiMe_3)_2\}_3]$ (M = K (**29**), Rb (**30**), Cs (**31**)), $[M(THF)_x][U^{VI}O_2\{N(SiMe_3)_2\}_3]$ (M = Li, *x* = 2 (**32**) or 4 (**33**); M = Na, *x* = 2 (**34**) or 6 (**35**); M = K, *x* = 6 (**36**)), $[M(2,2,2\text{-crypt})][U^{VI}O_2\{N(SiMe_3)_2\}_3]$ (M = Li (**37**), Na (**38**), K (**39**), Rb (**40**), Cs (**41**)) and $[M(L)_2][U^{VI}O_2\{N(SiMe_3)_2\}_3]$ (M = Li, L = 12-c-4 (**42**); M = Na, L = 15-c-5 (**43**); M = K, L = 15-c-5 (**44**); M = Rb, L = 15-c-5 (**45**); M = Cs, L = 15-c-5 (**46**), -c- = -crown-), have also recently been reported, formed by the interaction of Group 1 cations with the uranyl bis(silyl)amide anion, $[U^{VI}O_2\{N(SiMe_3)_2\}_3]^-$.[34,42,43] It was stated that the oxophilicity of Li^+ versus the heavier Group 1 congeners is the key driver in decreasing $U^{VI}-O_{yl}$ bond lengths descending the series. However, it should be noted that while the $U^{VI}-O_{yl}$ bond length for the Li^+ functionalized compound is significantly longer than the remainder in the series (1.88(1) Å), these differences are statistically insignificant for the remainder of the Group 1 cations as they range from 1.810(5) Å for Na^+ to 1.804(3) Å and 1.80(3) Å for K^+ and Rb^+, respectively.[34,42,43]

The only examples of nongroup 1 functionalized $[U^{VI}O_2]^{2+}$ derive from coordination of Pb^{II} in the bottom N_4-donor compartment of the mono(uranyl) "Pacman" complex, **11-THF** or **11-py**. This produces $[U^{VI}O(OPb)(THF)(L^{Me})]$ (**47-THF**), $[U^{VI}O\{OPb(py)\}(py)(L^{Me})]$ (**47-py**) or $[U^{VI}O\{OPb(py)\}(Opy)(L^{Me})]$ (**48**; Scheme 5) in which the $U^{VI}-O$ bond

Scheme 4. Synthesis of $K_2[K(OEt_2)_2]_2[U^{VI}O_2(^{dipp}AP)_2]_2$ (24; ^{dipp}AP = 4,6-di-*tert*-Butyl-2-{(2,6-diisopropylphenyl)amido}phenolate) from $[U^{VI}O_2(^{dipp}ISQ)_2(THF)]$ (25; ^{dipp}ISQ = 4,6-Di-*tert*-butyl-2-{(2,6-diisopropylphenyl)imino}semiquinone) and 2 equiv of KC_8 (dipp = 2,6-Di-*iso*-propylphenyl).[41]

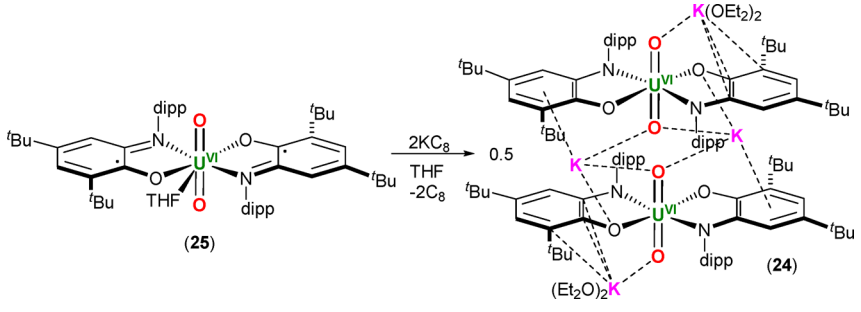

DOI: 10.1021/acs.chemrev.9b00048
Chem. Rev. XXXX, XXX, XXX−XXX

Scheme 5. Synthesis of Complexes 47 and 48.[44]

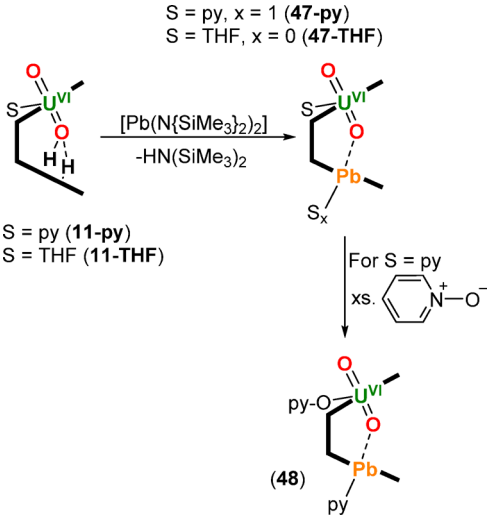

lengths range from 1.759(7)−1.853(8) Å. These bond distances are similar to other $U^{VI}-O_{yl}$ functionalized complexes, with the exception being the longer, 1.853(8) Å bond for **48**, which is consistent with its IR spectrum (ν[OUO asym.] = 893 cm^{-1}). No oxo-coordination to Pb^{2+} was reported for the larger anthracenyl-hinged macrocycle, H_4L^A (see Scheme 45 in Section 5 for a depiction of the H_4L^A ligand).[44]

The structural data (U−O and O−X bond lengths, O−U−O and U−O−X bond angles; X = oxo-functionalizing unit) determined by single crystal X-ray diffraction, and characteristic spectroscopic data (OUO vibrational stretching frequency) determined by FTIR or Raman spectroscopies for unfunctionalized and functionalized uranyl(VI) complexes reported since 2010 are provided in Tables 1 and 2, respectively, and their trends are discussed in more detail in Section 7 (*vide infra*). Elongated U−O bond lengths in uranyl(VI) complexes (*i.e.* greater than 1.83 Å) may be accessible when employing strong equatorial σ-donors (i.e., silylamides, alkyl, ketimides, amides, and other *O*-donor ligands), providing a "push" by way of the equatorial ligands, and a "pull" of $U^{VI}-O_{yl}$ through Lewis adduct formation, and they appears primarily to be an electronic effect.[63,64] While deviations from linearity of the OUO unit are scarce across many of these compounds, bond lengths vary considerably and are dependent on equatorial ligand coordination, with steric forces and crystal packing effects appearing to have little structural influence.

3. $U^{VI} \rightarrow U^{V}$ REDUCTIVE FUNCTIONALIZATION

The combination of the strongly electron donating β-ketoiminate ligand, ^{Ar}acnac (^{Ar}acnac = Ar*N*C(Ph)CHC(Ph)*O*; Ar = 3,5-^{t}Bu$_2$C$_6$H$_3$) and single oxo-group coordination by the Lewis acidic borane $B(C_6F_5)_3$ resulted in the activation of the uranyl(VI) ion toward reductive silylation, providing both uranyl(V) and uranium(IV) dioxo products (see Section 6, *vide infra*). To expand the scope of this borane-mediated silylation, dibenzoylmethanate (dbm; *O*C(Ph)CHC(Ph)*O*) was used as an equatorially coordinating ligand; $[U^{VI}O_2(dbm)_2(THF)]$ (**49**) was prepared by treating $[U^{VI}O_2Cl_2(THF)_2]$ (**4-THF**) with 2 equiv of Na[dbm]. When **49** was treated with 1 equiv of R_3SiH (R = Et, Ph) and 1 equiv of $B(C_6F_5)_3$, the complexes $[U^V\{OB(C_6F_5)_3\}(OSiR_3)(dbm)_2(THF)]$ were obtained (R = Et (**50**), Ph (**51**); Scheme 6). Complexes **50** and **51** are products of $U^{VI} \rightarrow U^V$ reductive silylation, in which one oxo ligand has been converted into a siloxy ligand and the other is coordinated to the borane. The U−O bond lengths are significantly elongated compared to those of uranyl(VI) complexes, with $U-O_B$ bond lengths of 1.960(2) and 1.952(2) Å and $U-O_{Si}$ bond lengths of 2.011(2) and 2.024(2) Å for **50** and **51**, respectively; the uranyl(V) units also remain linear with O_B-U-O_{Si} bond angles of 178.43(8) and 175.06(8)° for **50** and **51**, respectively. The yields of **50** and **51** are higher when 0.25 equiv of THF are added to the crystallization solutions, and THF-free **50** may be isolated in the absence of excess THF, affording $[U^V\{\kappa^2\text{-}O,F\text{-}OB(C_6F_5)_3\}(OSiEt_3)(dbm)_2]$ (**52**). Complex **52** possesses a short $U\cdots F_{ortho}$ intramolecular contact with one C_6F_5 ring, with considerably elongated $U-O_B$ and $U-O_{Si}$ bond lengths of 1.915(2) and 1.981(3) Å, respectively, and retains a linear O_B-U-O_{Si} angle of 169.3(1)°.[69]

Alternatively, **49** reacts with 2 equiv of Ph_3SiOTf in the absence of a borane activator, forming $[U^V(OSiPh_3)_2(dbm)_2(OTf)]$ (**53**; Scheme 7), which possesses two siloxy ligands *trans*-coordinated to the U^V center, with an O−U−O bond angle of 178.81(8)° and U−O bond lengths of 2.005(2) and 2.018(2) Å.[70]

A similar result is achieved if the uranyl(VI) bis(β-ketoiminate) complex, $[U^{VI}O_2(^{Ar}acnac)_2]$ (**54**), is treated with 2 equiv of Ph_3SiOTf in CH_2Cl_2, in which $U^{VI} \rightarrow U^V$ reductive silylation is achieved, yielding $[U^V(OSiPh_3)_2(^{Ar}acnac)_2][OTf]$ (**55**; Scheme 8).[70] Compound **54** also reacts with excess Me_3SiI to afford $[U^V(OSiMe_3)_2I_2(^{Ar}acnac)]$ (**56**) and ArNC(Ph)CHC(Ph)OSiMe$_3$ (^{Ar}acnacSiMe$_3$) and 0.5 equiv of I_2 as reaction byproducts, or with excess Me_3SiX to yield $[U^{VI}O_2X_2(OEt_2)_n(^{Ar}acnacH)_2]$ (X = OTf, *n* = 1 (**57**); X = Cl, *n* = 0 (**58**); Scheme 8).[46] Both oxo ligands in **55** and **56** have been converted into siloxy ligands, and the U−O bond lengths range from 1.986(5)−2.044(2) Å[46,70] and are indicative of $U^{VI} \rightarrow U^V$ reduction, whereas the equivalent metrics of 1.750(6) and 1.746(6) Å in **57** indicated that no reduction of the U^{VI} center had occurred.[46] The identity of the reducing agent in the formation of **53** and **55** is not immediately obvious, since 2 equiv of Ph_3SiOTf is required but only 1 equiv of $[OTf]^-$ is incorporated into the final product, but it is thought that 1 equiv of either the dbm or ^{Ar}acnac ligand undergoes a one-electron oxidation, yielding a ligand-based radical which then reacts to abstract an H atom from solvent.[70] This hypothesis is based on the observation of unreacted Ph_3SiOTf and Hdbm in the ^{1}H NMR spectrum recorded during the formation of **53**. On the other hand, the reducing agent in the formation of **56** is hypothesized to be I^-, which forms I_2 as a reaction byproduct. The formation of I_2 in this reaction has been experimentally verified by adding PPh_3 into the reaction mixture, forming Ph_3PI_2. The $U^{VI} \rightarrow U^V$ reduction is facilitated by a shift in the uranyl reduction potential to a more positive value upon Me_3Si^+ coordination to the uranyl oxo groups (in a similar fashion to the effects of coordinating the Lewis acid $B(C_6F_5)_3$ to uranyl), as well as the difference in Si−I and Si−O bond dissociation energies.[46]

The exploitation of the Pacman ligand framework in uranyl chemistry has led to a wide variety of new reactions that enable the controlled reductive functionalization of the uranyl dication. While treating the uranyl(VI) Pacman complex, $[U^{VI}O_2(S)(H_2L^{Me})]$ (S = THF (**11-THF**), py (**11-py**)), with 1

DOI: 10.1021/acs.chemrev.9b00048
Chem. Rev. XXXX, XXX, XXX−XXX

Table 1. Structural and Spectroscopic Data for Unfunctionalized Uranyl(VI) Complexes Reported since 2010[a]

Compound	U−O [Å]	O−X [Å]	O−U−O [deg]	U−O−X [deg]	ν(OUO) [cm^{-1}]	Refs
$[UO_2\{N(SiMe_3)_2\}_2(py)_2]$ (**2-py**)	1.779(3)	–	170.5(2)	–	935 (asym.)	29,45
$[UO_2(THF)(H_2L^{Me})]$ (**11-THF**)	1.787(3), 1.770(3)	–	177.0(2)	–	908 (asym.)	39
$[FeCl(MeIm)][UO_2(Ar_2nacnac)(\kappa^1\text{-}N\text{-}C_4H_5N_2)_2]$ (**14**)	1.777(4), 1.780(4)	–	177.2(2)	–	911 (asym.)	36
$[CoCl(MeIm)][UO_2(Ar_2nacnac)(\kappa^1\text{-}N\text{-}C_4H_5N_2)_2]$ (**15**)	1.767(5), 1.771(4)	–	178.0(2)	–	911 (asym.)	36
$[UO_2(^{dipp}ISQ)_2(THF)]$ (**25**)	1.762(4), 1.786(3)	–	175.4(2)	–	Unassigned	41
$[K(THF)_2(18\text{-}c\text{-}6)]_2[UO_2(^{dipp}AP)_2(THF)]$ (**26**)	1.812(2), 1.814(2)	–	174.5(1)	–	Unassigned	41
$[Li(THF)_4][UO_2\{N(SiMe_3)_2\}_3]$ (**33**)	1.784(4)	–	179.8(2)	–	969 (asym., soln.)	42
$[Na(THF)_6][UO_2\{N(SiMe_3)_2\}_3]$ (**35**)	1.791(3)	–	179.8(1)	–	973 (asym., soln.)	42
$[K(THF)_6][UO_2\{N(SiMe_3)_2\}_3]$ (**36**)	1.786(3)	–	179.6(1)	–	973 (asym., soln.)	42
$[Li(2,2,2\text{-crypt})][UO_2\{N(SiMe_3)_2\}_3]$ (**37**)	1.797(3)	–	179.0(2)	–	964 (asym.), 809 (sym.)	42
$[Na(2,2,2\text{-crypt})][UO_2\{N(SiMe_3)_2\}_3]$ (**38**)	1.772(8)	–	179.8(4)	–	963 (asym.), 811 (sym.)	42
$[K(2,2,2\text{-crypt})][UO_2\{N(SiMe_3)_2\}_3]$ (**39**)	1.801(2)	–	178.58(9)	–	963 (asym.), 809 (sym.)	42
$[Rb(2,2,2\text{-crypt})][UO_2\{N(SiMe_3)_2\}_3]$ (**40**)	1.80(1)	–	180.0	–	964 (asym.), 810 (sym.)	42
$[Cs(2,2,2\text{-crypt})][UO_2\{N(SiMe_3)_2\}_3]$ (**41**)	1.80(2)	–	180.0	–	961 (asym.), 809 (sym.)	42
$[Li(12\text{-}c\text{-}4)_2][UO_2\{N(SiMe_3)_2\}_3]$ (**42**)	1.787(4)	–	178.8(2)	–	962 (asym.), 808 (sym.)	42
$[Na(15\text{-}c\text{-}5)_2][UO_2\{N(SiMe_3)_2\}_3]$ (**43**)	1.79(2)	–	178.0(8)	–	960 (asym.), 810 (sym.)	42
$[K(15\text{-}c\text{-}5)_2][UO_2\{N(SiMe_3)_2\}_3]$ (**44**)	1.79(1)	–	180.0	–	964 (asym.), 811 (sym.)	42
$[Rb(15\text{-}c\text{-}5)_2][UO_2\{N(SiMe_3)_2\}_3]$ (**45**)	1.788(2)	–	178.7(2)	–	964 (asym.), 805 (sym.)	42
$[Cs(15\text{-}c\text{-}5)_2][UO_2\{N(SiMe_3)_2\}_3]$ (**46**)	1.789(3)	–	178.0(2)	–	964 (asym.), 804 (sym.)	42
$[UO_2(OTf)_2(^{Ar}acnacH)_2(OEt_2)]$ (**57**)	1.750(6), 1.746(6)	–	176.5(3)	–	940 (asym.)	46
$[UO_2\{N(SiMe_2Ph)_2\}_2(py)_2]$ (**69**)	1.782(3)	–	180.0	–	Unassigned	45
$[UO_2(THF)(H_2L^{Et})]$ (**89-THF**)	1.768(3), 1.790(3)	–	175.1(2)	–	907 (asym.)	47
$[UO_2(dpaea)]$ (**120**)	1.75(3)	–	176.9(7)	–	913 (asym.)	48
$[UO_2(SCS)(py)_2]$ (**126**)	1.776(5), 1.787(5)	–	171.8(2)	–	920 (asym.)	49
$[UO_2(Mesaldien)]$ (**150**)	1.779(3), 1.784(3), 1.770(3), 1.786(3)	–	173.3(2), 174.1(1)	–	Unassigned	50
$[UO_2Cl(L^{nacnac})]$ (**152**)	1.757(9), 1.785(8)	–	178.4(4)	–	Unassigned	51
$[\{UO_2(L^{nacnac})\}_2(\mu\text{-}O)]$ (**153**)	1.79(1), 1.80(1), 1.80(1), 1.82(1), 1.81(1), 1.82(1), 1.79(1), 1.79(1)	–	176.2(5), 172.8(5), 175.2(5), 173.0(6)	–	Unassigned	51
$[UO_2(salfen\text{-}^tBu_2)]$ (**167**)	1.778(3)	–	177.1(2)	–	Unassigned	52
$[UO_2(PhCOO)_2(py)_2]$ (**176**)	1.769(5)	–	180.0	–	Unassigned	53
$[Cp^*UO_2(^{Mes}PDI^{Me})]$ (**181**)	1.799(5), 1.790(5)	–	168.3(2)	–	876 (asym.), 788 (sym.)	54
$[Cp^*UO_2(^tBu\text{-}^{Mes}PDI^{Me})]$ (**182**)	1.77(1)	–	167.4(4)	–	878 (asym.), 787 (sym.)	54
$[UO_2Cl(L')]$ (**205**)	1.766(4), 1.763(4)	–	175.5(2)	–	920 (asym.)[b]	55
$[CoCp_2][UO_2Cl(L'')]$ (**208**)	1.772(3), 1.779(3)	–	176.5(1)	–	Unassigned	55
$[\{UO_2(py)\}_2(L^A)]$ (**209**)	1.747(4), 1.779(4)	–	174.0(2)	–	912 (asym.)	56
$[UO_2(^{tBu}acnac)_2]$ (**220**)	1.770(3)	–	180.0	–	907 (asym.), 823 (sym.)	57
$[UO_2(L')][B\{3,5\text{-}(CF_3)_2\text{-}C_6H_3\}_4]$ (**229**)	1.753(2), 1.762(2)	–	173.6(1)	–	952 (asym.)	58
$[UO_2(OTf)(L')]$ (**230**)	1.763(3), 1.759(3)	–	176.5(1)	–	Unassigned	58
$[UO_2(HOEt)(L^{salen})]$ (**240**)	1.773(8), 1.816(9)	–	177.6(4)	–	908 (asym.), 850 (sym.)	59
$\{[K(py)_2][UO_2(C_6H_5COO)_3]\}_n$ (**244**)	1.773(7)		179(1)		Unassigned	60
$[K(THF)_5][UO_2(NPh^F_2)_3(THF)]$	1.770(6), 1.772(5)	–	177.0(2)	–	Unassigned	37
$[K(THF)_5]_2[UO_2(NPh^FPh)_4]$	1.765(3)	–	180.0(2)	–	Unassigned	37
$[K(18\text{-}c\text{-}6)(dme)]_2[UO_2(NAr^FPh)_4]$	1.789(4), 1.792(4)	–	178.9(2)	–	Unassigned	37

DOI: 10.1021/acs.chemrev.9b00048
Chem. Rev. XXXX, XXX, XXX−XXX

Table 1. continued

Compound	U−O [Å]	O−X [Å]	O−U−O [deg]	U−O−X [deg]	ν(OUO) [cm^{-1}]	Refs
$[UO_2(DOPO^q)_2]$	1.765(4), 1.768(5)	–	179.9(2)	–	937 (asym.), 843 (sym.)	61
$[UO_2Cl_2(^HN4)]$	1.776(5), 1.785(5)	–	164.1(3)	–	813 (sym.)	62
$[UO_2Cl_2(^{Me}N4)]$	1.779(6)	–	168.2(3)	–	815 (sym.)	62
$[UO_2(OTf)_2(^HN4)]$	1.759(6), 1.781(6)	–	162.8(3)	–	833 (sym.)	62
$[UO_2(OTf)(THF)(^{Me}N4)][OTf]$	1.76(1), 1.77(1)	–	161.7(5)	–	831 (sym.)	62
$[\{UO\{OGe(THF)\}(THF)\}(L^A)]$	1.757(2), 1.762(2)	–	175.2(1)	–	925 (asym.), 928/910 (soln.)	44
$[\{UO\{OSn(THF)\}(THF)\}(L^A)]$	1.781(3), 1.782(3)	–	175.6(2)	–	921 (asym.), 927/911 (soln.)	44
$[\{UO\{OPb(THF)\}(THF)\}(L^A)]$	1.761(4), 1.764(4), 1.767(4), 1.780(4)	–	174.6(2), 175.1(2)	–	916 (asym.), 905 (soln.)	44
$[\{UO\{OPb(THF)\}(Opy)\}(L^A)]$	1.779(7), 1.787(7)	–	178.5(2)	–	Unassigned	44
$[\{UO\{OPb(py)\}(Opy)\}(L^A)]$	1.776(4), 1.779(4)	–	178.8(1)	–	902 (asym.)	44
$[UO_2(tmtaaH)\{N(SiMe_3)_2\}(THF)]$	1.787(5), 1.789(4)	–	174.0(2)	–	805 (sym.)	31
$[UO_2(tmtaaH)_2]$	1.752(7)	–	180.0	–	805 (sym.)	31
$[UO_2(L^{tBu})]$	1.778(2), 1.790(2)	–	175.83(9)	–	Unassigned	63
$[UO_2(L^{nap})]$	1.789(3), 1.780(3)	–	175.9(1)	–	Unassigned	63
$[UO_2(L^m)]$	1.786(5), 1.774(6)	–	180.0	–	Unassigned	64
$[Li(12\text{-}c\text{-}4)_2][UO_2\{N(HSiMe_2)(^tBu)\}_3]$	1.787(6)	–	179.2(5)	–	Unassigned	34
$[UO_2(^tBu\text{-}bipy)\{N(HSiMe_2)(^tBu)\}_2]$	1.748(5), 1.803(5)	–	175.8(2)	–	Unassigned	34
$[UO_2(BIPM^{TMS})(DMAP)_2]$	1.794(2), 1.785(2)	–	167.2(1)	–	860 (asym.)	65
$[UO_2(Htrensal)]$	1.783(3), 1.787(3)	–	173.5(1)	–	Unassigned	66
$[\{UO_2(trensal)\}_2Fe(py)_2]$	1.789(2), 1.785(2)	–	175.52(8)	–	Unassigned	66
$[UO_2(dpaea)(OH_2)]$	1.777(4), 1.780(4)	–	170.7(2)	–	Unassigned	48
$[UO_2(SCHS)(OTf)(OEt_2)]$	1.759(8), 1.764(8)	–	177.8(4)	–	929 (asym.)	49
$[UO_2(SCHS)_2]$	1.767(2), 1.769(2)	–	178.8(1)	–	916 (asym.)	49
$[UO_2Cl_2(DPPFO_2)]$	1.764(4), 1.760(4)	–	176.9(2)	–	916 (asym.)	67
$[UO_2(dipy^{tolyl})_2(THF)]$	1.765(5), 1.768(5), 1.758(5), 1.755(4)	–	170.9(2), 177.4(2)	–	963 (asym., DMAP adduct)	68
$[UO_2(dipy^{anis})_2(THF)]$	1.759(4), 1.764(4), 1.762(4), 1.762(4)	–	176.8(2), 170.5(2)	–	963 (asym., DMAP adduct)	68
$[UO_2(dipy^{Fc})_2(THF)]$	1.773(3)	–	177.0(2)	–	963 (asym., DMAP adduct)	68
$[UO_2(dipy^{Mes})_2(DMAP)]$	1.776(4), 1.764(4)	–	176.9(2)	–	963 (asym.)	68
$[UO_2(OTf)_2(^{dipp}IQ)(THF)]$	1.745(5)	–	179.1(2)	–	Unassigned	41
$[UO_2Cl(^{dipp}ISQ)(^{dipp}IQ)]$	1.757(3), 1.758(3)	–	175.1(1)	–	Unassigned	41

[a]With respect to the tabulated IR data, sym. refers to the symmetric OUO stretching frequency determined by Raman spectroscopy and asym. refers to the asymmetric OUO stretching frequency determined by IR spectroscopy. soln. = solution-state. The compounds are numbered within the table according to how they appear in the text, and any lattice solvent molecules are not included in the chemical formulae. [b]Reassigned or reclassified as unassigned in light of more recent information on this and related complexes since the original publication appeared.

equiv of $LiN(SiMe_3)_2$ results in the formation of $[U^{VI}O_2(S)(LiHL^{Me})]$ (S = THF (**10-THF**), py (**10-py**); see Figure 1 in Section 2), the reaction of **11-THF** or **11-py** with 2 equiv of a LiR base (R = N^{i}Pr$_2$, C_5H_5, CPh_3, NH_2, H) results in $U^{VI} \rightarrow U^V$ reduction and formation of $[U^VO(OLi)(S)(LiHL^{Me})]$ (S = THF (**59-THF**), py (**59-py**); Scheme 9), in which one of the pyrrole groups in the bottom N_4-donor pocket and the *exo*-oxo ligand have been metalated. Furthermore, treating **11-THF** or **11-py** with 3 equiv of $LiN(SiMe_3)_2$ in pyridine yields $[U^VO(OLi)(py)(Li_2L^{Me})]$ (**60**), which is the product of $U^{VI} \rightarrow U^V$ reduction and metalation of both pyrrole groups and the *exo*-oxo ligand; further treating **11-THF** or **11-py** with 4 equiv of $LiN(SiMe_3)_2$ in THF provides $Li[U^VO\{OLiN(SiMe_3)_2\}(THF)(Li_2L^{Me})]$ (**61**; Scheme 9), in which $U^{VI} \rightarrow U^V$ reduction has been achieved, both pyrrole groups in the bottom N_4-donor pocket have been metalated and the *exo*-oxo ligand has been functionalized with $LiN(SiMe_3)_2$. In this structure a Li^+ cation is present to balance the charge (Scheme 9). Performing the 3 equiv reaction in THF results in the formation of a mixture of paramagnetic species. Complexes **59-py**, **60**, and **61** crystallize as $[\{U^VO\{OLi(py)_3\}(py)\}\{(py)LiHL^{Me}\}]$ (**62-py**), $[\{U^VO[OLi(py)_3](py)\}(\{(py)Li\}_2L^{Me})]$ (**63-py**) and $[(U^VO\{OLiN(SiMe_3)_2(THF)\})(\{(THF)Li\}_3L^{Me})]$ (**64-THF**), respectively, which possess U−O bond lengths of 1.834(4) and 1.879(5) Å, 1.894(2) and 1.859(2) Å, and 1.850(2) and 1.921(2) Å, respectively. These values are in the range expected for uranyl(V) (see Tables 3, 4, 6, and Section 7).[35]

When **11-THF** or **11-py** is reacted with 2 equiv of the weakly reducing silylamide $LiN(SiMe_3)_2$, both diamagnetic and paramagnetic products are observed by ^{1}H NMR spectroscopy, with complex **60** as the paramagnetic component. However, the addition of dihydroanthracene (DHA) to the reaction mixture results in the sole formation of **59**. This divergent reactivity relative to the other LiR bases stems from the presence of two different operative mechanisms during U^{VI}

DOI: 10.1021/acs.chemrev.9b00048
Chem. Rev. XXXX, XXX, XXX−XXX

Table 2. Structural and Spectroscopic Data for Functionalized Uranyl(VI) Complexes Reported since 2010[a]

Compound	U−O [Å]	O−X [Å]	O−U−O [deg]	U−O−X [deg]	ν(OUO) [cm^{-1}]	Reference
$[Li(py)_2][UO_2\{N(SiMe_3)_2\}_3]$ (**1**)	1.81(1), 1.88(1)	1.83(3)	178.2(5)	169(2)	935 (asym.), 969 (asym., soln.) 799 (sym.)	29,42
$[Li(dme)_{1.5})]_2[UO_2(CH_2SiMe_3)_4]$ (**3**)	1.885(4)	1.87(1)	180	141.3(4)	Unassigned	30
$[Li(THF)]_2[UO_2\{N(SiMe_3)_2\}$ (tmtaa)] (**5**)	1.80(2), 1.77(2)	1.95(5)	175.9(9)	132(2)	Unassigned	31
$[Li(THF)_3][Li(THF)_2]$ $[(UO_2Cl_2)_2$(tmtaa)] (**6**)	1.764(6), 1.792(6), 1.776(5), 1.786(6)	1.88(2), 1.93(2)	176.8(3), 178.0(3),	168.9(6), 171.8(6)	Unassigned	32
$[Li(THF)](TMEDA)][UO_2(N{=}C^tBu_2)_3]$ (**7**)	1.804(5), 1.830(5)	1.85(1)	179.4(2)	172.2(5)	Unassigned	33
$[Li(THF)(OEt_2)]_2[UO_2(N{=}C^tBuPh)_4]$ (**8**)	1.838(4), 1.822(4)	1.97(1), 1.94(1)	180.0	106.2(4), 107.7(4)	Unassigned	33
$[Li(THF)_3][UO_2\{N(SiMe_2H)$ $(^tBu)\}_3]$ (**9**)	1.785(4), 1.853(5)	1.88(1)	179.7(2)	174.21(6)	Unassigned	34
$[UO_2(THF)\{(THF)LiHL^{Me}\}]$ (**10-THF**)	1.794(3), 1.767(3)	2.06(1)	176.1(2)	120.7(3)	899 (asym.)	35
$[Li(MeIm)][UO_2(Ar_2nacnac)(\kappa^1$-C-$C_4H_5N_2)_2]$ (**12**)	1.778(4), 1.788(4)	2.19(1)	176.1(2)	108.2(4)	886 (asym.), 806 (sym.)	36
$\{[K(THF)_3][UO_2(NPh^Fpy)_3]\}_n$ (**16**)	1.769(7), 1.775(7), 1.779(7), 1.783(7)	2.707(7), 2.716(7), 2.738(7), 2.693(8)	178.0(4), 178.4(4)	157.1(4), 176.1(4)	Unassigned	37
$[K(\eta^6$-$C_6H_5CH_3)_2]_2[UO_2(NAr^FPh)_4]$ (**17**)	1.802(2), 1.806(2)	2.589(2), 2.615(3)	177.8(1)	139.3(1), 149.5(1)	Unassigned	37
$[K(py)_3]_2[K(py)]_2[(UO_2)_2(\mu$-$O_2)$ $(L^{Me})]$ (**18**)	1.788(6), 1.781(6), 1.787(6), 1.784(5)	2.884(7), 2.642(6), 2.722(6), 3.325(6)	176.0(3), 176.1(3)	107.8(3), 174.0(3), 122.7(3), 165.3(3)	924 (asym.)	38
$[K(py)_3]_2[K(py)]_2[(UO_2)_2(\mu$-O) $(L^{Me})]$ (**20**)	1.817(7), 1.803(6), 1.786(6), 1.798(7)	3.079(8), 3.283(8), 2.951(7), 2.699(6), 2.583(6)	177.5(3), 176.5(3)	101.5(3), 99.1(3), 176.1(3), 124.3(3), 162.7(3)	Unassigned	38
$[\{UO_2(OH)K(C_6H_6)(H_2L^{Me})\}_2]$ (**21**)	1.796(2), 1.803(2)	2.813(2), 2.838(2)	179.16(7)	108.19(7), 123.01(8)	894 (asym.)	39
$[UO_2(OH)K(THF)_2(H_2L^{Me})]$ (**23**)	1.788(6), 1.821(6)	3.194(7)	178.5(3)	100.9(2)	895 (asym.)	39
$K_2[K(OEt_2)_2]_2[UO_2(^{dipp}AP)_2]_2$ (**24**)	1.824(3), 1.834(3)	2.701(3), 2.741(3), 2.688(3)	172.2(1)	139.3(1), 111.4(1), 129.1(1)	Unassigned	41
$[K(THF)_3][UO_2\{N(SiMe_3)_2\}_3]$ (**29**)	1.776(3), 1.804(3)	2.669(3)	179.4(2)	174.0(2)	940 (asym.), 799 (sym.), 973 (soln.)	42
$[Rb][(UO_2\{N(SiMe_3)_2\}_3]$ (**30**)	1.80(3)	2.74(3)	180.0	159.6(3)	940 (asym.), 804 (sym.), 973 (soln.)	42
$[Cs][UO_2\{N(SiMe_3)_2\}_3]$ (**31**)	1.79(1)	2.93(1)	180.0	155.0(2)	941 (asym.), 804 (sym.), 971 (soln.)	42
$[Li(THF)_2][UO_2\{N(SiMe_3)_2\}_3]$ (**32**)	1.786(4), 1.841(4)[34]	1.89(1)[34]	179.2(1)[34]	166.5(4)[34]	943 (asym.), 798 (sym.), 969 (soln.)[42]	34,42
$[Na(THF)_2][UO_2\{N(SiMe_3)_2\}_3]$ (**34**)	1.781(5), 1.810(5)[42]	2.201(6)[42]	179.3(2)[42]	161.7(2)[42]	938 (asym.),[42] 928 (asym.),[43] 973 (soln.),[42] 795 (sym.),[42] 805 (sym.)[43]	42,43
$[\{UO(OPb)(THF)\}(L^{Me})]$ (**47-THF**)	1.78(1), 1.817(9)	2.5	176.5(4)	137.8(4)	896 (asym.), 898 (soln.)	44
$[\{UO\{OPb(py)\}(py)\}(L^{Me})]$ (**47-py**)	1.77(1)	2.91(1)	175.3(6)	149.5(6)	908 (asym.), 895 (soln)	44
$[\{UO\{OPb(py)\}(Opy)\}(L^{Me})]$ (**48**)	1.759(7), 1.853(8)	2.612(8)	177.5(3)	121.3(3)	893 (asym.)	44

[a]With respect to the tabulated IR data, sym. refers to the symmetric OUO stretching frequency determined by Raman spectroscopy and asym. refers to the asymmetric OUO stretching frequency determined by IR spectroscopy. soln. = solution-state; the compounds are numbered within the table according to how they appear in the text, and any lattice solvent molecules are not included in the chemical formulae.

DOI: 10.1021/acs.chemrev.9b00048
Chem. Rev. XXXX, XXX, XXX−XXX

Scheme 6. Borane-Assisted $U^{VI} \rightarrow U^{V}$ Reductive Silylation of a Dibenzoylmethanate-Coordinated Uranyl(VI) Complex, $[U^{VI}O_2(dbm)_2(THF)]$ (49)[69]

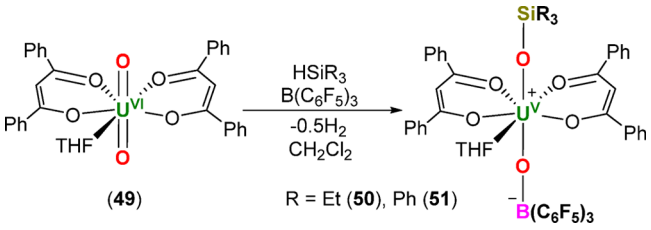

Scheme 7. $U^{VI} \rightarrow U^{V}$ Reductive Silylation of $[U^{VI}O_2(dbm)_2(THF)]$ (49) *via* Double Silylation of the Uranyl Oxo Ligands, Forming $[U^{V}(OSiPh_3)_2(dbm)_2(OTf)]$ (53)[70]

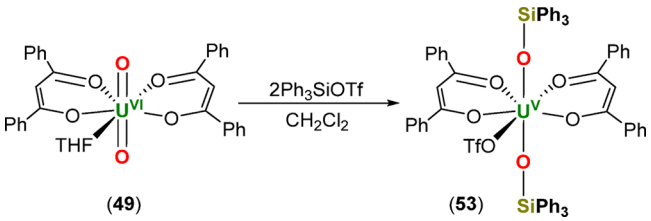

Scheme 8. $U^{VI} \rightarrow U^{V}$ Reductive Silylation of Both Uranyl Oxo Ligands in $[U^{VI}O_2(^{Ar}acnac)_2]$ (54) Using Either 2 equiv of Ph_3SiOTf or Excess Me_3SiI, Providing $[U^{V}(OSiPh_3)_2(^{Ar}acnac)_2][OTf]$ (55) and $[U^{V}(OSiMe_3)_2I_2(^{Ar}acnac)]$ (56)[a]

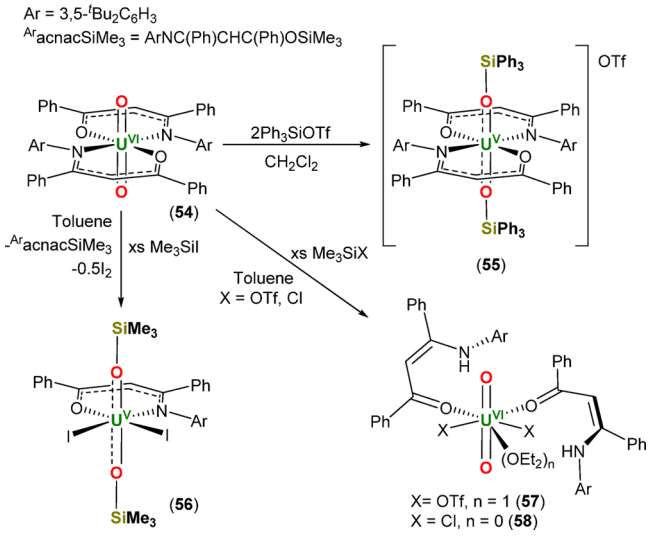

[a]Alternatively, **54** reacts with excess Me_3SiX (X = OTf, Cl) to yield $[U^{VI}O_2X_2(OEt_2)_n(^{Ar}acnacH)_2]$ (X = OTf, n = 1 (**57**); X = Cl, n = 0 (**58**)).[46,70]

$\rightarrow U^{V}$ reduction and metalation. The LiR bases (R = $N^{i}Pr_2$, CPh_3, C_5H_5, NH_2, H) act as simple reductants with release of a radical (R•), which is quenched by the Pacman ligand through H atom abstraction (as determined by ^2H NMR spectroscopy and incorporation of deuterium into the Pacman ligand). Alternatively, in the case of $LiN(SiMe_3)_2$, an H atom abstraction mechanism by the uranyl complex is invoked, requiring the presence of the H atom donor DHA for clean reactivity. However, it is unknown whether a U═O group or a pyrrolyl radical is responsible for C−H bond cleavage (Scheme 10); DFT calculations were unable to distinguish between the two mechanisms. Treatment of **11-THF** or **11-py** with 2 equiv of either $LiNH_2$ or LiH also forms a mixture of **60**, **10**, and unreacted **11**; heating this mixture drives the reaction toward **59**. Overall, this reactivity suggests that endogenous bonding of a lithium cation to the uranyl oxo group facilitates reduction chemistry.[35]

Scheme 9. Uranyl(VI) Pacman Complex, $[U^{VI}O_2(S)(H_2L^{Me})]$ (S = THF (11-THF), py (11-py)), Reacts with 1 equiv of $LiN(SiMe_3)_2$ or 2 equiv of LiR (R = $N^{i}Pr_2$, C_5H_5, CPh_3, NH_2, H) To Provide $[U^{VI}O_2(S)(LiHL^{Me})]$ (S = THF (10-THF), py (10-py)) and $[U^{V}O(OLi)(S)(LiHL^{Me})]$ (S = THF (59-THF), py (59-py)), respectively[a]

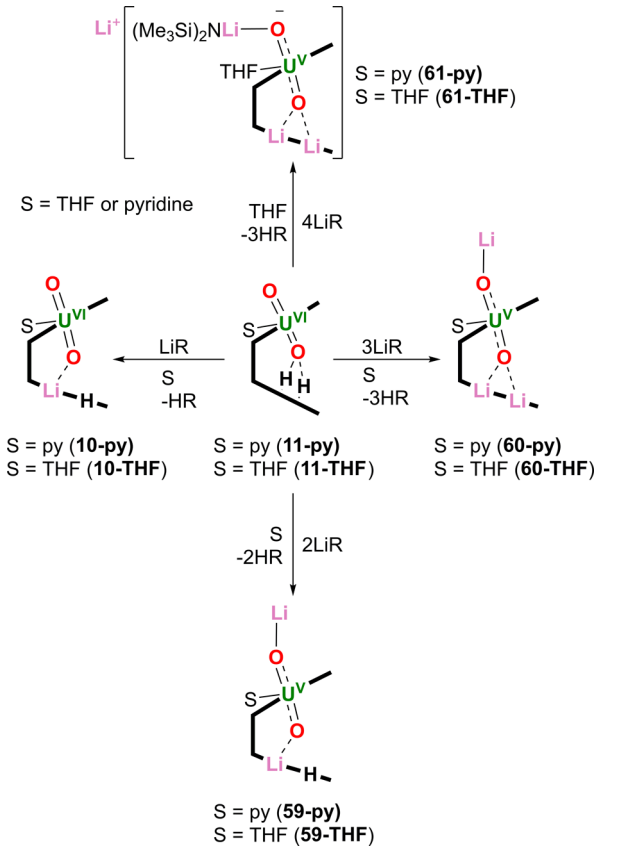

[a]Alternatively, **11-THF** or **11-py** reacts with 3 equiv of $LiN(SiMe_3)_2$ in pyridine to provide $[U^{V}O(OLi)(py)(Li_2L^{Me})]$ (**60**) or with 4 equiv of $LiN(SiMe_3)_2$ in THF to afford $Li[U^{V}O\{OLiN(SiMe_3)_2\}(THF)\text{-}(Li_2L^{Me})]$ (**61**).[35]

Treating **59-py** with 2 equiv of HCl provides the uranyl(V) hydroxide $[U^{V}O(OH)(py)(H_2L^{Me})]$ (**65**); **59-py** can be regenerated by treating **65** with 2 equiv of $LiN(SiMe_3)_2$ (Scheme 11). While **65** was not crystallographically characterized, its identity was verified by NMR and IR spectroscopy; an asymmetric OUO stretch located at 765 cm^{-1} in the corresponding IR spectrum confirms the presence of a U^{V} center. Complex **11-py** may be regenerated from **65** either by treatment with Ph_3CCl, forming 0.5 equiv of Gomberg's dimer, **11-py**, and HCl, or by treatment with TEMPO, forming **11-py** by H atom abstraction (Scheme 11).[71]

Complex **65** also reacts with chorosilanes, $ClSiR_3$ (SiR_3 = $SiMe_3$, $SiMe_2{}^{t}Bu$, $SiPh_2H$), to provide the uranyl(V) mono oxo-silylated products, $[U^{V}O(OSiR_3)(py)(H_2L^{Me})]$ (SiR_3 =

DOI: 10.1021/acs.chemrev.9b00048
Chem. Rev. XXXX, XXX, XXX−XXX

Table 3. Structural and Spectroscopic Data for Reductively Functionalized Mixed Uranyl(VI)/Uranyl(V) and Uranyl(V) Complexes Reported since 2010 and Discussed in Section 3[a]

Compound	U−O [Å]	O−X [Å]	O−U−O [deg]	U−O−X [deg]	ν(OUO) [cm^{-1}][c]	Refs
		Mixed $[U^{VI}O_2]^{2+}/[U^{V}O_2]^{+}$				
$[\{\{U^{V}O(OSiMe_3)\}(U^{V}O_2)(L^{Me})\}U^{VI}O_2(\mu\text{-}OH)_2(THF)_2]_2$ (**76**)	$[U^{VI}O_2]^{2+}$: 1.757(9), 1.760(8) $[U^{V}O_2]^{+}$: 1.909(7), 2.052(7), 2.170(8), 2.034(7), 2.045(8), 2.099(8)	$[U^{V}O_2]^{+}$: 1.666(8) (X = Si), 2.312(7) (X = U^{VI})	$[U^{VI}O_2]^{2+}$: 173.8(4) $[U^{V}O_2]^{+}$: 174.7(3), 173.9(3)	$[U^{V}O_2]^{+}$: 153.5(5) (X = Si), 168.8(4) (X = U^{VI})	Unassigned	45
$[U^{VI}O_2(BIPMH)(\mu\text{-Cl})U^{V}O_2(BIPMH)]$ (**124**)	$[U^{VI}O_2]^{2+}$: 1.785(4), 1.776(4) $[U^{V}O_2]^{+}$:1.932(4), 1.843(5)	$[U^{V}O_2]^{+}$:2.316(4)	$[U^{VI}O_2]^{2+}$:177.4(2) $[U^{V}O_2]^{+}$:171.0(2)	$[U^{V}O_2]^{+}$:126.4(2)	$[U^{VI}O_2]^{2+}$:906 (asym.) $[U^{V}O_2]^{+}$: 835, 803 (asym.)	77
$[U^{VI}O_2(BIPMH)(\mu_3\text{-Cl})\{U^{V}O_2(BIPMH)\}_2]$ (**127**)	$[U^{VI}O_2]^{2+}$:1.776(4), 1.812(4) $[U^{V}O_2]^{+}$:1.825(4), 1.966(4), 1.822(4), 1.903(4)	$[U^{VI}O_2]^{2+}$:2.544(4) $[U^{V}O_2]^{+}$:2.239(4), 2.360(4)	$[U^{VI}O_2]^{2+}$:177.9(2) $[U^{V}O_2]^{+}$:175.5(2), 173.7(2)	$[U^{VI}O_2]^{2+}$:127.8(2) $[U^{V}O_2]^{+}$:132.4(2), 132.5(2)	900−802 (asym.; multiple broad stretches)	77
$[Cp^*_2Co][\{U^{VI}O_2(salen)\}\{U^{V}O_2(salen)(py)\}]$ (**143**)	$[U^{VI}O_2]^{2+}$:1.79(1), 1.80(1) $[U^{V}O_2]^{+}$:1.82(1), 1.93(1)	$[U^{V}O_2]^{+}$:2.28(1)	$[U^{VI}O_2]^{2+}$:173.6(5) $[U^{V}O_2]^{+}$:179.0(6)	$[U^{V}O_2]^{+}$:163.0(6)	Unassigned	78
		$[U^{V}O_2]^{+}$				
$\{K_2[(U^{V}O_2)_2(L^{Me})]\}_n$ (THF solvate) (**19-THF**)[b]	1.867(7), 2.077(5)	2.598(7), 2.753(8)	176.4(3)	143.8(4), 113.1(3)	Unassigned	38
$[K(py)_3]_2[K(py)]_2[(U^{V}O_2)_2(L^{Me})]_2$ (**19-py**)[b]	1.851(5), 2.090(5), 2.101(5), 1.871(6)	2.658(6), 2.748(6), 2.764(6)	172.9(2), 173.7(2)	118.8(3), 114.0(2), 128.5(3)	Unassigned	38
$[U(OB\{C_6F_5\}_3)(OSiEt_3)(dbm)_2(THF)]$ (**50**)	2.011(2) (U−O_{Si}), 1.960(2) (U−O_B)	1.681(2) (X = Si), 1.503(4) (X = B)	178.43(8)	153.5(1) (X = Si), 165.8(2) (X = B)	Unassigned	69
$[U(OB\{C_6F_5\}_3)(OSiPh_3)(dbm)_2(THF)]$ (**51**)	2.024(2) (U−O_{Si}), 1.952(2) (U−O_B)	1.665(2) (X = Si), 1.525(4) (X = B)	175.06(8)	164.0(1) (X = Si), 172.0(2) (X = B)	Unassigned	69
$[U\{\kappa^2\text{-}O,F\text{-}OB(C_6F_5)_3\}(OSiEt_3)(dbm)_2]$ (**52**)	1.981(3) (U−O_{Si}), 1.915(2) (U−O_B)	1.720(3) (X = Si), 1.546(5) (X = B)	169.3(1)	148.7(2) (X = Si), 151.6(2) (X = B)	Unassigned	69
$[U(OSiPh_3)_2(dbm)_2(OTf)]$ (**53**)	2.005(2), 2.018(2)	1.669(2), 1.668(2)	178.81(8)	169.0(1), 176.1(1)	Unassigned	70
$[U(OSiPh_3)_2(^{Ar}acnac)_2][OTf]$ (**55**)	2.044(2)	1.664(2)	180.0	164.8(1)	Unassigned	70
$[U(OSiMe_3)_2I_2(^{Ar}acnac)]$ (**56**)	1.996(5), 1.986(5)	1.687(6), 1.682(6)	179.1(2)	154.9(4), 171.4(4)	Unassigned	46
$[\{UO\{OLi(py)_3\}(py)\}\{(py)LiHL^{Me}\}]$ (**62-py**)	1.834(4), 1.879(5)	1.93(1), 1.94(2)	174.8(2)	167.3(4), 113.6(7)	Unassigned[b]	35
$[\{UO\{OLi(py)_3\}(py)\}\{\{(py)Li\}_2L^{Me}\}]$ (**63-py**)	1.894(2), 1.859(2)	1.914(7), 1.979(7), 1.976(7)	174.2(1)	169.2(3), 123.8(2), 123.1(2)	704 (asym.)	35
$[(UO\{OLiN(SiMe_3)_2(THF)\})(\{(THF)Li\}_3L^{Me})]$ (**64-THF**)	1.850(2), 1.921(2)	1.876(6), 2.016(7), 2.171(6), 2.027(7)	175.35(9)	174.0(3), 111.7(2), 142.8(2), 111.8(2)	Unassigned	35
$[UO(OSiMe_3)(py)(H_2L^{Me})]$ (**66**)	1.854(4), 2.034(4)	1.667(5)	176.0(2)	160.2(3)	860 (asym.)	71
$[\{UO(OSiMe_3)\}_2(L^{Me})]$ (**70**)[b]	2.034(4), 2.099(4), 2.085(4), 2.040(4)	1.666(4), 1.665(4)	173.4(2), 174.9(2)	157.7(3), 155.1(3)	862, 802 (asym.)	45
$[\{UO(OSiMe_2Ph)\}_2(L^{Me})]$ (**71**)[b]	2.030(5), 2.081(5), 2.087(5), 2.039(5)	1.665(5), 1.664(5)	174.4(2), 176.7(2)	156.1(3), 155.5(3)	890−850 (asym.)	45
$[(Me_3SiOUO)(THF)(ZnCl)_2(L^{Me})]$ (**81-THF**)	1.84(1), 1.99(1)	1.70(1) (X = Si); 1.96(1) (X = Zn)	172.9(5)	160.2(8) (X = Si); 149.6(7) (X = Zn)	Unassigned	72
$[(py)Cl_2ZnOUO(py)\{Zn(py)\}(HL^{Me})]$ (**82**)	1.933(2), 1.887(3)	1.962(2), 1.989(3)	170.4(1)	119.5(1), 172.9(2)	Unassigned	72
$[(py)I_2ZnOUO(THF)\{Zn(py)\}(HL^{Me})]$ (**83**)	1.909(3), 1.879(3)	1.965(3), 1.987(3)	173.0(1)	118.9(2), 172.3(2)	Unassigned	72
$[\{(py)_2\{(Me_3Si)_2N\}MgOUO\}(py)\{Mg(py)\}(HL^{Me})]$ (**84**)	1.85(1), 1.87(1)	2.04(1), 1.97(1)	172.6(5)	162.1(6), 172.9(8)	Unassigned	72
$[UO\{OAlMe_2(py)\}(py)(H_2L^{Me})]$ (**87**)	1.856(3), 1.962(3)	1.777(3)	174.3(1)	166.2(2)	893 (asym.)	73
$[UO\{OAl^iBu_2(py)\}(THF)(H_2L^{Me})$ (**88**)	1.855(3), 1.962(2)	1.785(3)	175.1(1)	167.0(2)	892 (asym.; py adduct)	73

DOI: 10.1021/acs.chemrev.9b00048
Chem. Rev. XXXX, XXX, XXX−XXX

Table 3. continued

Compound	U−O [Å]	O−X [Å]	O−U−O [deg]	U−O−X [deg]	ν(OUO) [cm^{-1}][c]	Refs
		$[U^{V}O_2]^+$				
$[UO(OUCp_3)(THF)(H_2L^{Me})]$ (**90**)	1.840(3), 1.976(3)	2.262(3)	178.1(1)	170.7(2)	897 (asym.)	47
$[UO(OUCp_3)(THF)(H_2L^{Et})]$ (**91**)	1.844(3), 1.986(3)	2.245(3)	176.9(1)	171.3(1)	893 (asym.)	47
$[UO(ONpCp_3)(THF)(H_2L^{Me})]$ (**92**)	1.842(4), 1.975(4)	2.256(4)	178.1(2)	171.2(2)	891 (asym.)	47
$[UO(ONpCp_3)(THF)(H_2L^{Et})]$ (**93**)	1.826(7), 1.975(7)	2.249(7)	176.9(3)	170.5(4)	892 (asym.)	47
$[\{UO\{OLi(py)_3\}\}_2(L^{Me})]$ (**95**)[b]	1.877(4), 2.111(4), 2.100(4), 1.883(4)	1.87(1), 1.93(1)	175.1(2), 172.7(2)	166.8(5), 150.2(5)	Unassigned	29
$[\{UO(OSn^{n}Bu_3)\}_2(L^{Me})]$ (**96**)[b]	1.982(9), 2.073(8), 2.122(7), 1.991(9)	2.015(9), 2.00(1)	177.1(3), 174.5(3)	154.2(5), 154.8(5)	869 (asym.)	29
$[\{UO(OSnPh_3)\}_2(L^{Me})]$ (**97**)[b]	1.987(8), 2.057(8), 2.11(1), 2.00(1)	1.996(8), 2.01(1)	170.2(3), 176.1(3)	167.2(5), 168.0(5)	Unassigned	29
$[\{UO\{OLi(py)_3\}\}\{UO(O^{i}Pr)\}(L^{Me})]$ (**99**)[b]	2.034(2), 2.111(2), 2.076(2), 1.865(2)	1.438(4) (X = C); 1.922(8) (X = Li)	174.32(9), 174.34(9)	163.1(2) (X = C); 175.2(2) (X = Li)	Unassigned	29
$[\{UO(O^{i}Pr)\}_2(L^{Me})]$ (**100**)[b]	2.013(8), 2.105(6), 2.081(5), 2.011(6)	1.48(3)[d], 1.43(1)	174.7(3), 174.4(2)	155.8(2)[d], 149.5(8)	841 (asym.)	29
$[\{UO\{OLi(py)_3\}\}\{UO(OSiMe_3)\}(L^{Me})]$ (**101**)[b]	2.056(2), 2.113(2), 2.077(2), 1.857(3)	1.655(3) (X = Si); 1.929(8) (X = Li)	172.3(1), 175.2(1)	157.4(2) (X = Si); 171.6(3) (X = Li)	883 (asym.)	29
$[\{UO_2Sc(py)_2(L^{Me})\}_2]$ (**102**)	1.925(2), 1.939(2)	2.048(2)	174.56(8)	171.5(1)	Unassigned	74
$[\{UO_2Y(py)_2(L^{Me})\}_2]$ (**103**)	1.919(4), 1.965(3)	2.155(4)	175.3(2)	177.3(3)	722 (asym.)	74,75
$[\{UO_2Ce(py)_2(L^{Me})\}_2]$ (**104**)	1.895(5), 1.924(5)	2.253(5)	175.6(2)	173.3(3)	766 (asym.)	74
$[\{UO_2Sm(py)_2(L^{Me})\}_2]$ (**105**)	1.890(5), 1.941(5)	2.238(5)	174.4(2)	174.5(3)	724 (asym.)	74,75
$[\{UO_2Eu(py)_2(L^{Me})\}_2]$ (**106**)	1.904(2), 1.932(2)	2.200(2)	175.4(1)	177.0(1)	564 (asym.)	74
$[\{UO_2Dy(py)_2(L^{Me})\}_2]$ (**108**)	1.901(4), 1.942(4)	2.179(4)	175.2(2)	177.5(3)	765 (asym.)	74
$[\{UO_2Er(py)_2(L^{Me})\}_2]$ (**109**)	1.911(4), 1.939(3)	2.159(4)	175.6(2)	177.3(2)	770 (asym.)	74
$[\{UO_2Yb(py)_2(L^{Me})\}_2]$ (**110**)	1.905(6), 1.947(6)	2.143(6)	174.3(3)	170.9(4)	Unassigned	74
$[\{UO_2Lu(py)_2(L^{Me})\}_2]$ (**111**)	1.909(3), 1.941(3)	2.141(3)	173.3(1)	172.7(2)	Unassigned	74
$[(py)_3LiOUO(\mu\text{-}Cl)Sm(py)L^{Me}]$ (**114**)	1.916(8), 1.855(9)	2.286(8) (X = Sm); 1.90(3) (X = Li)	174.9(4)	119.3(4) (X = Sm); 172(1) (X = Li)	Unassigned	74
$[Cp^*_2Co][UO_2(dpaea)]$ (**122**)	1.83(1), 1.84(1)	–	177.0(6)	–	787 (asym.)	48
$[\{UO_2Sm(THF)_2(L^{Me})\}_2]$	1.903(8), 1.942(7)	2.238(8)	174.2(3)	174.9(5)	771 (asym.)	74
$[\{UO_2Sm(py)_2(L^{Et})\}_2]$	1.900(2), 1.939(2)	2.234(2)	174.4(1)	171.4(1)	Unassigned	74

[a]With respect to the tabulated IR data, sym. refers to the symmetric OUO stretching frequency determined by Raman spectroscopy and asym. refers to the asymmetric OUO stretching frequency determined by IR spectroscopy. [b]=U−O bond lengths are provided for the *trans*-uranyl oxo ligands because they possess multiple bond character, whereas the U−O bond lengths corresponding to the uranyl oxo groups bound in a *cis*-arrangement within the bridging-oxo butterfly motif are not provided because they do not possess any multiple bond character and as a result are not representative of the uranium oxidation state. [c]Reassigned or reclassified as unassigned in light of more recent information on this and related complexes since the original publication appeared. [d]Averaged value due to two site disorder of the isopropyl carbon atoms. The compounds are numbered within Table 3 according to how they appear in the text, and any lattice solvent molecules are not included in the chemical formulas.

DOI: 10.1021/acs.chemrev.9b00048
Chem. Rev. XXXX, XXX, XXX−XXX

Table 4. Structural and Spectroscopic Data for Functionalized Uranyl(V) Complexes Reported Since 2010 and Discussed in Section 4[a]

Compound	U−O [Å]	O−X [Å]	O−U−O [deg]	U−O−X [deg]	ν(OUO) [cm^{-1}]	Refs
[K(18-c-6)][UO_2(salan-^{t}Bu$_2$)(py)] (**131**)	1.853(2), 1.868(2)	2.651(3)	177.4(1)	138.0(1)	Unassigned[b]	81
[Cp*$_2$Co][UO_2(salan-^{t}Bu$_2$)(py)] (**132**)	1.846(9), 1.866(9)	–	178.7(4)	–	Unassigned	81
{[K(THF)$_2$][UO_2(salophen-^{t}Bu$_2$)(THF)]}$_n$ (**134-THF**)	1.853(2), 1.850(2)	2.630(2), 2.685(2)	177.14(8)	144.55(9), 115.75(9)	Unassigned	81
[K(18-c-6)]$_2$[K_2{UO_2(acacen)}$_4$] (**136**)	1.85(1), 1.94(1), 1.86(1), 1.973(9)	**X = K:**2.65(1), 2.89(1), 3.06(1), 2.88(1), 2.93(1)	177.4(5), 179.3(5)	**X = K:**137.7(5), 96.4(5), 88.2(3), 94.1(4), 84.1(4), 97.1(4), 96.2(3), 89.4(3)	Unassigned	78
		X = U^V:2.40(1), 2.344(9)		**X = U^V:**175.0(7), 172.2(6)		
[K(2.2.2-crypt)]$_2$[K_2{UO_2(acacen)}$_4$] (**137**)	1.77(1), 1.91(1), 1.799(9), 1.91(1)	**X = K:**2.907(8), 3.05(1), 2.885(9), 3.118(9)	179.3(4), 179.2(4)	**X = K:**97.4(3), 89.2(3), 95.5(3), 84.1(3), 98.6(3), 87.7(3), 93.2(3), 84.7(3)	Unassigned	78
		X = U^V:2.40(1), 2.40(1)		**X = U^V:**173.4(5), 173.4(4)		
[K(18-c-6)(THF)$_2$][{U^VO_2(salophen)}$_4$(μ_8-K)$_2$(μ_5-KI)$_2$]I_2 (**138**)	1.871(4), 1.942(3), 1.818(3), 1.954(3)	**X = K:**2.372(3), 2.816(3), 2.856(3), 3.121(3), 2.815(3)	175.4(1), 174.7(2)	**X = K:**90.3(1), 99.5(1), 94.1(1), 136.2(2), 90.4(1), 83.30(9)	Unassigned	78
		X = U^V:2.404(3), 2.374(3)		**X = U^V:**154.4(2), 155.3(2)		
[Rb(18-c-6)]$_2$[Rb_2{UO_2(salen)}$_4$] (**141**)	1.84(1), 1.928(9), 1.882(8), 1.909(9)	**X = Rb:**3.065(8), 3.154(9), 3.04(1), 3.41(1), 2.742(9)	175.3(3), 177.1(5)	**X = Rb:**100.3(3), 86.9(3), 95.0(3), 88.7(3), 97.6(4), 88.6(3), 91.0(4), 82.3(3), 148.1(6)	Unassigned	78
		X = U^V:2.414(9), 2.419(9)		**X = U^V:**171.2(4), 171.2(6)		
[Ca_2{UO_2(salen)}$_4$] (**146**)	1.80(1), 1.96(1), 1.79(1), 1.93(1)	**X = Ca:**2.553(1), 2.81(1), 2.56(1), 2.83(2)	174.6(5), 177.1(7)	**X = Ca:**102.0(5), 92.0(4), 102.2(5), 91.9(5), 94.9(5), 86.5(4), 94.2(6), 86.2(4)	756 (asym.)	82
		X = U^V:2.32(1), 2.37(1)		**X = U^V:**159.4(7), 178.5(8)		
[{Mn(py)$_3$}$_6${UO_2(salen)}$_{12}$] (**147**)	1.85(1), 1.88(1), 1.87(1), 1.88(2), 1.89(1), 1.89(1), 1.84(2), 1.89(2), 1.90(1), 1.90(2), 1.79(2), 1.90(2)	2.15(1), 2.18(2), 2.17(2), 2.18(2), 2.18(2), 2.12(2), 2.17(1), 2.12(2), 2.18(2), 2.12(2)	176.1(6), 169.9(6), 171.4(7), 176.5(9), 172.4(6), 175.2(8)	155.6(8), 145.9(7), 167.8(9), 169.1(9), 148.0(8), 154.2(8), 169.8(8), 147.4(8), 155.6(8)	752 (asym.)	82
[UO_2(Mesaldien)K]$_n$ (**148**)	1.79(2), 1.86(2), 1.79(2), 1.83(2)	2.63(2), 2.80(2), 2.72(2), 2.82(2)	174.1(9), 177.4(9)	151(1), 108.9(7), 154(1), 103.3(7)	Unassigned	50
{[{U^VO_2(Mesaldien)}{U^{IV}(Mesaldien)}]$_2$(μ-O)} (**149**)	1.82(1), 2.00(1)	2.20(1)	176.5(6)	162.8(7)	Unassigned	50
[UO_2(L^{nacnac})]$_3$ (**151**)	1.84(1), 1.91(1), 1.844(9), 1.940(8), 1.820(8), 1.906(8)	2.374(8), 2.371(9), 2.356(9)	176.7(4), 176.4(3), 176.7(4)	157.1(5), 156.4(4), 154.9(5)	Unassigned	51
[{UO_2(Mesaldien)}{FeCl(TPA)}$_2$]I (**154**)	1.917(4), 1.877(4)	1.998(4), 2.132(4)	174.8(2)	163.8(2), 175.4(2)	Unassigned	83
[{UO_2(Mesaldien)}{MnI(TPA)}$_2$]I (**155**)	1.91(1), 1.90(1)	2.05(1), 2.06(1)	175.7(4)	168.1(8), 171.4(7)	Unassigned	83
[{UO_2(Mesaldien)}{CdI(TPA)}$_2$]I (**156**)	1.89(2)	2.20(2)	172.7(8)	168.7(8)	Unassigned	84
[{UO_2(Mesaldien)}{Co(TPA)}]I (**157**)	1.837(3), 1.934(3)	1.924(3)	175.0(2)	151.5(2)	Unassigned	85
[{UO_2(Mesaldien)}{Ni(BPPA)(py)}$_2$]I (**158**)	1.896(5), 1.891(5)	2.068(5), 2.026(5)	175.0(2)	174.4(3), 168.5(3)	Unassigned	83
[{UO_2(Mesaldien)}{Fe(BPPA)(py)}$_2$]I (**159**)	1.917(4), 1.895(4)	2.006(4), 2.049(4)	174.1(2)	167.9(3), 168.9(3)	Unassigned	83
[{UO_2(Mesaldien)}{Co(BPPA)}$_2$]I (**160**)	1.913(6), 1.897(6)	1.983(6), 2.037(7)	173.8(3)	175.2(4), 170.9(4)	Unassigned	85
[{UO_2(salen)(py)}{Cd(NO_3)(py)$_4$}]$_n$ (**161**)	1.87(1), 1.88(1), 1.88(1), 1.88(1), 1.87(1), 1.89(1)	2.30(1), 2.28(1), 2.30(1), 2.34(1), 2.34(1), 2.32(1), 2.30(1)	178.7(5), 177.5(5), 178.7(5)	173.5(6), 161.8(7), 166.0(7), 170.0(6), 175.1(7), 162.8(7)	Unassigned	86

DOI: 10.1021/acs.chemrev.9b00048
Chem. Rev. XXXX, XXX, XXX−XXX

Table 4. continued

Compound	U−O [Å]	O−X [Å]	O−U−O [deg]	U−O−X [deg]	ν(OUO) [cm^{-1}]	Refs
[$CoCp^*_2$][UO_2(Mesaldien)] (**163**)	1.845(8), 1.846(8)	–	171.5(4)	–	Unassigned	87
{[UO_2(Mesaldien)][Mn(NO_3)(py)$_2$]}$_n$ (**164**)	1.900(3), 1.910(3)	2.066(3), 2.090(4)	171.6(2)	164.4(2), 177.2(2)	Unassigned	87
[{K(18-c-6)}UO_2(salfen-^{t}Bu$_2$)] (**165**)	1.831(4), 1.853(4), 1.838(4), 1.860(4)	2.568(4), 2.791(4)	176.8(2), 177.5(2)	150.7(2), 110.2(2)	Unassigned	52
[K(2.2.2-crypt)][UO_2(dpaea)] (**168**)	1.837(2), 1.847(2)	–	176.06(8)	–	794 (asym.)	48
[K(2.2.2-crypt)]$_2$[UO_2(trensal)] (**171**)	1.87(2), 1.82(2)	2.83(2)	173.7(6)	160.0(7)	Unassigned	66
[UO_2(trensal)Fe(py)$_3$] (**172**)	1.837(3), 1.930(2)	2.018(3)	177.1(1)	173.5(2)	Unassigned	66
[{UO_2(trensal)Fe(py)$_3$}$_2$Fe(py)$_3$]I_2 (**173**)	1.920(4), 1.935(4), 1.927(4), 1.927(5)	2.067(4), 1.984(4), 1.992(5), 2.055(5)	175.5(2), 175.3(2)	173.2(2), 166.6(3), 153.1(3), 171.1(3)	Unassigned	66
[UO_2(trensal)Fe(py)$_3$U(trensal)]I (**174**)	1.960(6), 1.922(6)	2.317(6) (X = U), 2.144(6) (X = Fe)	177.2(2)	171.2(3) (X = U), 170.3(3) (X = Fe)	Unassigned	66
[{(UO_2)Li(py)(H_2L^{Me})}$_2$] (**177**)	1.908(2), 1.891(2)	1.901(7)	177.7(1)	147.2(2)	894 (asym.)	73
[UO{ONa(py)$_3$}(py)(H_2L^{Me})] (**178**)	1.844(5), 1.856(7)	2.15(2), 2.28(2)[c]	174.2(3)	167.7(6), 170.3(8)[c]	891 (asym.)	73
[UO{OK(py)$_3$}(py)(H_2L^{Me})] (**179**)	1.871(2), 1.837(2)	2.707(3)	176.1(1)	116.0(1)	894 (asym.)	73
[UO{OLi(py)$_3$}(py)(H_2L^{Me})] (**180**)	1.853(6), 1.884(7)	1.94(2)	173.8(3)	166.7(8)	891 (asym.)	73

[a]With respect to the tabulated IR data, sym. refers to the symmetric OUO stretching frequency determined by Raman spectroscopy and asym. refers to the asymmetric OUO stretching frequency determined by IR spectroscopy. [b]Reassigned or reclassified as unassigned in light of more recent information on this and related complexes since the original publication appeared. [c]Two values are provided due to two site disorder of the Na cation. The compounds are numbered within Table 4 according to how they appear in the text, and any lattice solvent molecules are not included in the chemical formulas.

DOI: 10.1021/acs.chemrev.9b00048
Chem. Rev. XXXX, XXX, XXX−XXX

Table 5. Structural and Spectroscopic Data for Reductively Functionalized Uranium(IV) Dioxo Complexes Reported Since 2010 and Discussed in Section 5[a]

Compound	U−O [Å]	O−X [Å]	O−U−O [deg]	U−O−X [deg]	ν(OUO) [cm^{-1}]	Refs
$[UI_2(OSiMe_3)_2(^{Mes}PDI^{Me})]$ (**183**)	2.09(1), 2.10(1)	1.63(1), 1.64(1)	172.3(4)	173.6(7), 156.5(7)	Unassigned	54
$[U(OSiPh_3)_2Cl_2(OPPh_3)_2]$ (**186**)	2.112(5)	1.638(5)	178.9(2)	171.0(3)	Unassigned	88
$[U(OSiMe_3)_2(SPh)_2(OPPh_3)_2]$ (**187**)	2.113(5)	1.640(6)	174.2(3)	162.8(4)	Unassigned	88
$[U(OSiMe_3)_2Cl_2(OPPh_3)_2]$ (**188**)	2.127(2), 2.104(2)	1.620(2), 1.639(8)	173.56(7)	169.6(1), 158.9(4)	Unassigned	89
$[U(OSiMe_3)_2I_2(OPPh_3)_2]$ (**189**)	2.082(6)	1.607(7)	180.0	167.4(5)	Unassigned	88
$[U(OSiMe_3)_2(OTf)_2(OPPh_3)_2]$ (**190**)	2.053(6), 2.066(6)	1.667(6), 1.675(6)	176.9(2)	178.1(3), 173.9(3)	Unassigned	88
$[U(OSiEt_3)_2Cl_2(OPPh_3)_2]$ (**192**)	2.107(2), 2.108(2)	1.70(1), 1.650(7), 1.601(8), 1.632(2)[b]	174.56(9)	163.9(3), 173.3(3), 166.7(2), 145.4(5)	Unassigned	89
$[U(OSiHPh_2)_2Cl_2(OPPh_3)_2]$ (**196**)	2.120(5), 2.138(5)	1.608(5), 1.600(5)	177.4(2)	174.0(3), 174.2(3)	Unassigned	89
$[U(OSiMe_3)_2(OTf)_2(2,2'\text{-bipy})_2]$ (**201**)	2.12(1), 2.16(1)	1.62(1), 1.61(1)	155.5(5)	162.8(9), 154.4(8)	Unassigned	89
$[U(OTiClCp_2)_2(Cl)(L')]$ (**206**)	2.066(7), 2.061(6)	1.843(7), 1.841(7)	177.0(2)	170.9(4), 169.1(3)	630 (asym.)	55
$[(py)(pinBO)UOU(OBpin)(py)(L^A)]$ (**210**)	2.161(2), 2.139(2), 2.112(2), 2.172(2)	1.334(4), 1.341(4)	169.05(8), 96.51(7)	145.7(2), 166.9(2)	566 (asym.)	91
$[(py)\{cat(py)BO\}UOU(OBcat)(py)(L^A)]$ (**211**)	2.092(2), 2.219(2), 2.176(2), 2.068(2)	1.400(5), 1.315(5)	170.7(1), 99.2(1)	158.8(3), 171.1(3)	580, 531 (asym., tentative)	91
$[(py)(HPh_2SiO)UOU(OSiPh_2H)(py)(L^A)]$ (**213**)	2.142(2), 2.1486(3)	1.623(3)	172.09(9)	146.9(2)	Unassigned	91
$[(THF)(HPh_2SiO)UOU(OSiPh_2H)(THF)(L^A)]$	2.135(2), 2.1425(3)	2.160(2)	169.23(9)	154.0(2)	Unassigned	91
$[U(OSiMe_3)_2BrI(OPPh_3)_2]$[b]	2.078(3)	1.631(8), 1.63(1)	180.0	166.1(5), 170.2(8)	Unassigned	89
$[U(OSiMePh_2)_2Cl_{0.25}I_{1.75}(OPPh_3)_2]$[b]	2.116(2), 2.104(4), 2.100(2), 2.119(4)	1.632(2)	176.73(8), 172.5(1)	168.7(1), 163.4(1), 157.4(1), 153.2(1)	Unassigned	89

[a]With respect to the tabulated IR data, sym. refers to the symmetric OUO stretching frequency determined by Raman spectroscopy and asym. refers to the asymmetric OUO stretching frequency determined by IR spectroscopy. [b]Structure contains positional disorder. The compounds are numbered within Table 5 according to how they appear in the text, and any lattice solvent molecules are not included in the chemical formulas.

Table 6. Structural and Spectroscopic Data for Reductively Functionalized Uranyl(V) and Uranium(IV) Dioxo Complexes Reported Since 2010 and Discussed in Section 6[a]

Compound	U−O [Å]	O−X [Å]	O−U−O [deg]	U−O−X [deg]	ν(OUO) [cm^{-1}]	Refs
		$[U^VO_2]^+$				
$[U\{OB(C_6F_5)_3\}(OSiPh_3)(^{Ar}acnac)_2]$ (**214**)	1.941(8) (U−O_B), 2.034(9) (U−O_{Si})	1.666(9) (X = Si), 1.52(2) (X = B)	174.6(3)	173.2(5) (X = Si), 170.2(7) (X = B)	Unassigned	93
$[U(OSiEt_3)_2(^{Ar}acnac)_2][HB(C_6F_5)_3]$ (**216**)	2.011(4), 2.013(4)	1.678(4), 1.684(4)	180.0	161.5(3), 159.4(3)	Unassigned	94
$[U\{OB(C_6F_5)_3\}(OSiEt_3)(^{Ar}acnac)_2]$ (**217**)	2.017(6) (U−O_{Si}), 1.957(6) (U−O_B)	1.664(7) (X = Si), 1.53(1) (X = B)	175.0(3)	168.0(4) (X = Si), 166.6(6) (X = B)	Unassigned	94
$[Ph_3PI][U(OSiMe_3)_2I_4]$ (**221**)	1.976(8), 1.990(6)	1.688(8), 1.674(7)	180.0	176.9(5), 177.8(4)	Unassigned	57
$[UO_2(L')]_2$ (**226**)	1.928(2), 1.829(3)	3.5351(2)	174.5(1)	109.97(9)	783 (asym.)	58
$[UO\{OB(C_6F_5)_3\}(L')]$ (**227**)	1.914(7), 1.785(7)	1.53(1)	178.7(3)	167.4(6)	837 (asym.)	58
$[U\{OB(C_6F_5)_3\}_2(L')]$ (**228**)	1.922(3), 1.917(3)	1.578(5), 1.554(5)	176.4(1)	174.6(2), 172.9(2)	Unassigned	58
$[\{UO_2(py)_5\}_2(SmI_4)]I$ (**233**)	1.802(6), 1.915(6)	2.331(6)	177.8(3)	176.1(3)	818 (asym.)	95
$[\{UO_2(py)_5\}_2(DyI_4)]I$ (**234**)	1.808(5), 1.919(5)	2.270(5)	177.6(2)	176.9(3)	825 (asym.)	95
$[(UO_2I_4)\{Sm(NCMe)_6\}]_n$ (**235**)	1.868(5), 1.883(4)	2.351(5), 2.318(4)	179.3(2)	179.2(3), 169.5(3)	722 (asym.)	95
		$[U^{IV}O_2]$				
$[CoCp_2][U\{OB(C_6F_5)_3\}(OSiPh_3)(^{Ar}acnac)_2]$ (**215**)	2.173(8) (U−O_{Si}), 2.056(8) (U−O_B)	1.610(9) (X = Si), 1.44(2) (X = B)	175.3(3)	170.3(6) (X = Si), 176.9(8) (X = B)	Unassigned	93
$[U(OSiEt_3)_2(^{Ar}acnac)_2]$ (**219**)	2.129(2)	1.628(2)	180.0	159.0(2)	Unassigned	94
$[U(OSiMe_3)_2I_2(bipy)_2]$ (**222**)	2.084(4)	1.639(4)	115.5(2)	165.4(3)	Unassigned	57
$[U(OSiMe_3)_2I(THF)_4][I_3]$ (**224**)	2.065(6), 2.080(6)	1.670(6), 1.659(6)	173.8(3)	170.0(4), 172.8(4)	Unassigned	57
$[Cp^*_2Fe][U\{OB(C_6F_5)_3\}_2(L')]$ (**231**)	2.030(5), 2.022(5)	1.51(1), 1.475(9)	170.6(2)	163.1(5), 170.0(5)	631 (asym.)	58
$[U\{OB(C_6F_5)_3\}\{OB(C_6F_5)_2\}(L')]$ (**232**)	2.196(4), 1.990(3)	1.323(6), 1.490(6)	162.8(1)	152.0(3), 166.8(3)	Unassigned	58
$[(UO_2I_4)\{UICl(py)_4\}_2]$ (**236**)	2.166(5)	2.042(5)	180.0	173.8(3)	Unassigned	95
$[(UO_2I_4)\{DyI(py)_5\}_2]$ (**237**)	2.058(3), 2.068(3)	2.126(3), 2.119(3)	177.7(1)	170.5(2), 173.6(2)	Unassigned	95

[a]With respect to the tabulated IR data, sym. refers to the symmetric OUO stretching frequency determined by Raman spectroscopy and asym. refers to the asymmetric OUO stretching frequency determined by IR spectroscopy. The compounds are numbered within Table 6 according to how they appear in the text, and any lattice solvent molecules are not included in the chemical formulas.

DOI: 10.1021/acs.chemrev.9b00048
Chem. Rev. XXXX, XXX, XXX−XXX

Scheme 10. Two different mechanisms are operative for the synthesis of 60[a]

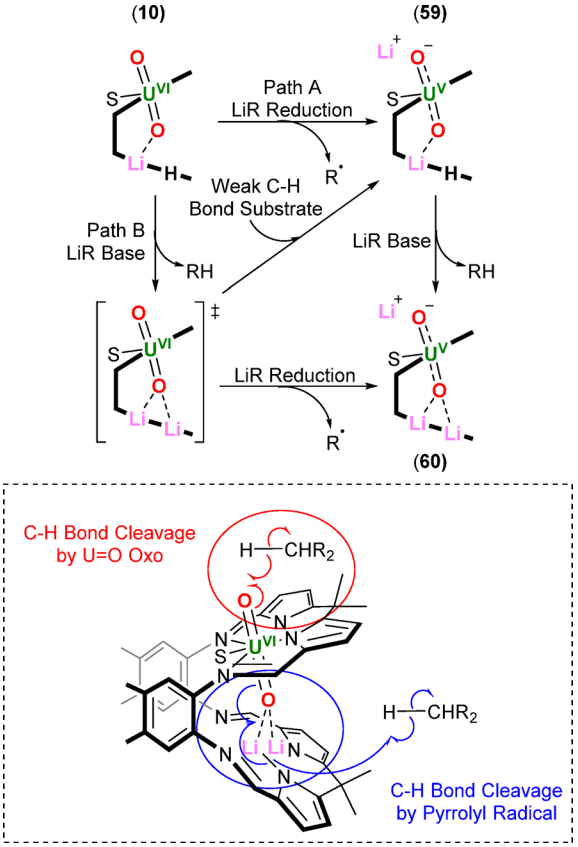

[a]The LiR reactant in Path A acts as a reductant, whereas the LiR reactant in Path B initially acts as a base, deprotonating the second pyrrole group in the bottom N_4-donor pocket. At that point, C−H bond cleavage in weak C−H bond substrates occurs either by the U═O group or a pyrrolyl radical, generating **60**.[35].

SiMe$_3$ (**66**), SiMe$_2$^{t}Bu (**67**), SiPh$_2$H (**68**); Scheme 11). While NMR and IR spectra were sufficient to determine the identity of complexes **66**−**68**, the solid-state structures of **66** and **67** were also obtained to verify their assignments, although due to issues with multiple twinning the structure of **67** only supports connectivity. The U−O$_{exo}$ and U−O$_{endo}$ bond lengths in **66** are 2.034(4) and 1.854(4) Å, respectively, and lie in the expected range for uranyl(V) complexes (see Tables 3, 4, and 6 and Section 7).[71]

[U^{VI}O$_2$(py)(H$_2$L^{Me})] (**11-py**) also reacts with an additional 1.5 equiv of [U^{VI}O$_2${N(SiR$_3$)$_2$}$_2$(py)$_2$] (SiR$_3$ = SiMe$_3$ (**2-py**), SiMe$_2$Ph (**69**)) to provide the butterfly shaped complexes [{U^{V}O(OSiR$_3$)}$_2$(L^{Me})] (SiR$_3$ = SiMe$_3$ (**70**), SiMe$_2$Ph (**71**); Scheme 12a). Alternatively, H$_4$L^{Me} reacts with 2.5 equiv of **2-py** to generate **70**, although in only 37% yield. Complexes **70** and **71** are the products of U^{VI} → U^{V} reduction of both U centers that have been installed into the [L^{Me}]$^{4-}$ Pacman ligand and silylation of both *exo*-oxo ligands. Compounds **70** and **71** are butterfly shaped bis(uranyl(V)) dimers and display an unusual structural motif for high-valent uranium in which one of the four uranyl(V) oxo ligands has migrated from a *trans*-coordination position to a *cis*-coordination position, giving rise to a U^{V}$_2$O$_2$ core. The U−O bond lengths range from 2.034(4)−2.099(4) Å and 2.030(5)−2.087(5) Å in **70** and **71**, respectively, and the asymmetric OUO stretching

Scheme 11. [U^{VI}O$_2$(py)(H$_2$L^{Me})] (11-py) Reacts with 2 equiv of LiN^{i}Pr$_2$ To Provide [U^{V}O(OLi)(py)(LiHL^{Me})] (59-py), and 59-py reacts with 2 equiv of HCl To Yield [U^{V}O(OH)(py)(H$_2$L^{Me})] (65), Which Reacts with 2 equiv of LiN(SiMe$_3$)$_2$, 1 equiv of Ph$_3$CCl/TEMPO, or 1 equiv of Cl-SiR$_3$ To Regenerate 59-py, Regenerate 11-py, or Form [U^{V}O(OSiR$_3$)(py)(H$_2$L^{Me})] (SiR$_3$ = SiMe$_3$ (66), SiMe$_2$^{t}Bu (67), SiPh$_2$H (68)), respectively[71]

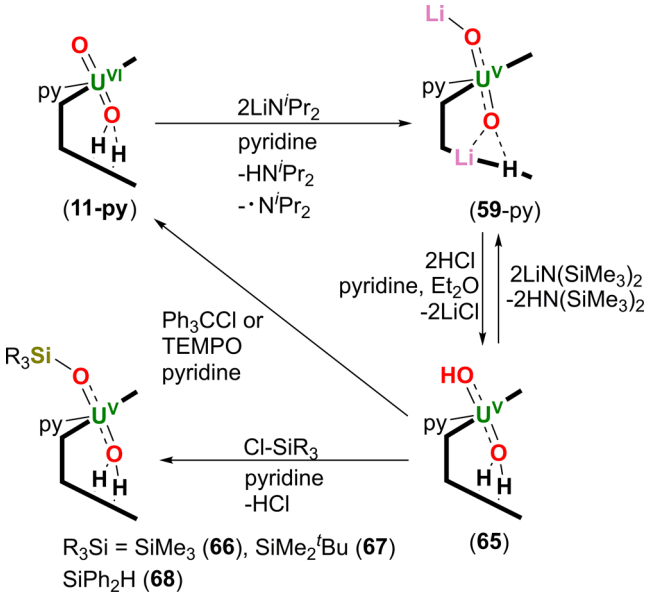

frequency is found at 862 and 802 cm^{-1} for **70** and between 890 and 850 cm^{-1} for **71**, which are indicative of uranyl(V). Furthermore, the U···U distance is very short in complexes **70** and **71**, which is 3.3557(5) and 3.3562(4) Å, respectively.[45]

During the formation of **70** and **71**, an insoluble aggregate mixture of uranyl-L^{Me} species was obtained in an approximate 30% yield and was identified as [U^{VI}O$_2$(py)$_2${(U^{V}O$_2$){U^{V}O(OH)}(L^{Me})}$_2$] (**72**), [{U^{V}O(OSiR$_3$)}{U^{V}O(OH)}(L^{Me})] (**73-Me/73-Ph**), and [{U^{V}O{OU^{VI}O$_2$(NHSiR$_3$)(py)}}{U^{V}O(OH)}(L^{Me})] (**74-Me/74-Ph**; Scheme 12a; **73-Me** and **74-Me** are derived from [U^{VI}O$_2${N(SiMe$_3$)$_2$}$_2$(py)$_2$], and **73-Ph** and **74-Ph** are derived from [U^{VI}O$_2${N(SiMe$_2$Ph)$_2$}$_2$(py)$_2$]). If H$_4$L^{Me} reacts with 2.5 equiv of [U^{VI}O$_2${N(SiR$_3$)$_2$}$_2$(py)$_2$] below 70 °C, only the paramagnetic aggregate mixture and 4 equiv of HN(SiR$_3$)$_2$ are observed by NMR spectroscopy. If this mixture is then heated to 120 °C, only trace amounts of **70** and **71** are produced. However, if the aggregate mixture is treated with Cl-SiR$_3$, complexes **70** and **71** are obtained in good yields (Scheme 12b). The aggregate mixture was identified as **72**, **73-Me/73-Ph**, and **74-Me/74-Ph** based on the following observations: (i) 4 equiv of HN(SiR$_3$)$_2$ is produced as a byproduct when treating H$_4$L^{Me} with 2.5 equiv of [U^{VI}O$_2${N(SiR$_3$)$_2$}$_2$(py)$_2$], 2.5 equiv of [U^{VI}O$_2$]$^{2+}$ is consumed per equivalent of [L^{Me}]$^{4-}$, and an additional equivalent of HN(SiR$_3$)$_2$ is produced upon treating the mixture of species **72**, **73-Me/73-Ph**, and **74-Me/74-Ph** with Cl-SiR$_3$, giving rise to an empirical formula of [(UO$_2$)$_{2.5}$(L^{Me}){NH(SiR$_3$)}(py)] (which is supported by elemental analysis; Scheme 12b); (ii) treating the mixture of species **72**, **73-Ph**, and **74-Ph** with Cl-SiMe$_3$ produced **70** (75%) and the mixed silylated [{U^{V}O(OSiMe$_3$)}{U^{V}O(OSiMe$_2$Ph)}(L^{Me})] (**75**; 25%), indicating that not all of the oxo groups in the mixture are silylated given that the silyl groups in complexes **70** and **71** are known to not

DOI: 10.1021/acs.chemrev.9b00048
Chem. Rev. XXXX, XXX, XXX−XXX

Scheme 12. (a) Synthesis of $[\{U^{V}O(OSiR_3)\}_2(L^{Me})]$ (SiR_3 = $SiMe_3$ (70), $SiMe_2Ph$ (71)) by Heating $[U^{VI}O_2(py)(H_2L^{Me})]$ (11-py) with 1.5 equiv of $[U^{VI}O_2\{N(SiR_3)_2\}_2(py)_2]$ in Pyridine, alongside 30% of an Aggregate Mixture with Empirical Formula $[(UO_2)_{2.5}(L^{Me})\{HN(SiR_3)\}]$. (b) When Heated between 20 and 70 °C, H_4L^{Me} Reacts with 2.5 equiv of $[U^{VI}O_2\{N(SiR_3)_2\}_2(py)_2]$ To Afford only the Aggregate Mixture, with Further Heating to 120 °C Providing Trace Amounts of 70 and 71. Alternatively, Adding Cl-SiR_3 to the Aggregate Mixture Provides 70 and 71 in High Yields. (c) Treating the Aggregate Mixture with Empirical Formula $[(UO_2)_{2.5}(L^{Me})\{NH(SiMe_2Ph)\}(py)]$ with Cl-$SiMe_3$ Results in the Formation of 70 (75%) and $[\{U^{V}O(OSiMe_3)\}\{U^{V}O(OSiMe_2Ph)\}(L^{Me})]$ (75; 25%), and (d) Exposure of the Aggregate Mixture with Empirical Formula $[(UO_2)_{2.5}(L^{Me})\{NH(SiMe_3)\}(py)]$ to Air Results in the Formation of $[\{\{U^{V}O(OSiMe_3)\}(U^{V}O_2)(L^{Me})\}U^{VI}O_2(\mu\text{-}OH)_2(THF)_2]_2$ (76)[45]

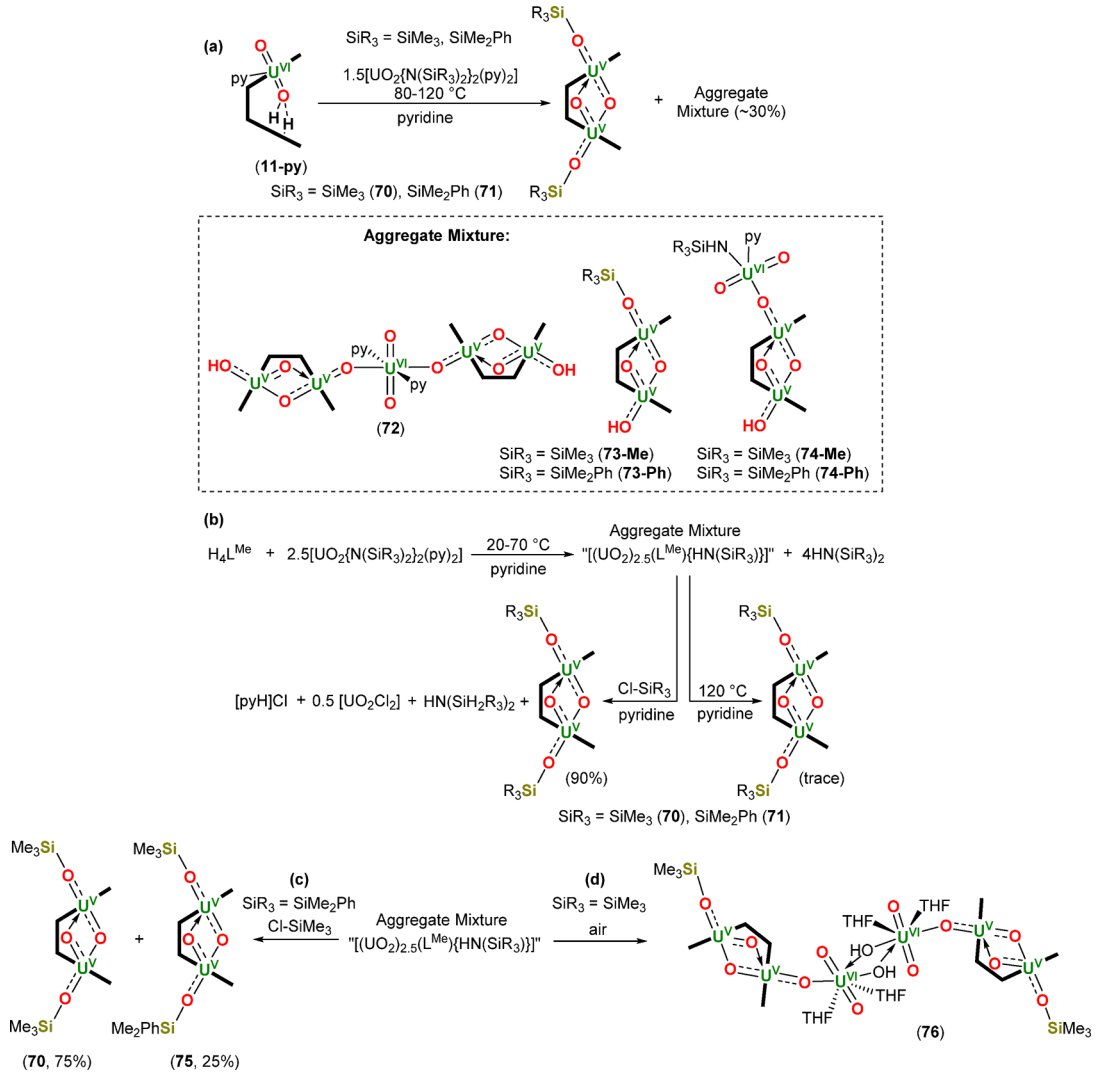

rearrange (Scheme 12c); (iii) laser desorption ionization (LDI) mass spectrometry supported this assignment; and (iv) an X-ray crystal structure of the mixed-valence complex, $[\{\{U^{V}O(OSiMe_3)\}(U^{V}O_2)(L^{Me})\}U^{VI}O_2(\mu\text{-}OH)_2(THF)_2]_2$ (**76**) was obtained following adventitious oxidation of the mixture of **72**, **73-Me**, and **74-Me** (Scheme 12d); mixed-valence **76** contains the $U^{V}_2O_2$ butterfly core with one *exo*-oxo ligand silylated and the other dimerized through the oxo groups as a uranyl(VI) hydroxide. The source of the silyl group in **70** and **71** can be traced back to the uranyl(VI) silylamide starting material and not the $HN(SiMe_3)_2$ byproduct, as there is no evidence for the formation of **70** or the mixed-silyl complex **75** upon treating **11-py** with 1.5 equiv of $[U^{VI}O_2\{N(SiMe_2Ph)_2\}_2(py)_2]$ in the presence of $N(SiMe_3)_3$. It is envisioned that initial one-electron $U^{VI} \rightarrow U^{V}$ reduction in **11-py** occurs *via* U−N bond homolysis upon the addition of 1.5 equiv of the uranyl silylamide starting material to **11-py** and that additional uranyl silylamide is required for reduction of the second U center and silylation by N−Si bond homolysis. Remarkably, complexes **70** and **71** decompose neither upon exposure as solids to air for 48 h nor in wet benzene solutions, which contrasts greatly to the known instability of uranyl(V) species toward disproportionation to uranyl(VI) and uranium(IV) dioxo species. Furthermore, the solution cyclic voltammagram (CV) of **70** and **71** did not show any electrochemical oxidation processes, which was further supported by a lack of reactivity between **70** and **71** with I_2 or $[Ce(OTf)_4]$. The electronic structure and magnetic behavior of **70** and **71** have also been investigated, but these results are beyond the scope of this review.[45]

The first example of covalent bond formation to a uranyl oxo group in the form of reductive silylation was reported in 2008

DOI: 10.1021/acs.chemrev.9b00048
Chem. Rev. XXXX, XXX, XXX−XXX

with the synthesis of $[U^{V}O(OSiMe_2R)(THF)(M_2X_2L^{Me})]$ (M = Fe, X = I, R = Me (**77**); M = Fe, X = I, R = Ph (**78**); M = Zn, X = I, R = Me (**79**); M = Zn, X = Cl, R = Me (**80**)) formed by reacting **11-THF** with the silylamido base, $KN(SiMe_3)_2$, in the presence of a transition metal dihalide.[40] Since the synthesis of complexes **77**–**80**, the mechanism of this reaction has been probed and compared to alternative reactions that lead to oxo-group metalation.[72] It was originally postulated that the Group 1 base was essential to this reaction and that the oxo-group reactivity was enhanced by coordination to a Lewis acidic metal in the bottom N_4-pocket of the Pacman ligand. When **11-THF** is treated with 2 equiv of $KN(SiMe_3)_2$ followed by 2 equiv of $ZnCl_2$, reductive silylation of the uranyl ion is observed, forming $[(Me_3SiOU^{V}O)(py)(ZnCl)_2(L^{Me})]$ (**81**; Scheme 13a). In contrast, treating **11-THF** with 2 equiv of the Group 1 metal bases $LiN^{i}Pr_2$ or KH followed by the addition of 2 equiv of ZnX_2 (X = Cl, I) results in reductive zincation of the uranyl ion, forming $[\{(py)X_2ZnOU^{V}O\}(py)\{Zn(py)\}(HL^{Me})]$ (X = Cl (**82**), I (**83**); Scheme 13b).[40] These different reaction pathways were explored by deploying various zinc(II) and magnesium(II) reagents. Complex **11-py** reacts with 2 equiv of $Mg(N'')_2$ (N'' = $N(SiMe_3)_2$) to afford $[\{(py)_2(N'')MgOU^{V}O\}(py)\{Mg(py)\}(HL^{Me})]$ (**84**), the product of $U^{VI} \rightarrow U^{V}$ reductive oxo-metalation of the uranyl and metalation of one of the two pyrroles in the bottom donor pocket of the ligand (Scheme 14a). One-electron reduction of the uranyl ion occurs through Mg–N bond homolysis.[72]

In contrast, **11-py** reacts with only 1 of 2 equiv of $Zn(N'')_2$ to afford $[U^{VI}O_2(py)\{Zn(py)\}(HL^{Me})]$ (**85**), in which reduction of the uranyl ion is not observed and both pyrrole NH groups have been metalated (Scheme 14b). Furthermore, **85** does not react with MgN''_2. These results indicate that coordination of the zinc cation to the *endo*-oxo group of uranyl is insufficiently activating to enable uranyl(VI) reduction by M–N bond homolysis, and it is likely that coordination of a more Lewis acidic metal dication (i.e., Mg^{2+}) to the *endo*-oxo group results in enhanced activation of the uranyl ion, thus enabling $U^{VI} \rightarrow U^{V}$ reduction by M–N bond homolysis. Importantly, it was found that the reaction between the mixed-ligand reagent ZnCl(N'') and **11-py** formed **81** in 62% yield; the remaining 38% was composed of **11-py**, **82**, and $[U^{VI}O_2(py)(ZnCl)(HL^{Me})]$ (**86**; Scheme 15a). Complex **86** was also prepared from **11-py** and 1 equiv of ZnCl(N'') and was characterized by NMR spectroscopy (Scheme 15b).[72]

Scheme 13. Treatment of $[U^{VI}O_2(py)(H_2L^{Me})]$ (11-py) First with a Group 1 Metal Base Followed by a Zinc Dihalide Leads to (a) $U^{VI} \rightarrow U^{V}$ Reductive Silylation, Yielding $[(Me_3SiOU^{V}O)(py)(ZnCl)_2(L^{Me})]$ (81), or (b) $U^{VI} \rightarrow U^{V}$ Reductive Metalation, Providing $[\{X_2(py)ZnOU^{V}O\}(py)\{Zn(py)\}(HL^{Me})]$ (X = Cl (82), I (83)).[72]

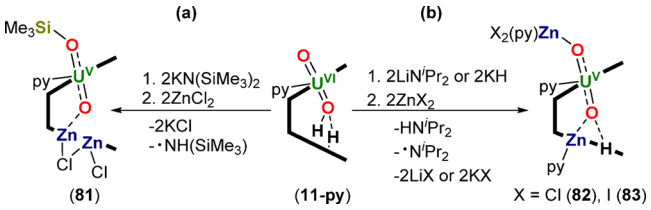

Scheme 14. Treatment of $[U^{VI}O_2(py)(H_2L^{Me})]$ (11-py) with (a) 2 equiv of MgN''_2 or (b) ZnN''_2 To Provide $[\{(py)_2N''MgOU^{V}O\}(py)\{Mg(py)\}(HL^{Me})]$ (84) and $[U^{VI}O_2(py)\{Zn(py)\}(HL^{Me})]$ (85), respectively.[72]

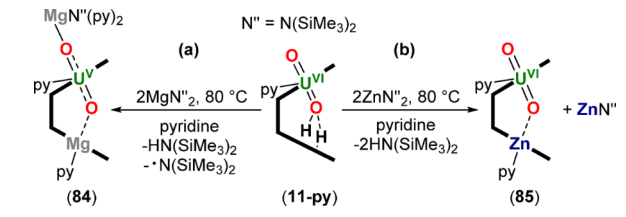

Scheme 15. Treatment of $[U^{VI}O_2(py)(H_2L)]$ (11-py) with (a) 2 equiv of ZnCl(N'') Provides a Mixture of 11-py, $[U^{VI}O_2(py)(ZnCl)(HL^{Me})]$ (86), $[(Me_3SiOU^{V}O)(py)(ZnCl)_2(L^{Me})]$ (81), and $[\{Cl_2(py)ZnOU^{V}O\}(py)\{Zn(py)\}(HL^{Me})]$ (82), and Treatment with (b) 1 equiv of ZnCl(N'') Provides only 86[72]

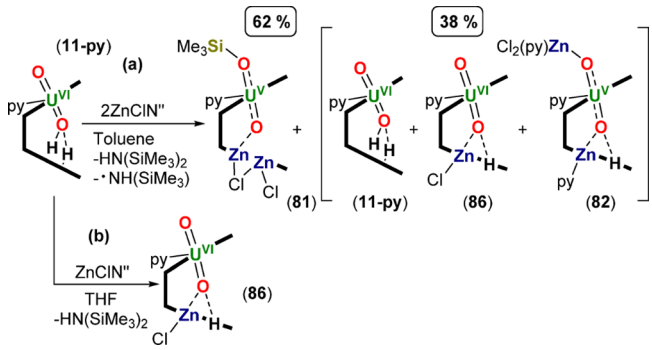

In order for oxo-silylation to be favored over oxo-metalation, N–Si bond homolysis must be preferred over M–N bond homolysis (M = Zn, Mg) within an oxo-coordinated M–N–SiR_3 group. Furthermore, the silylation pathway is driven by the formation of a strong Si–O bond and is enhanced when the alternative O–M bond is weaker. The zinc compound ZnCl(N'') is well suited to both oxo group activation and silyl group delivery, as is highlighted by the formation of both **81**, **82**, and **86** when reacted with complex **11-py**. However, its reduced Lewis acidity relative to $Mg(N'')_2$ dictates that oxo-silylation is preferred over oxo-metalation.[72]

The uranyl(VI) Pacman complex **11-py** reacts with either $[Cp_2TiCl(CH_2)(AlMe_2)]$ at room temperature or $HAl^{i}Bu_2$ at 70 °C to afford $[U^{V}O\{OAlR_2(py)\}(H_2L^{Me})]$ (R = Me (**87**), ^{i}Bu (**88**); Scheme 16), the product of $U^{VI} \rightarrow U^{V}$ reductive

Scheme 16. Reductive Alumination of $[U^{VI}O_2(py)(H_2L^{Me})]$ (11-py) Using Either $[Cp_2TiCl(CH_2)(AlMe_2)]$ or $HAl^{i}Bu_2$, Yielding $[U^{V}O\{OAlR_2(py)\}(H_2L^{Me})]$ (R = Me (87), ^{i}Bu (88))[73]

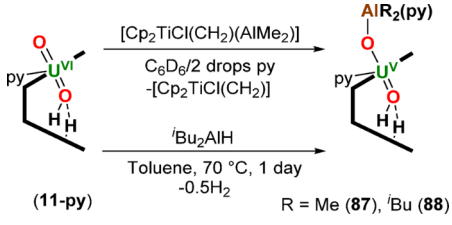

DOI: 10.1021/acs.chemrev.9b00048
Chem. Rev. XXXX, XXX, XXX–XXX

alumination of the uranyl ion. The U−O_{exo} and U−O_{endo} bond lengths in complexes **87** and **88** are 1.962(3)/1.962(2) and 1.856(3)/1.855(3) Å, respectively, which are elongated relative to those expected for uranyl(VI) complexes, and the O−U−O bond angles are 174.3(1) and 175.1(1)° for **87** and **88**, respectively. It is likely that the reducing electron required in the formation of **87** and **88** is derived from either Al−C or Al−H bond homolysis. Subsequent reactions of complexes **87** and **88** with alkyllithium reagents and metal hydrides are discussed in Section 4.[73]

The reductive functionalization chemistry of **11-THF** and $[U^{VI}O_2(S)(H_2L^{Et})]$ (S = THF (**89-THF**); H_2L^{Et} = macrocyclic Pacman-shaped Schiff-base ligand with ethyl substituents on the *meso*-carbon atoms) with common actinide precursors has also been explored, resulting in the first complex formed from reduction of the uranyl ion by a transuranic species (Scheme 17).[47]

Scheme 17. Reductive Functionalization of Uranyl in $[U^{VI}O_2(THF)(H_2L^{Me})]$ (11-THF) and $[U^{VI}O_2(THF)(H_2L^{Et})]$ (89-THF) by $[U^{III}Cp_3]$ or $[Np^{III}Cp_3]$, Providing $[U^{V}O(OU^{IV}Cp_3)(THF)(H_2L^{Me})]$ (90), $[U^{V}O(OU^{IV}Cp_3)(THF)(H_2L^{Et})]$ (91), $[U^{VI}O(ONp^{III}Cp_3)(THF)(H_2L^{Me})]$ (92), and $[U^{VI}O(ONp^{III}Cp_3)(THF)(H_2L^{Et})]$ (93)[47]

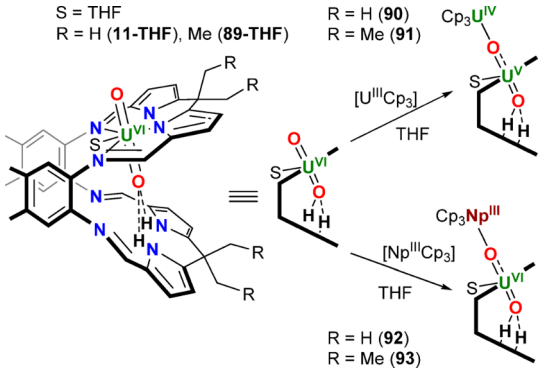

Complexes **11-THF** and **89-THF** react with $[U^{III}Cp_3]$ to yield oxo-functionalized $[U^{V}O(OU^{IV}Cp_3)(THF)(H_2L^{Me})]$ (**90**) and $[U^{V}O(OU^{IV}Cp_3)(THF)(H_2L^{Et})]$ (**91**; Scheme 17). Based on X-ray diffraction data (U−O_{exo} = 1.976(3)/1.986(3) Å, U−O_{endo} = 1.840(3)/1.844(3) Å, O−U−O = 178.1(1)/176.9(1)° for **90**/**91**, respectively), paramagnetic shifts in the resulting ^{1}H NMR spectra, IR spectra (ν[OUO asym.] = 897 and 893 cm^{-1}, respectively), and SQUID magnetometry measurements, these are best described as U^{IV}/U^{V} complexes formed upon $U^{VI} \rightarrow U^{V}$ reduction of the uranyl ion. **11-THF** and **89-THF** also react with $[Np^{III}Cp_3]$, in these cases to form $[U^{VI}O(ONp^{III}Cp_3)(THF)(H_2L^{Me})]$ (**92**) and $[U^{VI}O(ONp^{III}Cp_3)(THF)(H_2L^{Et})]$ (**93**; Scheme 17), in which the oxidation states are less clear-cut. While certain X-ray diffraction metrics for complexes **92** and **93** (U−O_{exo} = 1.975(4)/1.975(7) Å, U−O_{endo} = 1.842(4)/1.826(7) Å, O−U−O = 178.1(2)/176.9(3)° for **92**/**93**, respectively), paramagnetic shifts in the ^{1}H NMR spectra, and IR spectra (ν[OUO asym.] = 891 and 892 cm^{-1}, respectively) suggest $U^{VI} \rightarrow U^{V}$ reduction of the uranyl ion has occurred, the Np−O_{exo} bond lengths and SQUID magnetometry measurements suggest that complexes **92** and **93** are best described as donor−acceptor oxo-bridged Np^{III}/U^{VI} compounds with only partial electron transfer occurring; this assignment is further corroborated by DFT calculations which also suggest an explanation for the unexpectedly strong paramagnetically shifted resonances in the solution NMR spectra of **93**, as they find an anomalously high *s*-orbital contribution to key Np orbitals. The reactions of **11-THF** and **89-THF** with $[Pu^{III}Cp_3]$ were also investigated and, in agreement with the expected reducing capability of Pu^{III}, no oxo-coordination was observed; the reactions were carried out in THF, so there may have been an additional competition for the Pu center by the donor solvent.[47]

Uranyl(V) complexes are directly accessible from uranyl(VI) precursors. The Pacman ligand H_4L^{Me} reacts with 2.5 equiv of $[Li(py)_2][U^{VI}O_2\{N(SiMe_3)_2\}_3]$ (**94**) in boiling pyridine over 12 h to afford the doubly lithiated U^{V}/U^{V} complex, $[\{(py)_3LiOU^{V}O\}_2(L^{Me})]$ (**95**; Scheme 18a). Complex **95**

Scheme 18. (a) Synthesis of $[\{(py)_3LiOUO\}_2(L^{Me})]$ (95), (b) Subsequent Reactivity with Stannanes To Provide $[\{R_3SnOU^{V}O\}_2(L^{Me})]$ (R = ^{n}Bu (96), Ph (97)), and (c)/(d)/(e) Ti^{IV} Reagents To Yield $[\{(py)_3LiOU^{V}O\}(OU^{V}O^{i}Pr)(L^{Me})]$ (99) and $[(^{i}PrOUO)_2(L^{Me})]$ (100). (f) Synthesis of a Mixed Lithiated/Silylated U^{V}/U^{V} Bis(uranyl) Pacman Complex, $[\{(py)_3LiOU^{V}O\}(Me_3SiOU^{V}O)(L^{Me})]$ (101)[29]

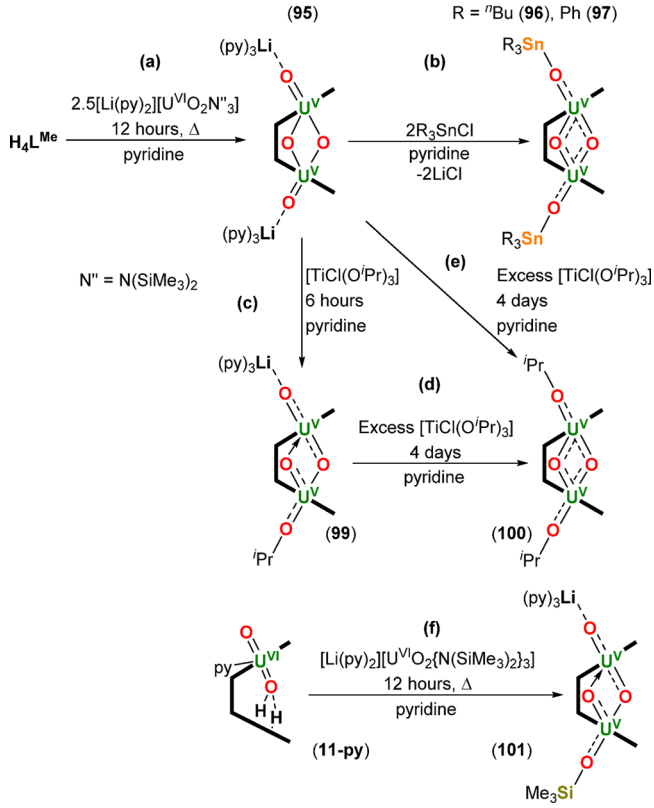

possesses Li-coordinated *exo*-oxo groups and a central diamond-shaped $[U^{V}_2O_2]$ core in which the two *endo*-oxo atoms bridge the uranium centers in axial and equatorial positions, similarly to the doubly silylated bis(uranyl(V)) complexes **70** and **71** (*vide supra*). **95** reacts with 2 equiv of a chlorostannane, R_3SnCl, to afford doubly stannylated $[\{R_3SnOU^{V}O\}_2(L^{Me})]$ complexes (R = ^{n}Bu (**96**), Ph (**97**); Scheme 18b). Complexes **96** and **97** could also be prepared from the dipotassium analogue of **95**, $[\{(py)_2KOU^{V}O\}_2(L^{Me})]$

DOI: 10.1021/acs.chemrev.9b00048
Chem. Rev. XXXX, XXX, XXX−XXX

(**98**), and the respective chlorostannane. Unexpectedly, reactions between **95** and $[Ti^{IV}Cl(O^iPr)_3]$ did not afford $[\{(^iPrO)_3TiOU^VO\}(L^{Me})]$ but instead provided $[\{(py)_3LiOU^VO\}(OU^VO^iPr)(L^{Me})]$ (**99**), in which one of the Li cations has been replaced by an isopropyl group (Scheme 18c). While **99** was stable as a solution in pyridine, attempts to isolate it on a bulk scale were unsuccessful and provided 0.5 equiv of dilithiated **95** and the doubly alkoxylated complex, $[(^iPrOUO)_2(L^{Me})]$ (**100**). **100** was also obtained by treating either **95** or **99** with excess $[Ti^{IV}Cl(O^iPr)_3]$ (Scheme 18d and 18e). Attempts to prepare both **99** and **100** from **95** and ^{i}PrCl were unsuccessful, providing intractable mixtures, so it is a realistic possibility that exchange of the lithiated uranyl oxo group by the Ti-derived O^{i}Pr group has occurred.[29]

Complex **11-py** reacts with $[Li(py)_2][U^{VI}O_2\{N(SiMe_3)_2\}_3]$ (**94**) to provide the lithiated/silylated U^V/U^V complex, $[\{(py)_3LiOU^VO\}(Me_3SiOU^VO)(L^{Me})]$ (**101**; Scheme 18f). Similarly to **95**, complexes **96**-**101** possess a diamond-shaped $[U^V_2O_2]$ core.[29]

Reduced and oxo-functionalized mixed uranyl(V)/lanthanide(III) Pacman complexes can be accessed for all of the rare earth cations (except *Pm*) using a Ln−N bond homolysis route (Scheme 19). Treatment of **11-py** with 1 equiv of the rare-earth silylamide $[Ln^{III}\{N(SiMe_3)_2\}_3]$ yields $[\{U^VO_2Ln^{III}(py)_2(L^{Me})\}_2]$ (Ln = Sc (**102**), Y (**103**), Ce (**104**), Sm (**105**), Eu (**106**), Gd (**107**), Dy (**108**), Er (**109**), Yb (**110**), and Lu (**111**)) in which the pyrrole groups of the bottom N_4-donor pocket have been deprotonated and coordinated to the Ln^{III} ion (Scheme 19a). Uranyl $U^{VI} \rightarrow U^V$ reduction occurs upon Ln−N bond homolysis of the third silylamido ligand, which then abstracts either a proton or deuterium from a solvent molecule. Complexes **102**−**111** exist as dimers with bridging $[U^V_2O_2]$ interactions holding the two uranyl units together, and dimerization is thought to occur subsequent to Ln−N bond homolysis and $U^{VI} \rightarrow U^V$ reduction, given the greater Lewis basicity of the U^V oxo groups. Even so, this dimer is readily split by alkali metal halides which satisfy both the Lewis acid and base requirements of the uranyl(V) center. The addition of either LiCl or LiI to $[\{U^VO_2Ln^{III}(py)_2(L^{Me})\}_2]$ (Ln = Y, La, Sm, Dy) provided the monomeric $[(py)_3LiOUO(\mu\text{-}X)Ln(py)(L^{Me})]$ complexes (X = Cl, Ln = Y (**112**), La (**113**), Sm (**114**), Dy (**115**); X = I, Ln = Y (**116**), La (**117**), Sm (**118**), Dy (**119**)), in which the *exo*-oxo ligand of the uranyl(V) ion is coordinated to a Li^+ cation, and a halide is residing in a bridging position between the U^V and Ln^{III} centers (Scheme 19b).[74,75] Single-electron reduction of the uranyl(VI) ion should also be possible if a suitable Ln−A (A = coligand) bond homolysis route is available, and indeed this has been verified through deployment of Ln^{III} aryloxides, $[Ln(OAr)_3]$ (Ar = C_6H_2-2,6-^{t}Bu$_2$-4-Me). While the variable-temperature SQUID magnetometry and IR, NIR, and EPR spectroscopies on complexes **102**−**119** have been studied to obtain a better understanding of the electronic structure of these complexes and their *f*-electron exchange interactions,[74] these observations are beyond the scope of this review and will not be discussed further.

The uranyl(VI) complex, $[U^{VI}O_2(dpaea)]$ (**120**), synthesized from $[U^{VI}O_2(NO_3)_2(OH_2)_6]$ (**121**) and H_2dpaea, reacts with 1 equiv of $[CoCp^*_2]$ to afford the uranyl(V) complex, $[Cp^*_2Co][U^VO_2(dpaea)]$ (H_2dpaea = bis(pyridyl-6-methyl-2-carboxylate)-ethylamine, **122**; Scheme 20). While this is not an example of reductive functionalization of the uranyl ion, it is a rare example of uranyl reduction with an outer-sphere reductant to afford a thermodynamically stable uranyl(V) product and is therefore noteworthy for inclusion in this review. Complex **122** possesses an O−U−O bond angle of 177.0(6)° and U−O bond lengths of 1.83(1) and 1.84(1) Å, which are significantly elongated relative to the uranyl(VI) starting complex (1.75(3) Å), although as a separated ion pair, it does not precisely fit the definition of oxo-functionalized. Furthermore, the asymmetric OUO stretching frequency was found at 787 cm^{-1} in the IR spectrum of **122**, which is at significantly lower frequency relative to uranyl(VI) **120** (913 cm^{-1}). Remarkably, isolated uranyl(V) **122** is stable with respect to ligand dissociation and disproportionation in D_2O.[48]

Lastly, in an attempt to prepare a uranyl(VI) carbene complex by deprotonation of a carbene analogue bound to uranyl(VI), $[U^{VI}O_2Cl(BIPMH)(THF)]$ (BIPMH = HC-$(PPh_2NSiMe_3)_2$, **123**), which was originally reported in 2003,[76] was treated with sodium benzyl, $NaCH_2C_6H_5$. However, this provided the bimetallic uranyl(VI)/uranyl(V) complex, $[U^{VI}O_2(BIPMH)(\mu\text{-}Cl)U^VO_2(BIPMH)]$ (**124**), along with NaCl and $(C_6H_5CH_2)_2$ as reaction byproducts (Scheme 21). The slow elimination of chloride enables trapping of the uranyl(V) fragment by unreacted uranyl(VI). Complex **124** is formed irrespective of the number of

Scheme 19. Synthesis of (a) Mixed Uranyl(V)/Lanthanide(III) Pacman Complexes 102−111 by Reduction of $[U^{VI}O_2]^{2+}$ by Ln−N Bond Homolysis (Ln = Sc (102),[74] Y (103),[75] Ce (104),[74] Sm (105),[75] Eu (106), Gd (107), Dy (108), Er (109), Yb (110), Lu (111)) and (b) Cleavage of the Subsequently Formed Dimer with LiCl or LiI, Providing Complexes 112−119 (X = Cl, Ln = Y (112), Ln = La (113), Sm (114), Dy (115); X = I, Ln = Y (116), La (117), Sm (118), Dy (119))[74]

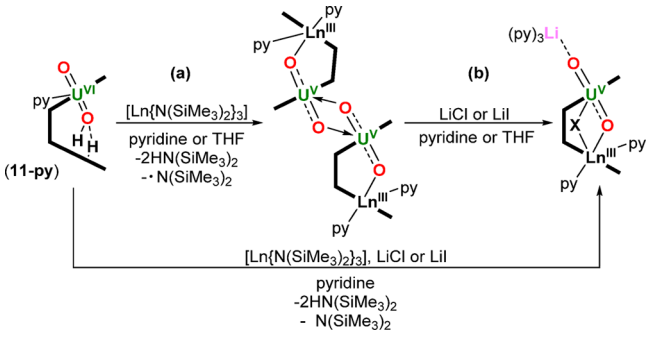

Scheme 20. $[U^{VI}O_2(dpaea)]$ (120) Reacts with $[CoCp^*_2]$ To Yield $[Cp^*_2Co][U^VO_2(dpaea)]$ (122)[a]

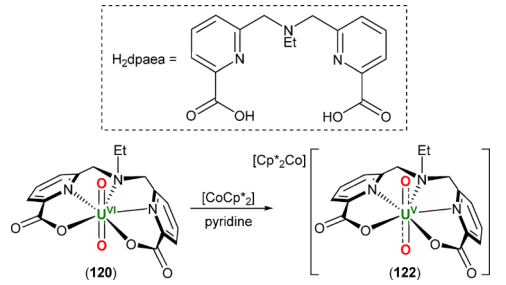

[a]The H_2dpaea ligand is depicted at the top of the scheme.[48]

DOI: 10.1021/acs.chemrev.9b00048
Chem. Rev. XXXX, XXX, XXX−XXX

Scheme 21. Synthesis of the Mixed-Valence Complexes $[U^{VI}O_2(BIPMH)(\mu\text{-}Cl)U^{V}O_2(BIPMH)]$ (124) and $[U^{VI}O_2(BIPMH)(\mu_3\text{-}Cl)\{U^{V}O_2(BIPMH)\}_2]$ (127) from $[U^{VI}O_2Cl(BIPMH)(THF)]$ (123) and 0.5 equiv of Sodium Benzyl[a]

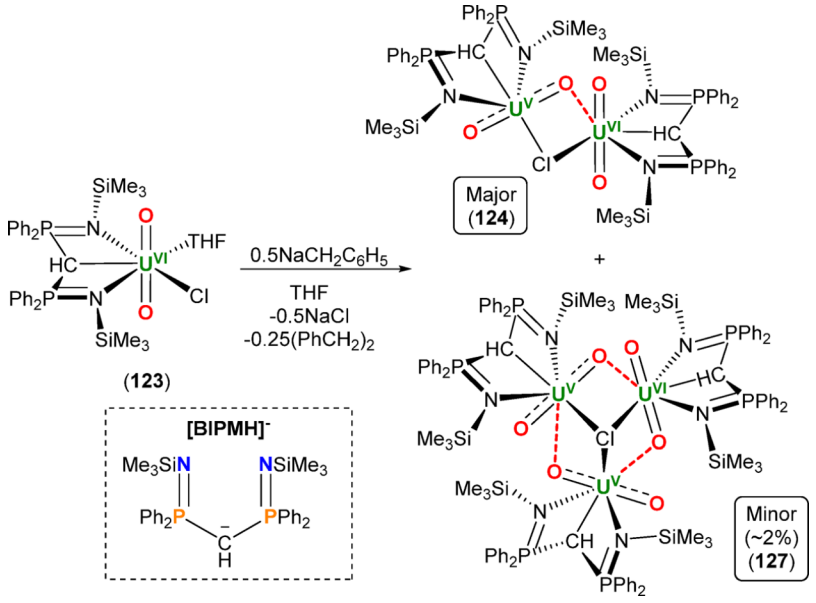

[a]The $[BIPMH]^-$ ligand is depicted in the bottom left hand corner of the scheme.[77]

equivalents of $NaCH_2C_6H_5$ used for the reaction, and attempts to prepare **124** by treating **123** with other alkali metal alkyls, amides, and hydrides resulted in the formation of intractable mixtures. The $^{31}P\{^1H\}$ NMR spectrum of **124** contains one sharp (δ −5.2) and one broadened resonance (δ −129), the magnetic moment of **124** measured in benzene at 298 K is 2.59 μ_B, and the IR spectrum contains asymmetric OUO stretching frequencies at 906, 835, and 803 cm^{-1}, all of which are indicative of one diamagnetic uranyl(VI) and one paramagnetic uranyl(V) ion being present in **124**.[77] This result contrasts to that reported from deployment of the $[C(PPh_2S)_2]^{2-}$ dianion, in which deprotonation of $CH_2(PPh_2S)_2$ with excess $LiNEt_2$ in the presence of $[U^{VI}O_2(OTf)_2]$ (**125**) was found to be a viable strategy for the synthesis of a uranyl(VI) carbene (ylid) complex, $[U^{VI}O_2(SCS)(py)_2]$ (**126**; SCS = $[C(PPh_2S)_2]^{2-}$).[49]

Also formed in the reaction between **123** and $NaCH_2C_6H_5$, albeit as a minor product (~2% yield), is the uranyl(VI)/uranyl(V)/uranyl(V) trimer, $[U^{VI}O_2(BIPMH)(\mu_3\text{-}Cl)\{U^{V}O_2(BIPMH)\}_2]$ (**127**; Scheme 21), in which oxo-bridging essentially generates the uranyl-functionalized oxo group. The $^{31}P\{^1H\}$ NMR spectrum of **127** contains a sharp signal at −5.2 ppm and a broad quartet at −149 ppm. Furthermore, the magnetic moment of **127** in benzene at 298 K is 4.01 μ_B, which is indicative of one uranyl(VI) and two uranyl(V) ions being present in **127**.[77]

Complex **124** bridges the uranyl(V) oxo group and the U^{VI} center through both oxo and chlorido ligands while complex **127** is trinuclear, with two bridging uranyl(V) oxo groups and one bridging U^{VI} oxo group. Furthermore, both **124** and **127** contain a chlorido ligand that is bridging the U cations; the chlorido ligand in **124** is bridging two metal centers whereas that in **127** is bridging three metal centers. The U−O bond lengths in the uranyl(VI) ion in **124** are 1.785(4) and 1.776(4) Å, whereas those in the uranyl(V) ion are 1.932(4) and 1.843(5) Å, in which the longer U−O bond length corresponds to the uranyl(V) oxo that is participating in the CCI. The U−O bond lengths in the uranyl(VI) ion in **127** are 1.776(4) and 1.812(4) Å, whereas those in the uranyl(V) ions range from 1.822(4)−1.966(4) Å. Similarly to **124**, the longer U−O bond length corresponds to the uranyl(V) oxo that is participating in the CCI. The O−U−O bond angles remain nearly linear in both compounds, ranging from 171.0(2)−177.9(2)°. The U···O bond length in the uranyl(V)/uranyl(VI) dimer in **124** is 2.316(4) Å whereas those in **127** are 2.544(4), 2.360(4), and 2.239(4) Å, in which the longest U···O distance is derived from the uranyl(VI) oxo group and a U^V center. This elongated distance could be a consequence of the decrease in Lewis basicity of the uranyl oxo ligand moving from U^V to U^{VI}, as well as a contraction in the U−oxo bond length in the uranyl(VI) ion, which combined with the geometric constraints imparted by the fused cubane core would prohibit close approach to another metal center. Solutions of **124** and **127** decompose upon standing in toluene at room temperature, producing a mixture of unidentified products.[77]

The structural data (U−O and O−X bond lengths, O−U−O and U−O−X bond angles; X = oxo-functionalizing unit) determined by single crystal X-ray diffraction and characteristic spectroscopic data (OUO vibrational stretching frequency) determined by FTIR or Raman spectroscopies for the reductively functionalized mixed uranyl(V)/uranyl(VI) and uranyl(VI) complexes reported since 2010 and discussed in section 3 (*vide supra*) are provided in Table 3, and their trends are discussed in more detail in section 7 (*vide infra*).

4. FURTHER FUNCTIONALIZATION OF URANYL(V) COMPLEXES THAT RETAIN THE U(V) OXIDATION STATE

This section highlights reactions that further functionalize the oxo ligands of isolated uranyl(V) complexes, therefore retaining the U(V) oxidation state and do not involve reduction of uranyl(VI). In our experience, the majority of reactions of uranyl(V) complexes designed to further function-

DOI: 10.1021/acs.chemrev.9b00048
Chem. Rev. XXXX, XXX, XXX−XXX

alize the oxo groups, for example by replacement of an alkali metal cation with a *p*-, *d*-, or *f*-block cation, result in either spontaneous reoxidation and isolation of the original uranyl(VI) complex or, in rare cases, in disproportionation to $U^{IV}O_2$ and $[U^{VI}O_2]^{2+}$. The success and diversity of the reactions outlined below is notable evidence of the maturity of this area, and it is now becoming possible to manipulate uranyl(V) complexes, despite their well-known kinetic instability, through the judicious choice of ligand design and selection of reaction conditions.

The readily available uranyl(V) starting complex, $[\{U^VO_2(py)_5\}\{KI_2(py)_2\}]_n$ (**128**), which was first reported in 2006,[79,80] reacts with the K_2salan-^{t}Bu$_2$ ligand (H_2salan-^{t}Bu$_2$ = *N*,*N*′-bis(2-hydroxybenzyl-3,5-di-*tert*-butyl)-1,2-dimethylaminomethane) in pyridine to provide polymeric $\{K[U^VO_2(salan\text{-}^tBu_2)(py)]\}_n$ (**129**; Scheme 23) in which the uranyl(V) oxo groups are coordinated to K^+ cations. Treatment of **128** or **129** with 18-c-6 in pyridine provides monomeric $[U^VO_2(py)_5]I$ (**130**) and $[K(18\text{-c-}6)][U^VO_2(salan\text{-}^tBu_2)(py)]$ (**131**), respectively (Scheme 22). The stability of **130** is remarkable considering the absence of coordinating cations and demonstrates the ability of pyridine to stabilize uranyl(V). **131** contains one potassium cation bound to 1 equiv of 18-c-6 and one of the uranyl(V) oxo ligands.[81]

Adding KI to a solution of $[Cp^*_2Co][U^VO_2(salan\text{-}^tBu_2)(py)]$ (**132**) in pyridine, which is prepared from $[U^{VI}O_2(salan\text{-}^tBu_2)(py)]$ (**133**) and excess decamethylcobaltocene, also affords polymeric **129**. All three uranyl(V)-salan-^{t}Bu$_2$ complexes, **129**, **131**, and **132**, exhibit the same stability with respect to disproportionation in pyridine and DMSO, up to 30 days. However, polymeric **129** exhibits lower stability with respect to disproportionation compared to monomeric **131** in THF. Only 33% of U(V) **129** remains after 14 days in THF whereas there is no loss of **131** after 30 days in THF, but 33% loss after 14 days in toluene solution.[81]

When **128** was treated with the Schiff-base ligand, K_2salophen (H_2salophen = *N*,*N*′-phenylene-bis(salicylideneimine)), in pyridine, a mixture of disproportionation products was obtained. However, when a bulkier Schiff base ligand, K_2salophen-^{t}Bu$_2$ (H_2salophen-^{t}Bu$_2$ = *N*,*N*′-phenylene-bis(3,5-di-*tert*-butylsalicylideneimine)), was deployed, polymeric $\{K[U^VO_2(salophen\text{-}^tBu_2)(py)]\}_n$ (**134-py**) was obtained (Scheme 23), which is stable toward disproportionation for up to 30 days in pyridine, DMSO, and toluene. This highlights the important effect that increasing the steric protection of the salophen ligand framework increases the stability of uranyl(V). If **134-py** is dissolved in THF, the pyridine coligand bound to U is displaced by THF, forming $\{K[U^VO_2(salophen\text{-}^tBu_2)(THF)]\}_n$ (**134-THF**; Scheme 23).[81]

The reactivity of **129** and **134-py** with stoichiometric amounts of H_2O was also investigated, where **129** reacts slowly with 1 equiv of H_2O to release free H_2salan-^{t}Bu$_2$; the reaction proceeds much quicker in the presence of 10 equiv of H_2O, resulting in complete disappearance of uranyl(V) after 24 h. Conversely, under similar conditions, ligand protonation and uranyl(V) oxidation is not observed in **134-py**, indicating the salophen-^{t}Bu$_2$ ligand provides greater stability for uranyl(V) than the salan-^{t}Bu$_2$ ligand. The electronic structure, electronic

Scheme 22. Synthesis of $\{K[U^VO_2(salan\text{-}^tBu_2)(py)]\}_n$ (129) from $[\{U^VO_2(py)_5\}\{KI_2(py)_2\}]_n$ (128) and K_2salan-^{t}Bu$_2$. 128 and 129 react with 18-c-6 to afford $[U^VO_2(py)_5]I$ (130) and $[K(18\text{-c-}6)][U^VO_2(salan\text{-}^tBu_2)(py)]$ (131), respectively. The K_2salan-^{t}Bu$_2$ ligand is depicted at the bottom of the scheme.[81]

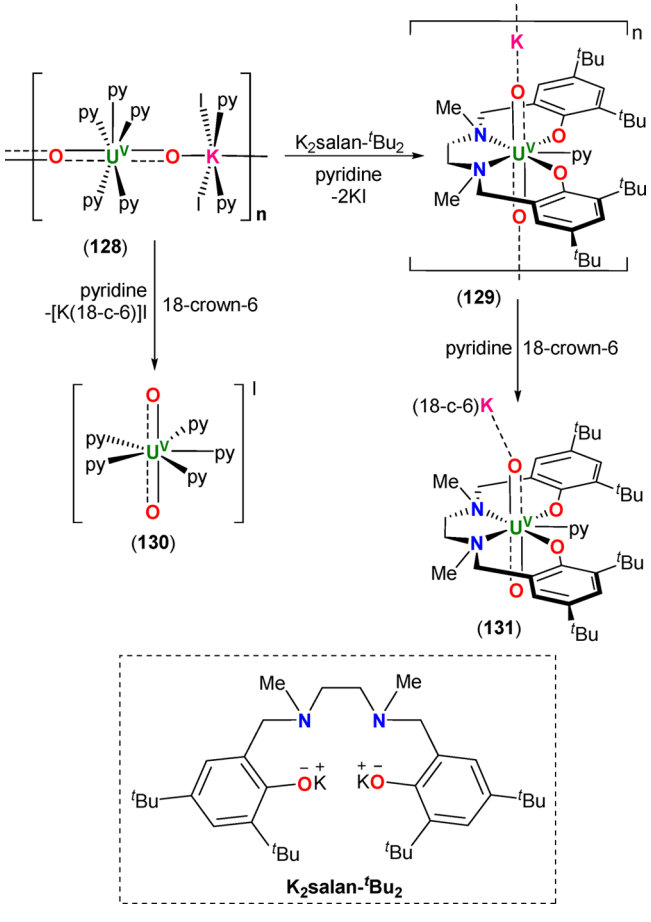

Scheme 23. Synthesis of $\{K[U^VO_2(salophen\text{-}^tBu_2)(py)]\}_n$ (134-py) from $[\{U^VO_2(py)_5\}\{KI_2(py)_2\}]_n$ (128) and K_2salophen-^{t}Bu$_2$ in Pyridine[a]

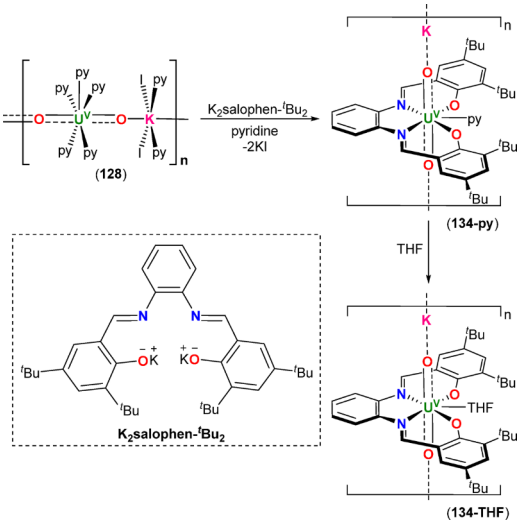

[a]Dissolving **134-py** in THF provides $\{K[U^VO_2(salophen\text{-}^tBu_2)(THF)]\}_n$ (**134-THF**). The K_2salophen-^{t}Bu$_2$ ligand is depicted in the bottom left corner of the scheme.[81]

DOI: 10.1021/acs.chemrev.9b00048
Chem. Rev. XXXX, XXX, XXX−XXX

Scheme 24. Synthesis of $[K(18\text{-c-}6)]_2[K_2\{U^VO_2(salen)\}_4]$ (135) and $[K(R)]_2[K_2\{U^VO_2(acecen)\}_4]$ (R = 18-c-6 (136), 2.2.2-cryptand (137)) from $[\{U^VO_2(py)_5\}\{KI_2(py)_2\}]_n$ (128) and K_2salen/2 equiv of 18-c-6 or K_2acacen/2 equiv of 18-c-6/2.2.2-cryptand, respectively[a]

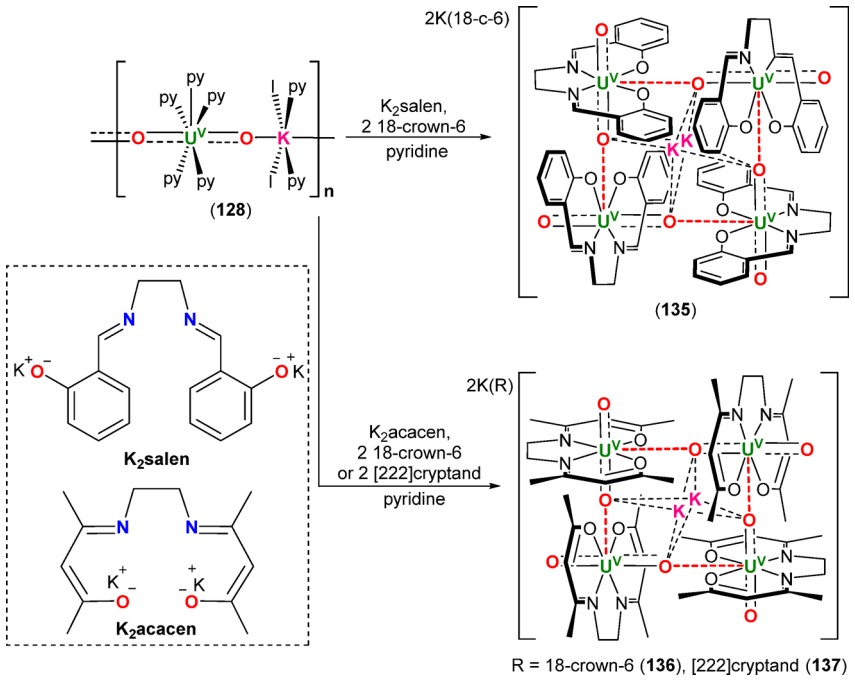

[a]The K_2salen and K_2acecen ligands are depicted in the bottom left corner of the scheme.[78]

spectroscopy, electrochemistry, and magnetic properties of complexes **129**−**131**, **133**, and **134-py** were studied in detail but are beyond the scope of this review.[81]

Complexes **129**−**132** and **134-THF** possess U−O bond lengths that range from 1.846(9)−1.868(2) Å, which are in the expected range for uranyl(V) compounds, and maintain near linear O−U−O bond angles, which range from 177.14(8)−178.7(4)°.[81]

$[\{U^VO_2(py)_5\}\{KI_2(py)_2\}]_n$ (**128**) reacts with K_2salen (H_2salen = *N*,*N*′-ethylene-bis(salicylideneimine), Scheme 24) in the presence of 18-c-6 to afford tetrameric $[K(18\text{-c-}6)]_2[K_2\{U^VO_2(salen)\}_4]$ (**135**), or with K_2acacen (H_2acacen = *N*,*N*′-ethylene-bis(acetylacetoneimine), Scheme 24) in the presence of either 18-c-6 or 2.2.2-cryptand to afford tetrameric $[K(R)]_2[K_2\{U^VO_2(acecen)\}_4]$ (R = 18-c-6 (**136**), 2.2.2-cryptand (**137**); Scheme 24). While both reactions were successful with respect to retaining the U^V oxidation state within the final product (i.e., stable with respect to disproportionation), the final products evaded isolation in the absence of 18-c-6 or 2.2.2-cryptand due to the formation of either polymeric or highly soluble species. Each U^V center possesses pentagonal bipyramidal geometry, coordinated by the N_2O_2 ligand donor set in the equatorial plane with the fifth coordination site occupied by an oxo group of a neighboring uranyl(V) ion, forming a T-shaped coordination geometry through oxo-bridging. The formation of the uranyl(V) tetramers **135**−**137** demonstrates the propensity for uranyl(V) to participate in oxo-bridging, the strength of which was highlighted by Pulsed-Field Gradient Stimulated Echo (PFGSTE) diffusion NMR spectroscopy in pyridine, in which calculating the Stokes radius of **135** and **137** relative to $[U^{VI}O_2(salophen)(py)]$ (**138**, used as an external reference) indicated that the tetrametallic motif was maintained in pyridine solution. In addition, complexes **135**−**137** are stable with respect to disproportionation.[78]

While **128** reacts cleanly with K_2salophen (H_2salophen = *N*,*N*′-phenylene-bis(salicylideneimine), Scheme 25) that has been pretreated with 18-c-6 to afford $[K(18\text{-c-}6)]_2[K_2(KI)_2\{U^VO_2(salophen)\}_4]$ (**138**), it undergoes rapid

Scheme 25. Synthesis of $[K(18\text{-c-}6)]_2[K_2(KI)_2\{U^VO_2(salophen)\}_4]$ (138) from $[\{U^VO_2(py)_5\}\{KI_2(py)_2\}]_n$ (128) and K_2salophen/18-c-6[a]

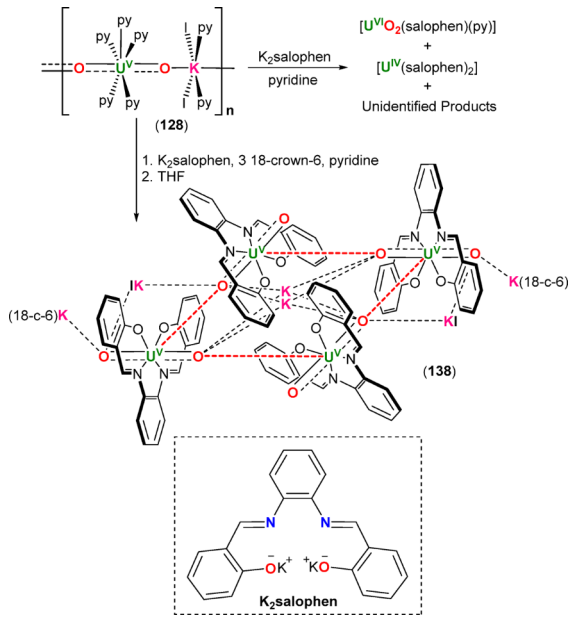

[a]The K_2salophen ligand is depicted at the bottom of the Scheme.[78]

DOI: 10.1021/acs.chemrev.9b00048
Chem. Rev. XXXX, XXX, XXX−XXX

Scheme 26. Synthesis of $[Cp^*_2Co][\{U^{VI}O_2(salen)\}\{U^{V}O_2(salen)(py)\}]$ (143), $[Rb(18\text{-c-}6)]_2[Rb_2\{U^{V}O_2(salen)\}_4]$ (141), and $[K(18\text{-c-}6)]_2[K_2\{U^{V}O_2(salen)\}_4]$ (135) from $[Cp^*_2Co][U^{V}O_2(salen)(py)]$ (140)[a]

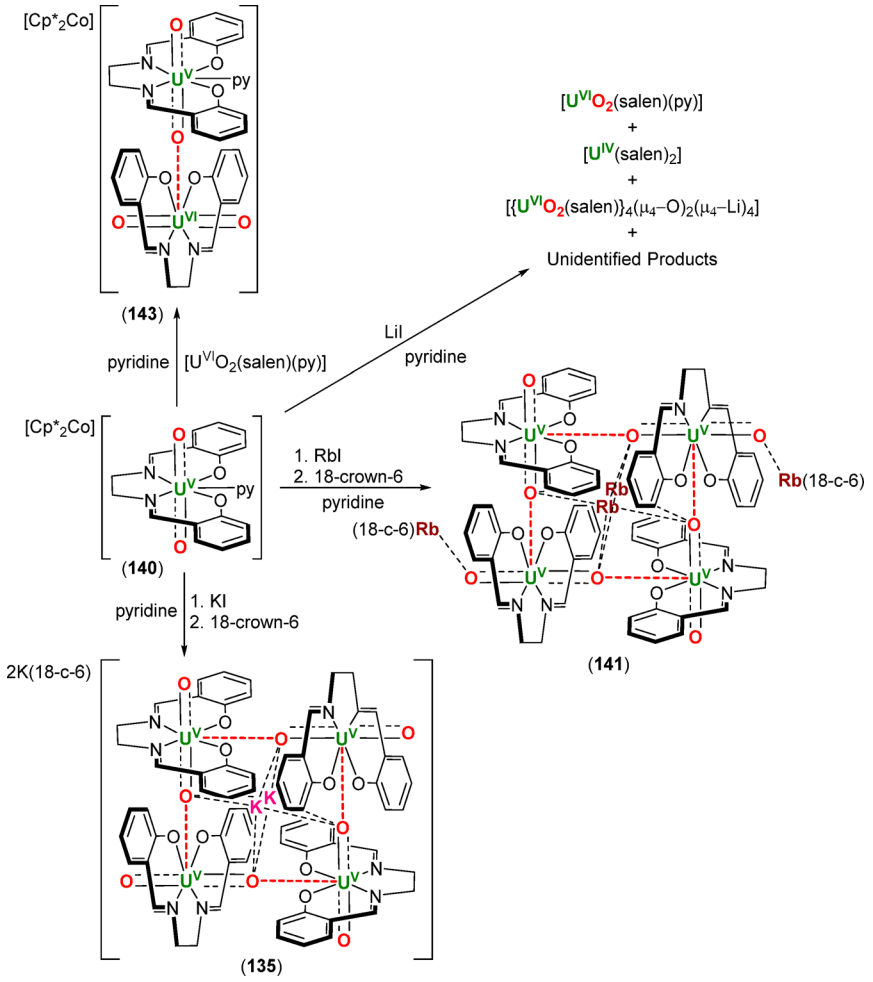

[a]**140** also reacts with LiI in pyridine to give a mixture of disproportionation products.[78]

disproportionation when reacted with K_2salophen in the absence of 18-c-6 (Scheme 25). This reactivity is remarkable given the similarities between the K_2salophen, K_2salen, and K_2acacen ligands. That said, once isolated, complex **138** is stable toward disproportionation for up to 30 days when redissolved in pyridine but undergoes complete disproportionation in 2 days in the presence of an excess of KI with respect to 18-crown-6 (0.1 equiv) in pyridine. **138** was recrystallized as $[K(18\text{-c-}6)(THF)_2][\{U^{V}O_2(salophen)\}_4(\mu_8\text{-}K)_2(\mu_5\text{-}KI)_2]I_2$ from THF and exists as a tetrameric structure with T-shaped coordination with respect to the uranyl(V) dimer similarly to complexes **135**–**137**. However, conversely to complexes **135**–**137**, PGFSTE diffusion NMR spectroscopy indicated that **138** exists as a monomer in pyridine. Complex **138** may also be prepared from $[Cp^*_2Co][U^{V}O_2(salophen)(py)]$ (**139**; synthesized from $[CoCp^*_2]$ and $[U^{VI}O_2(salophen)(py)]$) and K(18-c-6)I; adding KI to a pyridine solution of **139** results in rapid disproportionation.[78]

Complexes **136**–**138** possess uranyl(V) U–O bond lengths that range from 1.77(1)–1.973(9) Å, with the nonbridging U–oxo bond that is pointing away from the center of the tetramer significantly contracted relative to the bridging U–oxo bond (1.77(1)–1.871(4) Å vs 1.91(1)–1.973(9) Å, respectively). In addition, the bridging U–O bond lengths within the $[U^{V}O_2]^+\cdots[U^{V}O_2]^+$ units range from 2.344(9)–2.404(3) Å. In addition, 2 K^+ ions reside in the center of each tetramer and are coordinated to each of the *endo*-oxygen atoms and remain bound to the uranyl oxo groups even in the presence of excess 18-c-6 or 2.2.2-cryptand. It is therefore clear that potassium plays a key role in the formation of complexes **136**–**138** and their resulting structural integrity. The presence of coordinating K^+ cations also has an electronic effect in which the uranyl(V) center is stabilized against oxidation by decreasing the amount of negative charge on the uranyl oxygen atoms. To gain further insight into the importance of K^+ coordination with respect to other alkali metal cations, $[Cp^*_2Co][U^{V}O_2(salen)(py)]$ (**140**) was reacted with LiI, KI, and RbI in the presence of 18-c-6 (Scheme 27). **140** reacts with KI/18-c-6 and RbI/18-c-6 to afford tetrameric **135** and $[Rb(18\text{-c-}6)]_2[Rb_2\{U^{V}O_2(salen)\}_4]$ (**141**), respectively, which do not display any differences with respect to their reactivity/stability; both complexes are stable in pyridine with respect to disproportionation. However, **140** reacts with LiI/18-c-6 to afford a mixture of disproportionation products (Scheme 26). The difference in reactivity between Li^+, K^+ and Rb^+ may be attributed to the smaller size of Li^+, as well as its higher ratio of charge/ionic radius compared to K^+ and Rb^+.[78]

DOI: 10.1021/acs.chemrev.9b00048
Chem. Rev. XXXX, XXX, XXX–XXX

140 also reacts with 1 equiv of $[U^{VI}O_2(salen)(py)]$ (**142**) to yield the mixed-valence $[U^{V}O_2]^{+}/[U^{VI}O_2]^{2+}$ complex, $[Cp^*_2Co][\{U^{VI}O_2(salen)\}\{U^{V}O_2(salen)(py)\}]$ (**143**). The U−O bond lengths for the U^{VI} center in **143** (1.79(1), 1.80(1) Å) are shorter than those for the U^{V} center (1.82(1), 1.93(1) Å), indicating that the valence of each U center is localized. Each U center is pentagonal bipyramidal, with the axial coordination sites occupied by the U−oxo groups and 4 of the equatorial coordination sites occupied by the salen ligand. In terms of the U^{V} center, the fifth equatorial coordination site is occupied by pyridine, whereas for the U^{VI} center is occupied by a uranyl(V) oxo group; the uranyl(VI) and uranyl(V) ions in **143** participate in a T-shaped CCI similarly to complexes **135**−**138**.[78]

DFT studies on the mechanism of disproportionation of uranyl(V) in **135** in aqueous solution suggest that the protonation of a cation−cation intermediate is followed by electron transfer that occurs to yield uranyl(VI), U^{IV} aqua complexes, and water.[5] This was supported experimentally, in which **135** was reacted with 1 equiv of [HPy]Cl per uranium to immediately afford the disproportionation products $[U^{VI}O_2(salen)(py)]$ (**142**), $[U^{IV}(salen)_2]$ (**144**), and $[U^{IV}Cl_2(salen)]$ (**145**) in a ratio of 6:2:3 (Scheme 27; H_2O was also detected by ^1H NMR spectroscopy). The important role played by protons in this mechanism is highlighted and confirms that protonation of one uranyl oxygen atom to form a better leaving group is a key step, given that the U^{IV} disproportionation products no longer contain oxo ligands.[78]

Scheme 27. $[K(18\text{-c-}6)]_2[K_2\{U^{V}O_2(salen)\}_4]$ (135) Reacts with [HPy]Cl To Afford a Mixture of Disproportionation Products[78]

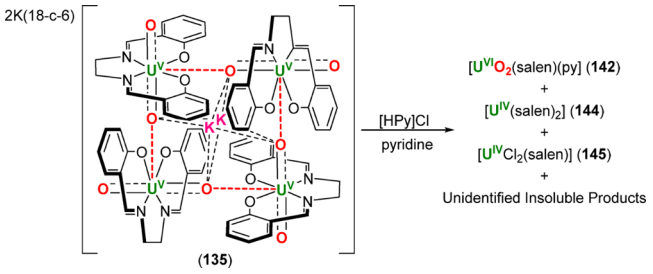

The tetranuclear complexes **135**−**137** give rise to well-resolved bands at 960 nm ($\varepsilon \sim 200$ L mol^{-1} cm^{-1}) in their respective UV−vis−NIR spectra in pyridine. In contrast, **129** and **138** (*vide supra*) give rise to large, poorly resolved bands in the region of 800−1000 nm ($\varepsilon \sim 200$ L mol^{-1} cm^{-1}). These spectral differences could arise from the differences in symmetry between the two types of structures and could prove useful for detecting the presence of oxo-clusters in solution.[78]

The reactivity of $[Cp^*_2Co][U^{V}O_2(salen)(py)]$ (**140**) with $[CaCl_2(dme)]$ and $Mn(NO_3)_2$ has also been investigated. Complex **140** reacts with $[CaCl_2(dme)]$ in a 2:1 ratio to provide tetrameric $[Ca_2\{U^{V}O_2(salen)\}_4]$ (**146**) and $[Cp^*_2Co]Cl$ as a reaction byproduct. Complex **146** is structurally analogous to complexes **135**−**137** and **141**, albeit with Ca^{2+} cations in the center of the tetramer and no cations on the periphery (Scheme 28). The U−O bond lengths in **146** range from 1.79(1)−1.96(1) Å, in which the bridging U^{V}−O bond is elongated relative to the terminal oxo. The O−U−O bond angles are 174.6(5) and 177.1(7)°, and the U···O bond distances between the bridging uranyl(V) oxo groups and U^{V} centers are 2.32(1) and 2.37(1) Å.[82]

Scheme 28. Synthesis of $[Ca_2\{U^{V}O_2(salen)\}_4]$ (146) and $[\{Mn^{II}(py)_3\}_6\{U^{V}O_2(salen)\}_{12}]$ (147) from $[Cp^*_2Co][U^{V}O_2(salen)(py)]$ (140) and $[CaCl_2(dme)]$ and $Mn(NO_3)_2$, respectively.[82]

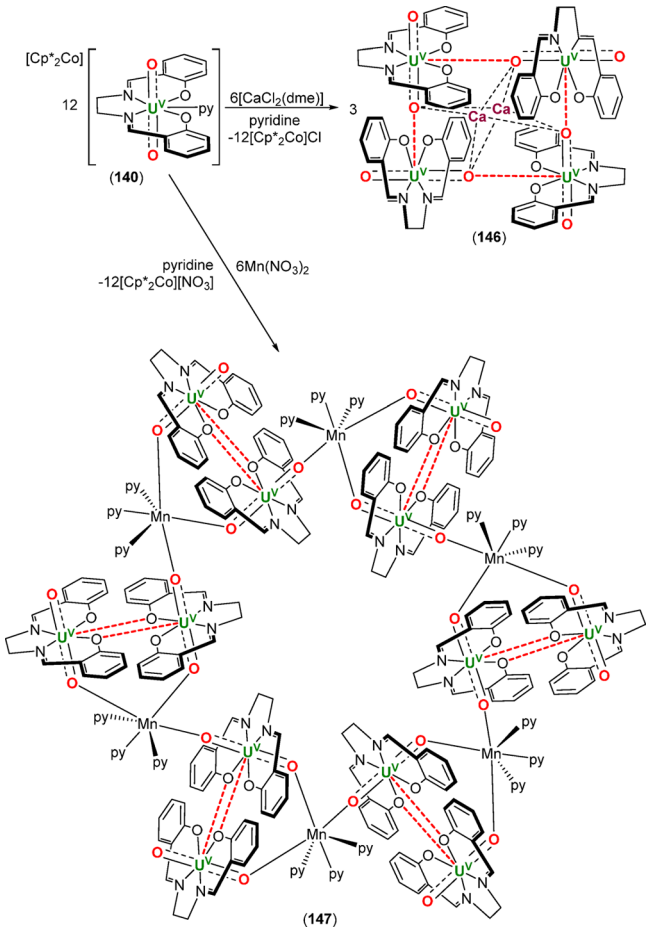

Compound **140** also reacts with $Mn(NO_3)_2$ in a 2:1 ratio, in this case to form the molecular wheel-shaped $[\{Mn^{II}(py)_3\}_6\{U^{V}O_2(salen)\}_{12}]$ (**147**), along with $[Cp^*_2Co][NO_3]$ as a reaction byproduct (Scheme 28). Complex **147** is held together by CCIs between the uranyl(V) oxo groups and the Mn^{II} ions, as opposed to the U^{V} center of a neighboring uranyl(V) ion, as is the case in complexes **135**−**137**, **141**, and **146** (*vide supra*). Six of the uranyl(V) ions in **147** form Mn-oxo-bridges through both uranyl oxo atoms, whereas the other six form bridges through just one oxo ligand. The U−O bond lengths range from 1.79(2)−1.90(2) Å, the O−U−O bond angles range from 169.9(6)−176.5(9)°, and the Mn···$O_{bridging}$ distances range from 2.12(2)−2.18(2) Å. The structural motif seen in **147** is likely a consequence of the 2:1 $[U^{V}O_2]^{+}$:$[Mn^{II}]^{2+}$ ratio, the 2+ charge of the Mn^{II} ion, and the preference of Mn^{II} to adopt an octahedral coordination geometry. As a result, the $[U^{V}O_2]^{+}$···Mn^{II} interactions in **147** play a structure-directing role. The magnetic properties of complexes **146** and **147** have also been studied.[82]

Polymeric $[U^{V}O_2(Mesaldien)K]_n$ (Mesaldien = *N*,*N*′-(2-aminomethyl)diethylenebis(salicylideneimine); **148**) can be obtained from the K_2Mesaldien and **128** and possesses U−O bond lengths ranging from 1.79(2)−1.86(2) Å, indicating that the U^{V} oxidation state is maintained. Complex **148** (6 equiv)

DOI: 10.1021/acs.chemrev.9b00048
Chem. Rev. XXXX, XXX, XXX−XXX

reacts with $[U^{IV}I_4(OEt_2)_2]$ (3 equiv) in the presence of K_2Mesaldien (3 equiv) in pyridine to afford tetrameric $\{[\{U^{V}O_2(\text{Mesaldien})\}\{U^{IV}(\text{Mesaldien})\}]_2(\mu\text{-O})\}$ (**149**) along with uranyl(VI) and $[U^{VI}O_2(\text{Mesaldien})]$ (**150**), from partial disproportionation (Scheme 29). Complex **149** is made

Scheme 29. Synthesis of $\{[\{U^{V}O_2(\text{Mesaldien})\}\{U^{IV}(\text{Mesaldien})\}]_2(\mu\text{-O})\}$ (149) and $[U^{VI}O_2(\text{Mesaldien})]$ (150) from $[U^{V}O_2(\text{Mesaldien})K]_n$ (148), K_2Mesaldien, and $[U^{IV}I_4(OEt_2)_2]$[a]

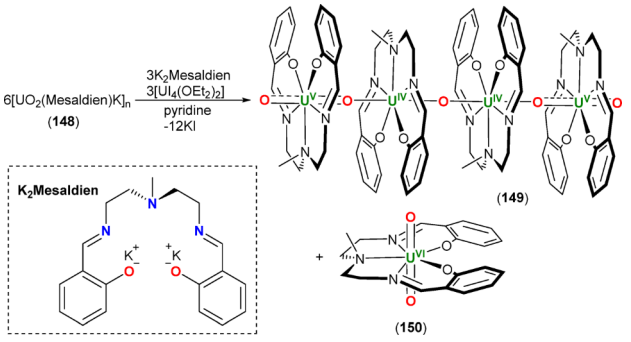

[a]The K_2Mesaldien ligand is depicted in the bottom left corner of the scheme.[50]

up of two uranyl(V)-Mesaldien/U^{IV}-Mesaldien units connected by a bridging oxo ligand. The U−O bond lengths in the uranyl(V) fragment are 1.82(1) and 2.00(1) Å, and the O−U−O unit retains its linearity (176.5(6)°).[50]

Complex **128** also reacts with the KL^{nacnac} ligand (KL^{nacnac} = 2-(4-tolyl)-1,3-bis(quinolyl)malondiiminate) in pyridine to afford the uranyl(V) trimer, $[U^{V}O_2(L^{nacnac})]_3$ (**151**; Scheme 30). Each U^{V} center possesses pentagonal bipyramidal geometry, coordinated by one equivalent of the tetradentate β-diketiminate ligand in the equatorial plane with the fifth coordination site occupied by an oxo group of a neighboring

Scheme 30. Synthesis of $[U^{V}O_2(L^{nacnac})]_3$ (151) from KL^{nacnac} and $[\{U^{V}O_2(py)_5\}\{KI_2(py)_2\}]_n$ (128). 151 Reacts Further with CH_2Cl_2 or Dry O_2 To Afford $[U^{VI}O_2Cl(L^{nacnac})]$ (152) and $[\{U^{VI}O_2(L^{nacnac})\}_2(\mu\text{-O})]$ (153), respectively[51]

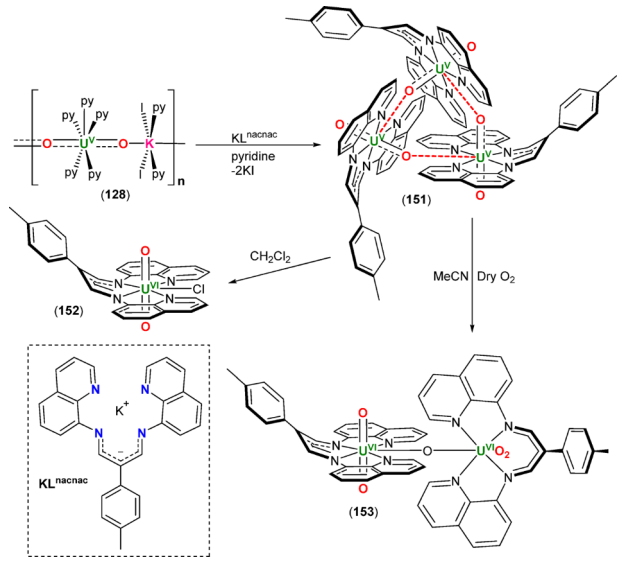

uranyl(V) ion. PFGSTE diffusion NMR spectroscopy in pyridine indicated that the trimetallic motif is maintained in solution. However, dissolution of **151** into DMSO does result in partial dissociation of the trimer.[51]

The U−O bond lengths in **151** range from 1.84(1)−1.940(8) Å, and the O−U−O bond angles range from 176.4(3)−176.7(4)°. Complex **151** reacts with oxidizing agents, forming uranyl(VI) $[U^{VI}O_2Cl(L^{nacnac})]$ (**152**) when dissolved in CH_2Cl_2 through chloride abstraction from the solvent, or $[\{U^{VI}O_2(L^{nacnac})\}_2(\mu\text{-O})]$ (**153**) when treated with dry O_2 in acetonitrile (Scheme 30). The U−O bond lengths range from 1.757(9)−1.82(1) Å in **152** and **153**, with the shorter of these in agreement with $U^{V} \rightarrow U^{VI}$ oxidation, although those around 1.8 Å are remarkably long for a formal U^{VI} oxidation state and the oxo-group reactions of these complexes may warrant further study.[51]

A series of trimetallic 3*d*-5*f* and 4*d*-5*f* complexes featuring the uranyl(V) ion, $[U^{V}O_2]^{+}$, have also been prepared to target single molecule magnetism in uranyl(V)-containing complexes, given its highly anisotropic nature and potential for magnetic exchange through metal−O−U^{V} linkages.[83−85]

$[U^{V}O_2(\text{Mesaldien})K]_n$ (**148**) reacts with 2 equiv of a 3*d*- or 4*d*-metal complex of the tetradentate tris(pyridyl)amine ligand, TPA (TPA = tris(2-pyridylmethyl)amine), to afford the trimetallic M^{II}−$OU^{V}O$−M^{II} complexes, $[\{U^{V}O_2(\text{Mesaldien})\}\{M^{II}X(TPA)\}_2]X$ (M = Fe, X = Cl (**154**); M = Mn, X = I (**155**); M = Cd, X = I (**156**); Scheme 31). Treatment of **148** with 1 equiv of $[Co^{II}I_2(TPA)]$ affords bimetallic $[\{U^{V}O_2(\text{Mesaldien})\}\{Co^{II}(TPA)\}]I$ (**157**, Scheme 31).[83−85]

Scheme 31. Synthesis of M^{II}−$OU^{V}O$−M^{II} and Co^{II}−$OU^{V}O$ Complexes, $[\{U^{V}O_2(\text{Mesaldien})\}\{M^{II}X(TPA)\}_2]X$ (M = Fe, X = Cl (154); M = Mn, X = I (155); M = Cd, X = I (156)) and $[\{U^{V}O_2(\text{Mesaldien})\}\{Co^{II}(TPA)\}]I$ (157), featuring uranyl(V).[83−85a]

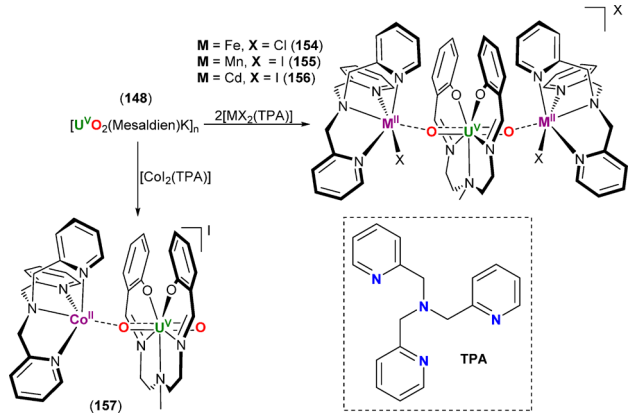

[a]The TPA ligand is depicted in the bottom right corner of the scheme.

Trimetallic M^{II}−$OU^{V}O$−M^{II} complexes may also be obtained from polymeric $[U^{V}O_2(\text{Mesaldien})K]_n$ and 2 equiv of $[M^{II}I(BPPA)]$ (BPPA = bis(2-picolyl)(2-oxybenzyl)amine), affording $[\{M^{II}(BPPA)(L)\}\{U^{V}O_2(\text{Mesaldien})\}\{M^{II}(BPPA)(py)\}]X$ (M = Ni, L = py (**158**); M = Fe, L = py (**159**); M = Co, L = vacant coordination site (**160**); Scheme 32).[83,85]

Alternatively, the uranyl(V) complex $[Cp^{*}_2Co][U^{V}O_2(salen)(py)]$ (**140**) reacts with the simple 3*d* or 4*d* metal precursors $M^{II}(NO_3)_2$ to yield polymeric

DOI: 10.1021/acs.chemrev.9b00048
Chem. Rev. XXXX, XXX, XXX−XXX

Scheme 32. Synthesis of $M^{II}-OU^{V}O-M^{II}$ Complexes, $[\{M^{II}(BPPA)(L)\}\{U^{V}O_2(Mesaldien)\}\{M^{II}(BPPA)(py)\}]I$ (M = Ni, L = py (158); M = Fe, L = py (159); M = Co, L = Vacant Coordination Site (160)), Featuring Uranyl(V)[83,85a]

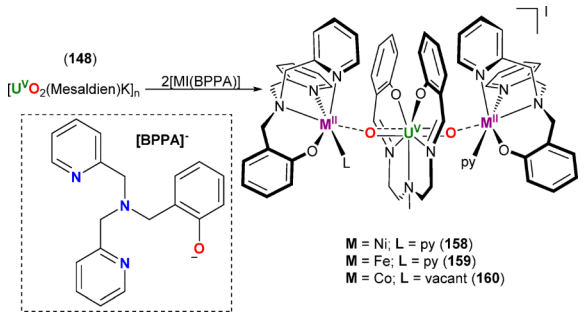

[a]The $[BPPA]^-$ ligand is depicted in the bottom left corner of the scheme.

$[\{U^{V}O_2(salen)(py)\}\{M^{II}(py)_4\}(NO_3)]_n$ (M = Cd (**161**); M = Mn (**162**); Scheme 33),[86] while $[Cp^*_2Co][U^{V}O_2(Mesaldien)]$

Scheme 33. Synthesis of Polymeric $M^{II}-OU^{V}O$ Complexes, $[\{U^{V}O_2(salen)(py)\}\{M^{II}(py)_4\}(NO_3)]_n$ (M = Cd (161); M = Mn (162)), of Uranyl(V)[86]

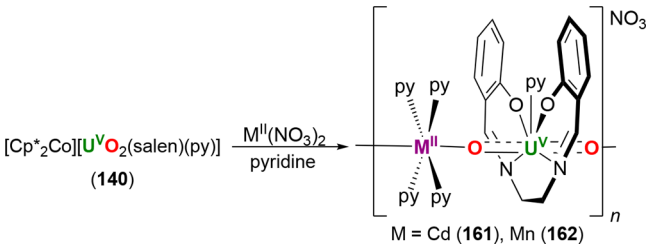

(**163**) reacts with $[Mn^{II}(NO_3)_2(py)_2]$ to afford polymeric $\{[U^{V}O_2(Mesaldien)][Mn^{II}(NO_3)(py)_2]\}_n$ (**164**).[87] Complexes **154**–**161** and **164** all contain the uranyl(V) ion with U–O bond lengths and O–U–O bond angles ranging from 1.837(3)–1.934(3) Å and 171.6(2)–178.7(5)°, respectively, and possess bridging $M^{II}-O-U^{V}-O-M^{II}$ interactions between cationic M^{II} and anionic U^{V} fragments.[83−87]

It has also been shown that the dipotassium salt of a ferrocene-based tetradentate Schiff-base ligand, K_2salfen-^{t}Bu$_2$, reacts with $[\{U^{V}O_2(py)_5\}\{KI_2(py)_2\}]_n$ (**128**) to afford $[\{K(18\text{-c-}6)\}U^{V}O_2(salfen\text{-}^t Bu_2)]$ (**165**, Scheme 34), which possesses U–O and $U-O_K$ bond lengths of 1.831(4)/1.838(4)

Scheme 34. Synthesis of $[\{K(18\text{-c-}6)\}U^{V}O_2(salfen\text{-}^t Bu_2)]$ (165) from $[\{U^{V}O_2(py)_5\}\{KI_2(py)_2\}]_n$ (128) and K_2salfen-^{t}Bu$_2$[52]

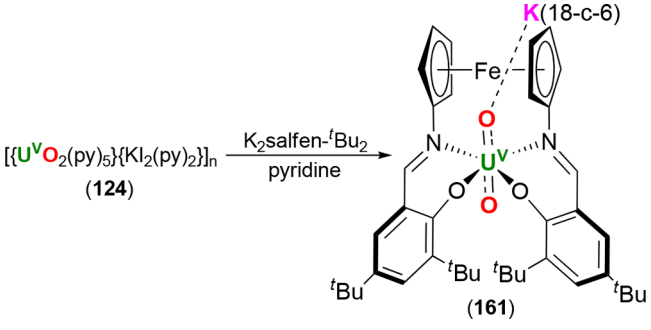

and 1.853(4)/1.860(4) Å, respectively, and O–U–O bond angle of 176.8(2)/177.5(2)° for two crystallographically independent molecules within the unit cell. K_2salfen-^{t}Bu$_2$ also reacts with $[U^{VI}O_2I_2(py)_3]$ (**166-py**) to yield $[U^{VI}O_2(salfen\text{-}^t Bu_2)]$ (**167**). If the less bulky K_2salfen (in which the *tert*-butyl groups are replaced with hydrogen atoms) is used, a mixture of U(IV) and $[U^{VI}O_2]^{2+}$ species are formed over 12 h through disproportionation of a transiently formed uranyl(V) species.[52]

$[\{U^{V}O_2(py)_5\}\{KI_2(py)_2\}]_n$ (**128**) also reacts with K_2dpaea in the presence of 2.2.2-cryptand in pyridine to yield the uranyl(V) complex, $[K(2.2.2\text{-crypt})][U^{V}O_2(dpaea)]$ (**168**; Scheme 35). Uranyl(V) **168** possesses a O–U–O bond

Scheme 35. Synthesis of $[K(2.2.2\text{-crypt})][U^{V}O_2(dpaea)]$ (168) from $[\{U^{V}O_2(py)_5\}\{KI_2(py)_2\}]_n$ (128), K_2dpaea, and 2.2.2-Cryptand[a]

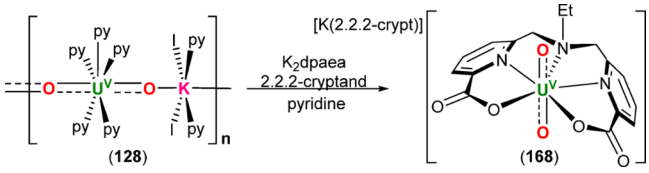

[a]See Scheme 20 in section 3 for a depiction of H_2dpaea.[48]

angle of 176.06(8)°, U–O bond lengths of 1.837(2) and 1.847(2) Å, and an asymmetric stretching frequency of 794 cm^{-1}. Complex **168** is stable in aprotic solvents for up to 4 months, or until the addition of 1 equiv of [HPy]OTf (in DMSO), which results in disproportionation; X-ray quality crystals of the U^{IV} species, $[U^{IV}(dpaea)_2]$ (**169**), were isolated from this reaction. Analogously to $[Cp^*_2Co][U^{V}O_2(dpaea)]$ (**122**), introduced in section 3, once isolated, **168** is stable against disproportionation when dissolved in D_2O. Complex **168** (7–15 mM, pH = 9.2–10) is in fact stable in D_2O for up to 2 weeks but slowly begins to precipitate from solution after this point. Small amounts of the disproportionation products begin to appear after 5 days in D_2O (16 mM of **168**, pH = 7) and more than 80% of **168** has undergone disproportionation after 2 days in 20 mM D_2O solutions at pH = 6. These results indicate that **168** is stable in aqueous solutions with a pH between 7 and 10 and that acid-induced disproportionation of **168** occurs rapidly in organic solutions in the presence of stoichiometric amounts of a proton source. CV studies on **168** indicate that the U^{VI}/U^{V} redox couple ($E_{1/2}$ = −1.25 V vs Fc/Fc^+) is reversible in pyridine but irreversible in aqueous solution (0.02 M HEPES buffered water solution, pH = 7; U^{V}/U^{VI} oxidation occurs at E = −0.16 to 0.00 V vs Ag/AgCl, U^{VI}/U^{V} reduction occurs at E = −1.56 to −1.65 V vs Ag/AgCl); the U^{V}/U^{IV} redox couple is not observed in aqueous solution. The different electrochemical behavior of **168** in pyridine versus aqueous solution has been attributed to $U-OH_2$ binding and/or the potential for proton exchange reactions to occur.[48]

$[\{U^{V}O_2(py)_5\}\{KI_2(py)_2\}]_n$ (**128**) also reacts with K_3trensal (H_3trensal = 2,2′,2′′-tris(salicylideneimino)triethylamine), to afford $K[U^{V}O_2(trensal)K]$ (**170**, Scheme 36a). Treating **170** with 2.2.2-cryptand allows for isolation of $[K(2.2.2\text{-cryptand})]_2[U^{V}O_2(trensal)]$ (**171**), in which one of the U–oxo groups is coordinated to a K^+ cation (Scheme 36b; U–O = 1.82(2) Å, $U-O_K$ = 1.87(2) Å). Alternatively, **170** reacts with 1 or 1.5 equiv of FeI_2 in pyridine to substitute the K^+ cation for a coordinated Fe^{II} fragment to afford $[U^{V}O_2(trensal)Fe^{II}(py)_3]$

DOI: 10.1021/acs.chemrev.9b00048
Chem. Rev. XXXX, XXX, XXX−XXX

Scheme 36. Synthesis of (a) K[$U^{V}O_2$(trensal)K] (170) from [{$U^{V}O_2$(py)$_5$}{KI_2(py)$_2$}]$_n$ (128) and K_3trensal, Followed by Conversion into (b) [K(2.2.2-crypt)]$_2$[$U^{V}O_2$(trensal)] (171), (c) [$U^{V}O_2$(trensal)Fe^{II}(py)$_3$] (172), (d) [{$U^{V}O_2$(trensal)Fe^{II}(py)$_3$}$_2$$Fe^{II}(py)_3$]$I_2$ (173), and (e) [$U^{V}O_2$(trensal)Fe^{II}(py)$_3U^{IV}$(trensal)]I (174) by Treatment with 2.2.2-cryptand, 1 and 1.5 equiv of FeI_2, and 1 equiv of [U^{IV}(trensal)], Respectively[66]

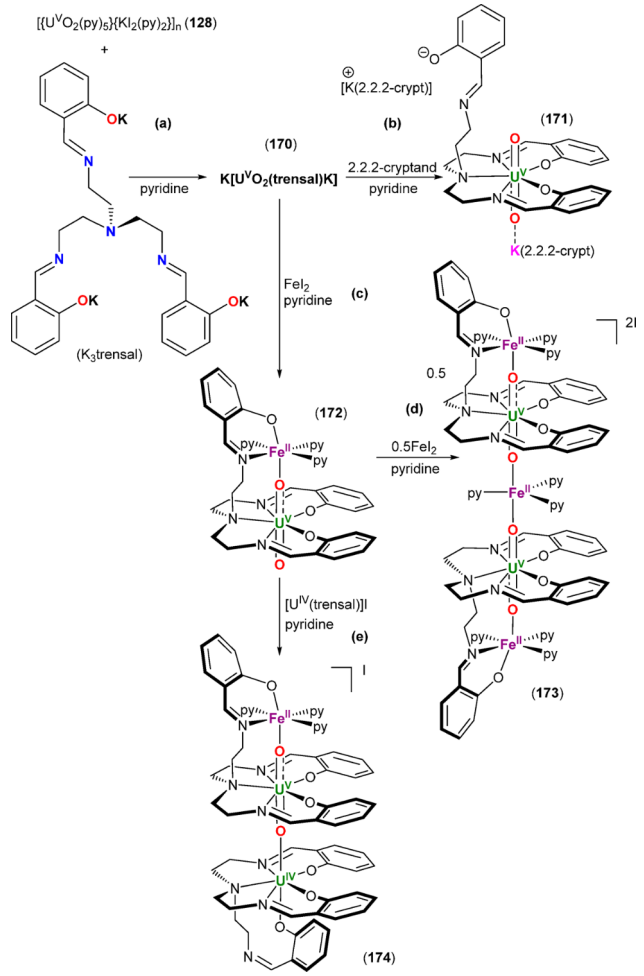

(**172**; U−O = 1.837(3) Å, U−O_{Fe} = 1.930(2) Å) and 0.5 equiv of [{$U^{V}O_2$(trensal)Fe^{II}(py)$_3$}$_2$$Fe^{II}(py)_3$]$I_2$ (**173**; U−O = 1.920(4)−1.935(4) Å), respectively (Scheme 36c and 36d). Both complexes **172** and **173** possess contracted U−O bond lengths at the unfunctionalized oxo group compared with the functionalized oxo group. Complex **170** also reacts with [U^{IV}(trensal)]I to afford [$U^{V}O_2$(trensal)Fe^{II}(py)$_3U^{IV}$(trensal)]I (**174**; Scheme 36e), which possesses a contracted Fe^{II}-functionalized U−O bond length (1.922(6) Å) relative to the U^{IV}-functionalized U−O group (1.960(6) Å). Complexes **171**−**174** possess O−U−O bond angles that range from 173.7(6)−177.2(2)°. Remarkably, complexes **172**−**174**, which exhibit Fe^{II} functionalization of a uranyl-oxo group, demonstrate increased stability with respect to proton-induced disproportionation. Complex **172** reacts with 2 equiv of pyridinium chloride ([HPy]Cl) to afford **174**, a product of partial disproportionation which possesses a Fe^{II}−[$OU^{V}O$]$^{+}$−U^{IV} core, whereas complexes **170** and **171** react with 2 equiv of [HPy]Cl to yield U^{IV} and [$U^{VI}O_2$]$^{2+}$ complexes via complete disproportionation. Furthermore, redox reactivity and CV experiments display an increased range of stability for the uranyl(V) species functionalized by Fe^{II} with respect to both oxidation and reduction reactions. As Fe^{II}-containing minerals are known to participate in [$U^{VI}O_2$]$^{2+}$ reduction and stabilization of uranyl(V) species with its exact role remaining ambiguous, these results shed light on the function of iron in the environmental mineral-mediated reduction of U^{VI}.[66]

While [{$U^{V}O_2$(py)$_5$}{KI_2(py)$_2$}]$_n$ (**128**) has been used as an effective starting uranyl(V) complex for further oxo-functionalization while maintaining the uranyl(V) oxidation state, it has been demonstrated to undergo immediate disproportionation in the presence of benzoic acid in pyridine, forming the hexanuclear U^{IV}-benzoate cluster, [$U^{IV}_6O_4$(OH)$_4$(PhCOO)$_{12}$(py)$_3$] (**175**), and the uranyl(VI) complex, [$U^{VI}O_2$(PhCOO)$_2$(py)$_2$] (**176**). Water, pyridinium iodide, and KI are formed as byproducts during this reaction.[53]

The synthesis of [U^{V}O{OAlR_2(py)}(H_2L^{Me})] (R = Me (**87**), ^{i}Bu (**88**); Scheme 16 in Section 3) from the uranyl(VI) Pacman complex **11-py** and [$Cp_2TiCl(CH_2)(AlMe_2)$] and $HAl^{i}Bu_2$, respectively, was discussed previously in section 3. The oxo-coordinated -AlR_2 group in **87** or **88** is readily replaced by Group 1 metal cations by treatment with alkyl lithium reagents (MeLi, $(Me_3Si)_2CHLi$, Me_3SiCH_2Li) in C_6D_6 to provide [{($OU^{V}O$)Li(py)(H_2L^{Me})}$_2$] (**177**; Scheme 37a).

Scheme 37. Transmetalation of the Oxo-Coordinated -AlR_2 Group with Group 1 Metal Cations Using Either Alkyl Lithium Reagents Affording (a) [{($OU^{V}O$)Li(py)(H_2L^{Me})}$_2$] (177) or Group 1 Metal Hydrides Providing (b) [U^{V}O{OLi(py)$_3$}(py){{Li(py)}$_2L^{Me}$}] (63-py) and (c) [U^{V}O{OM(py)$_3$}(py)(H_2L^{Me})] (M = Na (178), K (179)). Addition of Pyridine to 177 Provides (d) [U^{V}O{OLi(py)$_3$}(py)(H_2L^{Me})] (180)[73]

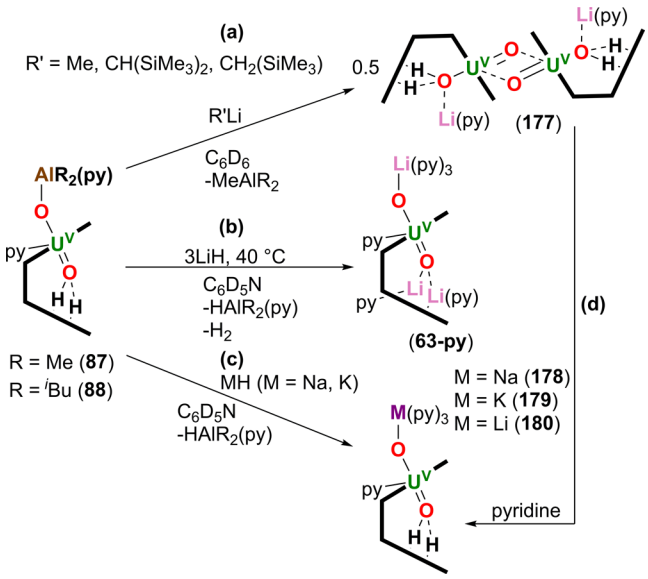

Alternatively, **87** and **88** react with LiH in pyridine to afford a trilithiated complex, [U^{V}O{OLi(py)$_3$}(py){{Li(py)}$_2L^{Me}$}] (**60-py**; Scheme 37b and Scheme 9 in Section 3) or with NaH or KH in pyridine to provide [U^{V}O{OM(py)$_3$}(py)(H_2L^{Me})] (M = Na (**178**), K (**179**); Scheme 37c). Furthermore, **177** may be converted into [U^{V}O{OLi(py)$_3$}(py)(H_2L^{Me})] (**180**) through the addition of pyridine (Scheme 37d).[73] This reactivity contrasts that of the

DOI: 10.1021/acs.chemrev.9b00048
Chem. Rev. XXXX, XXX, XXX−XXX

uranyl(VI) complex **11-py**, in which deprotonation of the acidic pyrrole NH groups[35] occurs instead of transmetalation of the oxo-coordinated functional group, suggesting that hydrogen-bonding between the uranyl *endo*-oxo group and the pyrrole protons is significant enough to negate deprotonation.[73]

Interestingly, this clean substitution of the AlR_2 group has enabled the development of a one-pot, DIBAL-catalyzed reduction of the U(VI) uranyl complexes to all three monoalkali metal uranyl(V) complexes **178**−**180** (Scheme 38). This DIBAL-catalyzed route could also have applications in *d*-block metal oxo chemistry.[73]

Scheme 38. Complexes 178−180 May Be Prepared Catalytically from $HAl(^iBu)_2$ (10 mol %) and Excess MH (M = Li, Na, K) in Toluene (70 °C, 3−4 days)[73]

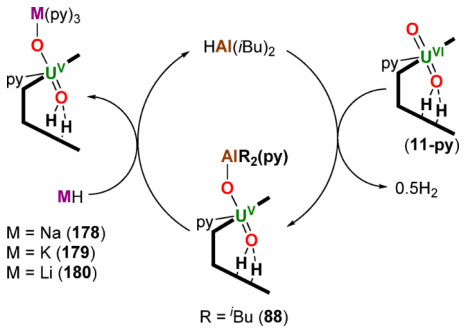

The structural data (U−O and O−X bond lengths, O−U−O and U−O−X bond angles; X = oxo-functionalizing unit) determined by single crystal X-ray diffraction and characteristic spectroscopic data (OUO vibrational stretching frequency) determined by FTIR or Raman spectroscopies for the functionalized uranyl(V) complexes reported since 2010 and discussed in Section 4 (*vide supra*) are provided in Table 4, and their trends are discussed in more detail in Section 7 (*vide infra*).

5. $U^{VI} \rightarrow U^{IV}$ REDUCTIVE FUNCTIONALIZATION

The treatment of the trianionic pyridine(diamine) uranium(IV) complexes $[Cp^*U^{IV}(^{Mes}PDI^{Me})(L)]$ ($^{Mes}PDI^{Me}$ = 2,6-((Mes)N=CMe)$_2$C$_5$H$_3$N; L = THF or $(Me_2N)_3PO$) and $[Cp^*U^{IV}(^tBu\text{-}^{Mes}PDI^{Me})(THF)]$ ($^tBu\text{-}^{Mes}PDI^{Me}$ = 2,6-((Mes)N=CMe)$_2$-*p*-C(CH$_3$)$_3$C$_5$H$_3$N) with *N*-methylmorpholine-*N*-oxide affords the uranyl(VI) complexes $[Cp^*U^{VI}O_2(^{Mes}PDI^{Me})]$ (**181**) and $[Cp^*U^{VI}O_2(^tBu\text{-}^{Mes}PDI^{Me})]$ (**182**), which are best described as containing uranyl(VI) supported by a singly reduced pyridine(diamine) ligand. Treatment of **181** or **182** with 2 equiv of Me_3SiI results in $U^{VI} \rightarrow U^{IV}$ reduction and silylation of both oxo ligands, forming $[U^{IV}I_2(OSiMe_3)_2(^{Mes}PDI^{Me})]$ (**183**) and $[U^{IV}I_2(OSiMe_3)_2(^tBu\text{-}^{Mes}PDI^{Me})]$ (**184**), respectively (Scheme 39).[54]

Only complex **183** was crystallographically characterized, and in the solid-state the U^{IV} center possesses pentagonal bipyramidal geometry with the *trans*-trimethylsiloxy ligands occupying the axial coordination sites. The formation of **183** was thought to progress from **181** via a U^V intermediate, which was identified as $[U^VOI(OSiMe_3)(^{Mes}PDI^{Me})]$ (**185**) by ^{1}H NMR and IR spectroscopy. Intermediate **185** is the product of homolytic cleavage of the U−Cp* bond with concomitant Me_3Si−I addition across one of the U=O bonds; its presence

Scheme 39. $U^{VI} \rightarrow U^{IV}$ Reductive Silylation of $[Cp^*U^{VI}O_2(^{Mes}PDI^{Me})]$ (181) with Me_3SiI, Affording $[U^{IV}I_2(OSiMe_3)_2(^{Mes}PDI^{Me})]$ (183) *via* Intermediate $[U^VOI(OSiMe_3)(^{Mes}PDI^{Me})]$ (185)[54]

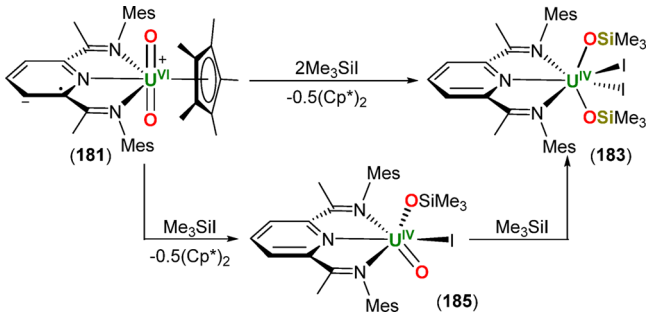

during the formation of **179** was verified by electronic absorption spectroscopy of the reaction solution. The formation of **184** is thought to proceed via an analogous intermediate.[54]

The scope of the reductive silylation of **181** using Me_3SiI was expanded to other silanes via a reductive functionalization strategy that entailed the addition of a Lewis base to generate the silylium ion, [base-SiR_3][X]. It was envisaged that the more electrophilic silylium ion would facilitate uranyl functionalization, and while previously the addition of Ph_3Si−Cl or Me_3Si-SPh to **181** did not result in a reaction and the addition of Me_3Si-Cl or Me_3Si-OTf yielded intractable mixtures, the introduction of 2 equiv of Ph_3P=O into the reaction mixtures resulted in complete conversion into $[(R_3SiO)_2U^{IV}X_2(OPPh_3)_2]$ (R = Ph, X = Cl (**186**); R = Me, X = SPh (**187**); R = Me, X = Cl (**188**); R = Me, X = I (**189**); R = Me, X = OTf (**190**); Scheme 40). The more sterically

Scheme 40. $U^{VI} \rightarrow U^{IV}$ Reductive Silylation of $[Cp^*U^{VI}O_2(^{Mes}PDI^{Me})]$ (181), Providing $[(R_3SiO)_2U^{IV}X_2(OPPh_3)_2]$ (R = Ph, X = Cl (186); R = Me, X = SPh (187); R = Me, X = Cl (188); R = Me, X = I (189); R = Me, X = OTf (190)).[88]

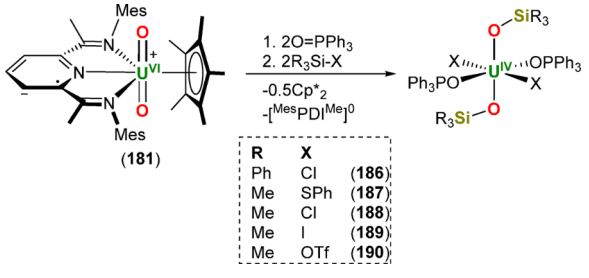

encumbered $^iPr_3Si$-Cl remained unreactive with **181**, which was attributed to the inability of O=PPh_3 to undertake nucleophilic attack at Si.[88,89] The reducing electrons for the two electron reduction of the U^{VI} center in **181** originate from the redox-active pyridine(diamine) ligand and from homolytic cleavage of the U−Cp* bond, forming $[^{Mes}PDI^{Me}]^0$ and Cp^*_2 as byproducts.[54]

The reductive functionalization of the simple uranyl(VI) compound $[U^{VI}O_2Cl_2(OPPh_3)_2]$ (**191**) has also been explored. Salt metathesis using M-R alkylating reagents (M-R = KCH_2Ph, ^{n}BuLi, MCH_2SiMe_3; M = Li, Na, K) forms the corresponding U^{VI} (dialkyl) complexes which undergo reductive elimination of the alkyl coligands upon addition of

DOI: 10.1021/acs.chemrev.9b00048
Chem. Rev. XXXX, XXX, XXX−XXX

R_3Si-X halosilanes across the U=O bond. The reductive elimination of alkane provides the two reducing electrons requisite for $U^{VI} \rightarrow U^{IV}$ reduction. Alkylation of **191** with 2 equiv of $NaCH_2SiMe_3$, followed by the addition of R_3Si-Cl, provided $[(R_3SiO)_2U^{IV}Cl_2(OPPh_3)_2]$ (R = Ph (**186**), Me (**188**), Et (**192**) or H (**193**); Scheme 41) in high yields. The use of this protocol with Me_2PhSi-Cl, $MePh_2Si$-Cl, Ph_2HSi-Cl, and Me_3Si-SPh also provided the desired U^{IV} bis(siloxide) products, $[(Me_3SiO)_2U^{IV}(SPh)_2(OPPh_3)_2]$ (**187**) and $[(R_3SiO)_2U^{IV}Cl_2(OPPh_3)_2]$ (R_3Si = Me_2PhSi (**194**), $MePh_2Si$ (**195**), and Ph_2HSi (**196**); Scheme 41). The same method was also applied to different uranyl and silyl starting materials, in particular, $[U^{VI}O_2X_2(OPPh_3)_2]$ (X = Br (**197**), I (**198**)) and $[U^{VI}O_2(OTf)_2(2,2'\text{-bipy})_2]$ (**199**), and Me_3Si-X (X = Br, I, OTf) which successfully generated the corresponding U^{IV} bis(siloxide) products, $[(Me_3SiO)U^{IV}Br_2(OPPh_3)]$ (**200**), $[(Me_3SiO)U^{IV}I_2(OPPh_3)]$ (**189**) and $[(Me_3SiO)$-$U^{IV}(OTf)_2(2,2'\text{-bipy})_2]$ (**201**), respectively (Scheme 41); the halide coligands incorporated with the uranyl starting materials were matched with the R_3Si-X halide to avoid halide scrambling.[89]

Cationic uranyl(VI) complexes have been studied in reductive silylation chemistry as they should be susceptible to reduction at more positive reduction potentials. However, treatment of the cationic uranyl(VI) complex $[U^{VI}O_2(dppmo)_2(OTf)][OTf]$ (**202**; dppmo = $Ph_2P(O)$-$CH_2P(O)PPh_2$) with 2 equiv of Ph_3SiOTf did not result in a reaction, which is likely due to the decrease in nucleophilicity of the uranyl oxo-ligands. In contrast, the addition of 2 equiv of $[CoCp_2]$ and 4 equiv of Ph_3SiOTf to **202** afforded $[U^{IV}(OTf)_4(dppmo)]$ (**203**), likely through initial $U^{VI} \rightarrow U^{V}$ reduction to render the uranyl oxo-groups more nucleophilic and susceptible to silylation. The formation of **203** proceeds through a U^{IV} bis(siloxide) intermediate, detected by ^1H NMR spectroscopy, and $[U^{IV}(OSiPh_3)(OTf)_2(dppmo)_2][OTf]$ (**204**), which was characterized crystallographically. **204** is the product of $U^{VI} \rightarrow U^{IV}$ reduction and oxo-group silylation followed by oxo-group abstraction; 2 equiv of $[Cp_2Co][OTf]$ and $Ph_3SiOSiPh_3$ were detected as byproducts during the formation of **204** (Scheme 42).[90]

It was recently demonstrated that the monoanionic, tetradentate dipyrrin ligand, L′ (Scheme 43) acts as a ligand for uranyl(VI) and that treatment with either inner- or outer-sphere reductants leads to different, and reagent-dependent, degrees of reduction of the complex. Treatment of $[U^{VI}O_2\{N(SiMe_3)_2\}_2(THF)_2]$ (**2-THF**) with HL′ followed by [HPy]Cl provided $[U^{VI}O_2Cl(L')]$ (**205**; Scheme 43). Alternatively, **205** may be obtained by treating HL′ with 0.5 equiv of **2-THF** and 0.5 equiv of $[U^{VI}O_2Cl_2(THF)_2]$ (**4-THF**; Scheme 43). Complex **205** reacts with the inner-sphere reductant, $[Cp_2TiCl]_2$, to yield the uranium(IV) complex $[U^{IV}(OTiClCp_2)_2(Cl)(L')]$ (**206**) which is the product of $U^{VI} \rightarrow U^{IV}$ reduction and titanation of each of the uranyl oxo groups (Scheme 44a). Attempts to react **205** with 0.5 equiv of $[Cp_2TiCl]_2$ to cleanly isolate the U^{V} analogue of **206**, $[U^{V}O(OTiClCp_2)(Cl)(L')]$ (**207**), were unsuccessful, as **207** slowly disproportionates into **205** and **206** over time. **205** reacts with a substoichiometric amount (0.95 equiv) of the outer-sphere reductant, $[CoCp_2]$, to provide $[CoCp_2]$-$[U^{VI}O_2Cl(L')]$ (**208**) which, based on EPR and NMR spectroscopy and X-ray crystallography, is best described as a ligand-centered radical of the uranyl(VI) ion (Scheme 44b). Despite CV data suggesting that $[CoCp_2]$ is reducing enough

Scheme 41. $U^{VI} \rightarrow U^{IV}$ Reductive Silylation of $[U^{VI}O_2X_2(OPPh_3)_2]$ (191, 197, 198) and $[U^{VI}O_2(OTf)_2(2,2'\text{-bipy})_2]$ (199): by (1) Alkylation Followed by (2) Bis(alkyl) Reductive Elimination and U−O Silylation, Forming $[(R_3SiO)U^{IV}X_2(OPPh_3)]$ (186−189, 192−196, 200) and $[(Me_3SiO)U^{IV}(OTf)_2(2,2'\text{-bipy})_2]$ (201)[89]

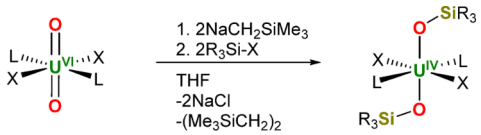

R_3Si	X	L	
Ph_3Si	Cl	$O=PPh_3$	(**186**)
Me_3Si	SPh	$O=PPh_3$	(**187**)
Me_3Si	Cl	$O=PPh_3$	(**188**)
Me_3Si	I	$O=PPh_3$	(**189**)
Et_3Si	Cl	$O=PPh_3$	(**192**)
H_3Si	Cl	$O=PPh_3$	(**193**)
Me_2PhSi	Cl	$O=PPh_3$	(**194**)
$MePh_2Si$	Cl	$O=PPh_3$	(**195**)
Ph_2HSi	Cl	$O=PPh_3$	(**196**)
Me_3Si	Br	$O=PPh_3$	(**200**)
Me_3Si	OTf	2,2′-bipy	(**201**)

Scheme 43. Synthesis of a Dipyrrin-Coordinated Uranyl(VI) Complex, $[U^{VI}O_2Cl(L')]$ (205).[55]

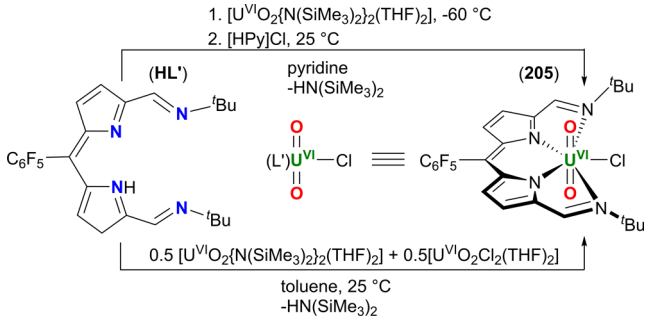

Scheme 42. $U^{VI} \rightarrow U^{IV}$ Reductive Silylation of Cationic $[U^{VI}O_2(OTf)(dppmo)][OTf]$ (202) Resulting in Oxo-Group Silylation and Abstraction, Yielding $[U^{IV}(OSiPh_3)(OTf)_2(dppmo)_2][OTf]$ (204)[90]

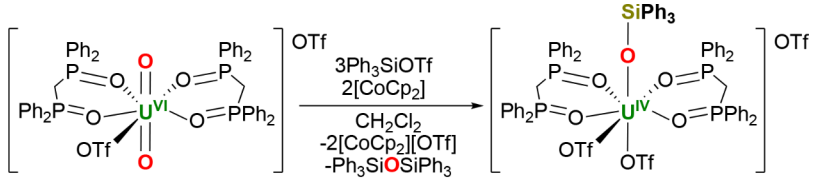

(**202**) (**204**)

DOI: 10.1021/acs.chemrev.9b00048
Chem. Rev. XXXX, XXX, XXX−XXX

Scheme 44. (a) $U^{VI} \rightarrow U^{IV}$ Reduction Observed upon Treating $[U^{VI}O_2Cl(L')]$ (205) with the Inner-Sphere Reductant, $[Cp_2TiCl]_2$, To Provide $[U^{IV}(OTiClCp_2)_2(Cl)(L')]$ (206) and (b) Ligand-Based Reduction Observed When Treating 205 with the Outer-Sphere Reductant, $[CoCp_2]$, To Provide $[CoCp_2][U^{VI}O_2Cl(L')]$ (208)[55]

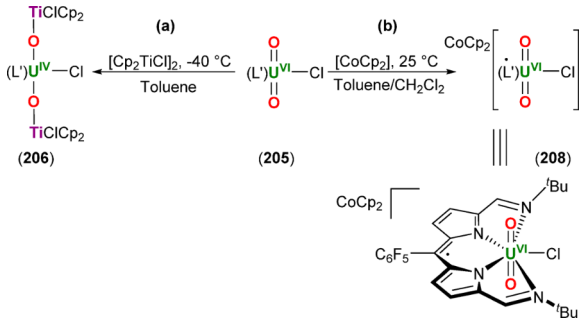

to access the reduced uranyl complex, $[CoCp_2]_2[U^VO_2(Cl)(L')]$, only the ligand-centered radical was observed.[55]

It is interesting to note that while $[Cp_2TiCl]_2$ and $[CoCp_2]$ possess similar reduction potentials, $U^{VI} \rightarrow U^{IV}$ reduction is seen when **205** reacts with the former (inner-sphere) reductant whereas ligand-based reduction is observed when **205** reacts with the latter (outer-sphere) reductant. It was determined by DFT calculations that in the case of the inner-sphere reductant, while the first reduction is ligand-based, coordination of the Lewis acidic Ti^{IV} ion to one of the uranyl oxo groups promotes electron transfer from the ligand to the U^{VI} center, resulting in $U^{VI} \rightarrow U^V$ reduction. The subsequent electron transfer and oxo group titanation step then occurs at the U center, resulting in $U^V \rightarrow U^{IV}$ reduction.[55]

When two uranyl(VI) ions are installed into the same ligand, facile reductive functionalization to uranium(IV) complexes is achieved using mild reducing agents such as boranes or silanes. $[\{U^{VI}O_2(py)\}_2(L^A)]$ (**209**), which is prepared from H_4L^A and 2.5 equiv of **2-THF** (H_4L^A = a Pacman-shaped macrocyclic Schiff-base ligand with ethyl substituents on the *meso*-carbon atoms and an anthracenyl hinge linking the N_4-donor pockets, Scheme 45), reacts with 2 equiv of B_2pin_2 or B_2cat_2 at 80 °C in pyridine to afford $[(py)(pinBO)U^{IV}OU^{IV}(OBpin)(py)(L^A)]$ (**210**) and $[(py)\{cat(py)BO\}U^{IV}OU^{IV}(OBcat)(py)(L^A)]$ (**211**), respectively (Scheme 45a). While complex **210** is isolated in 47% yield, **211** is only generated *in situ* or in small quantities (ca. 10 mg) and of reduced purity (ca. 90%) because it reacts with a third equiv of B_2cat_2 to ultimately yield $[(py)U^{IV}OU^{IV}(\mu\text{-}O_2C_6H_4)(L^A)]$ (**212**). Complex **209** also reacts with 10 equiv of HBpin or HBcat at 125 °C in pyridine to afford **210** and **211**/**212**, respectively. Alternatively, **209** reacts with excess Ph_2SiH_2 (15 equiv) in the presence of 0.25 equiv of MX salts (M = K, X = $N(SiMe_3)_2$ or O^{t}Bu; M = Li, X = $N(SiMe_3)_2$) at 125 °C in pyridine to afford the reductively silylated uranium(IV) complex $[(py)(HPh_2SiO)U^{IV}OU^{IV}(OSiPh_2H)(py)(L^A)]$ (**213**; Scheme 45b). Complexes **210**, **211**,, and **213** are the products of $U^{VI} \rightarrow U^{IV}$ reductive borylation or silylation, oxo-atom abstraction, and fusion of the former uranyl(VI) ions. Initial functionalization is thought to proceed through a U^V/U^V intermediate upon B−B or Si−H bond homolysis and borylation/silylation of the *exo*-oxo ligands. The ultimate $U^V \rightarrow U^{IV}$ reduction is anticipated to proceed through a second B−B or Si−H bond homolysis and

Scheme 45. (a) $U^{VI} \rightarrow U^{IV}$ Reductive Borylation of a Bis(uranyl(VI)) Complex $[\{U^{VI}O_2(py)\}_2(L^A)]$ (209) through Reaction with B_2pin_2 and B_2cat_2, Yielding $[(py)(pinBO)U^{IV}OU^{IV}(OBpin)(py)(L^A)]$ (210) and $[(py)\{cat(py)BO\}U^{IV}OU^{IV}(OBcat)(py)(L^A)]$ (211), and (b) $U^{VI} \rightarrow U^{IV}$ Reductive Silylation of 209 through Reaction with Ph_2SiH_2, Providing $[(py)(HPh_2SiO)U^{IV}OU^{IV}(OSiPh_2H)(py)(L^A)]$ (213)[a]

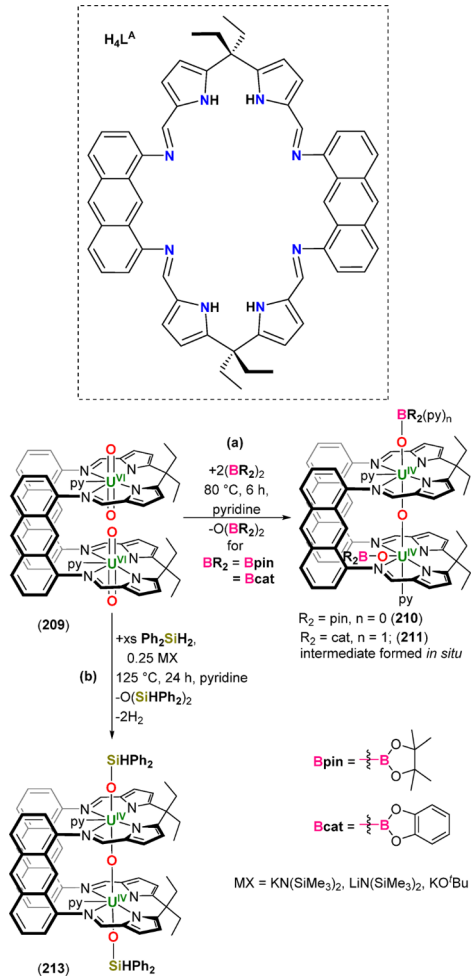

[a]The anthracenyl-Pacman ligand, H_4L^A, is depicted at the top of the scheme.[91]

attack at one of the *endo*-oxo-groups, resulting in loss of one of the *endo*-oxo-ligands and formation of $(R_2B)_2O$/$(HPh_2Si)_2O$.[91]

The structural data (U−O and O−X bond lengths, O−U−O and U−O−X bond angles; X = oxo-functionalizing unit) determined by single crystal X-ray diffraction and characteristic spectroscopic data (OUO vibrational stretching frequency) determined by FTIR or Raman spectroscopies for the reductively functionalized uranium(IV) dioxo complexes reported since 2010 and discussed in Section 5 (*vide supra*) are provided in Table 5, and their trends are discussed in more detail in Section 7 (*vide infra*).

6. $U^{VI} \rightarrow U^{IV}$ REDUCTIVE FUNCTIONALIZATION *VIA* CHARACTERIZED U(V) INTERMEDIATES

As discussed in Section 3, treating a uranyl(VI)−^{Ar}acnac complex (^{Ar}acnac = ArNC(Ph)CHC(Ph)O; Ar =

DOI: 10.1021/acs.chemrev.9b00048
Chem. Rev. XXXX, XXX, XXX−XXX

Scheme 46. (A) Monosilylation of an Oxo Group in $[U^{VI}O_2(^{Ar}acnac)_2]$ (54) by Treatment with $Ph_3SiH/B(C_6F_5)_3$, Providing $[U^{V}\{OB(C_6F_5)_3\}(OSiPh_3)(^{Ar}acnac)_2]$ (214), and Subsequent Reduction To Afford $[CoCp_2][U^{IV}\{OB(C_6F_5)_3\}(OSiPh_3)(^{Ar}acnac)_2]$ (215). (B) Disilylation of 54 using 2 equiv of Et_3SiH and 1 equiv of $B(C_6F_5)_3$, Providing $[U^{V}(OSiEt_3)_2(^{Ar}acnac)_2][HB(C_6F_5)_3]$ (216) and $[U^{V}\{OB(C_6F_5)_3\}(OSiEt_3)(^{Ar}acnac)_2]$ (217; Minor Component); 216 May Be Converted into 217 by Heating in Toluene at 85 °C for 24 h. 217 Reacts with $CoCp_2$ To Provide $[U^{IV}(OSiEt_3)_2(^{Ar}acnac)_2]$ (219)[93,94]

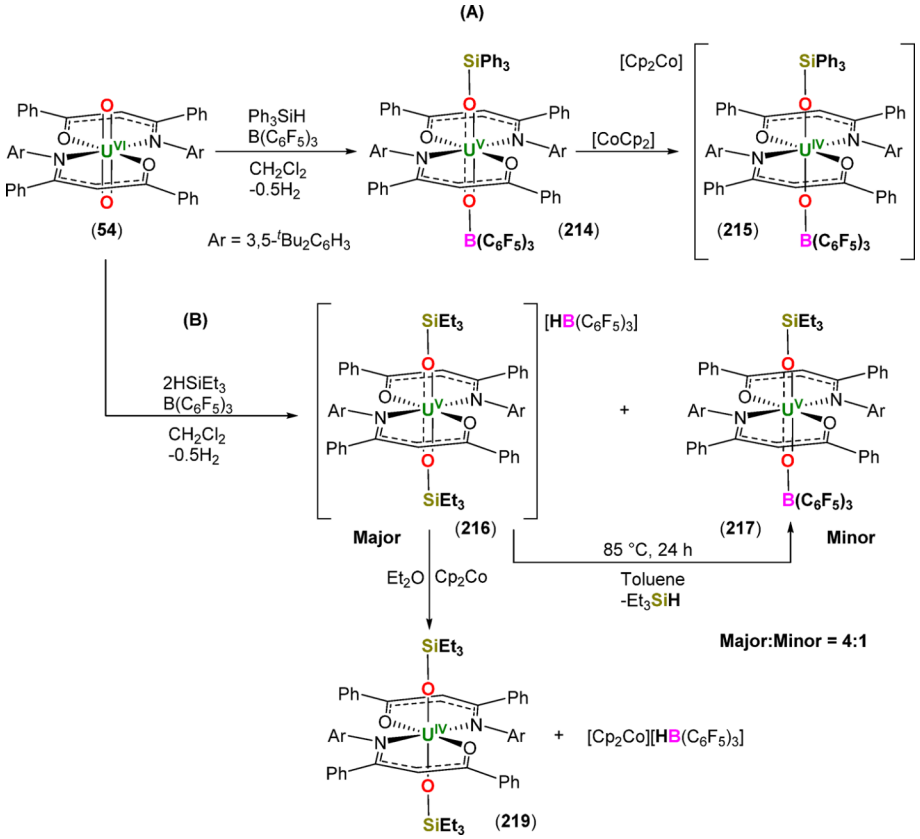

3,5-^{t}Bu$_2$C$_6$H$_3$) with either 2 equiv of Ph_3SiOTf or excess Me_3SiI results in $U^{VI} \rightarrow U^{V}$ reduction and silylation of the oxo groups. Attempts have been made to react the same uranyl(VI) starting complex, $[U^{VI}O_2(^{Ar}acnac)_2]$ (**54**), with Ph_3SiH, but no reaction occurs until $B(C_6F_5)_3$ is added to the reaction mixture, in which case $[U^{V}\{OB(C_6F_5)_3\}(OSiPh_3)(^{Ar}acnac)_2]$ (**214**; Scheme 46a) was formed. The addition of borane is thought to result in $Ph_3SiH \rightarrow B(C_6F_5)_3$ adduct formation, thus activating the silane and rendering it susceptible to nucleophilic attack by a uranyl oxo group. This hypothesis was verified by repeating the same reaction but with ^{i}Pr$_3$SiH, in which the sterically bulky iso-propyl substituents are known to disfavor $B(C_6F_5)_3$ coordination and activation, resulting in no reaction. Upon Ph_3Si^+ and $B(C_6F_5)_3$ coordination to the uranyl oxo ligands, $U^{VI} \rightarrow U^{V}$ reduction is facilitated by H^-, resulting in the formation of H_2. The CV indicated that an irreversible reduction feature was located at $E_{1/2}$ = −0.72 (vs Fc/Fc$^+$), which is shifted 0.49 V to a more positive reduction potential relative to $[Cp^*_2Co][U^{V}\{OB(C_6F_5)_3\}_2(^{Ar}acnac)_2]$ ($E_{1/2}$ = −1.21 V vs Fc/Fc$^+$)[92] and is attributed to coordination of the more Lewis acidic Ph_3Si^+ cation to one of the uranyl(V) oxo groups. Treating **214** with $[CoCp_2]$ resulted in the formation of $[Cp_2Co][U^{IV}\{OB(C_6F_5)_3\}(OSiPh_3)(^{Ar}acnac)_2]$ (**215**; Scheme 46a). The U−O bond lengths in **215** (U−O$_B$ = 2.056(8) Å, U−O$_{Si}$ = 2.173(8) Å) are elongated relative to those in **214** (U−O$_B$ = 1.941(8) Å, U−O$_{Si}$ = 2.034(9) Å), as expected for $[U^{IV}O_2]$ versus $[U^{V}O_2]^+$, and the O−U−O bond angles remain linear in both (175.3(3)° and 174.6(3)° in **215** and **214**, respectively). Attempts were made to oxidize **215** back to **54** using either I_2 or AgOTf but were unsuccessful.[93]

Alternatively, treating **54** with 2 equiv of Et_3SiH and 1 equiv of $B(C_6F_5)_3$ results in double silylation of the uranyl oxo groups, providing $[U^{V}(OSiEt_3)_2(^{Ar}acnac)_2][HB(C_6F_5)_3]$ (**216**) following $U^{VI} \rightarrow U^{V}$ reduction. During this reaction, $[U^{V}\{OB(C_6F_5)_3\}(OSiEt_3)(^{Ar}acnac)_2]$ (**217**) is formed as a minor product (**216**:**217** = 4:1) but can be isolated on a preparative scale either by heating **54** with equimolar quantities of Et_3SiH and $B(C_6F_5)_3$ or by heating **216** to 85 °C for 24 h in toluene (Scheme 46b). However, several unidentified decomposition products are observed when using the latter method. Complex **54** also reacts with 1 equiv of $Et_3SiH/B(C_6F_5)_3$ at room temperature to provide **216** and unreacted **54**. The formation of complexes **216** and **217** indicates that a $[U^{V}O_2]^+$-silylated intermediate, $[U^{V}O(OSiR_3)(^{Ar}acnac)_2]$ (R = Et, Ph), must be formed during the reaction. Furthermore, the silyl cation in $Et_3SiH \rightarrow B(C_6F_5)_3$ must be more prone to nucleophilic attack by the silylated-uranyl(V) oxo group and therefore reacts faster than uranyl → borane adduct formation compared to $Ph_3SiH \rightarrow B(C_6F_5)_3$, given that a doubly silylated product is isolated in the reaction involving the former reactive species while only a singly silylated product is isolated in the latter case.[94] A quasi-reversible redox couple was observed at −0.37 V (vs Fc/Fc$^+$) in the CV of **216**, which is shifted 0.35 and 0.84 V to a more positive reduction

DOI: 10.1021/acs.chemrev.9b00048
Chem. Rev. XXXX, XXX, XXX−XXX

potential relative to **214** and $[Cp^*_2Co][U^V\{OB(C_6F_5)_3\}_2(^{Ar}acnac)_2]$ (**218**), respectively, consistent with the positive charge on **216** versus the neutral and anionic charges on **214** and **218**, respectively. Complex **216** reacts with $[CoCp_2]$ to provide $[U^{IV}(OSiEt_3)(^{Ar}acnac)_2]$ (**219**), which possesses U−O bond lengths (2.129(2) Å) that are elongated relative to **216** (2.011(4), 2.013(4) Å) and **217** (2.017(6), 1.957(6) Å), and representative of a $[U^{IV}(OSiR_3)_2]^{2+}$ complex (Scheme 46b).[92,94]

The reductive silylation chemistry of uranyl(VI) of a *β*-ketoiminate ligand (i.e., acnac ligand) that possesses an *N*-bound *tert*-butyl substituent instead of an aryl substituent, $[U^{VI}O_2(^{tBu}acnac)_2]$ (**220**; ^{tBu}acnac = ^{t}Bu*N*C(Ph)CHC(Ph)*O*), has also been explored. In this case, treating **220** with excess Me_3SiI (10 equiv) in the presence of PPh_3 affords $[Ph_3PI][U^V(OSiMe_3)_2I_4]$ (**221**), in which both oxo groups of uranyl have been silylated, the U^{VI} center has undergone a one-electron reduction, and both ^{tBu}acnac ligands have been substituted for iodo ligands and converted into their silylated analogue, ^{tBu}acnacSiMe$_3$ (Scheme 47). The loss of both

Scheme 47. Treatment of $[U^{VI}O_2(^{tBu}acnac)_2]$ (220) with Excess Me_3SiI/PPh_3 Provides $[Ph_3PI][U^V(OSiMe_3)_2I_4]$ (221), the Addition of 2 equiv of Either 4,4′-Bipyridine (bipy) or 1,10-Phenanthroline (phen) to a Toluene Solution of 221 Affords $[U^{IV}(OSiMe_3)_2I_2(bipy)_2]$ (222) or $[U^{IV}(OSiMe_3)_2I_2(phen)_2]$ (223), Respectively, And the Addition of Excess THF Yields $[U^{IV}(OSiMe_3)_2I(THF)_4][I_3]$ (224)[57]

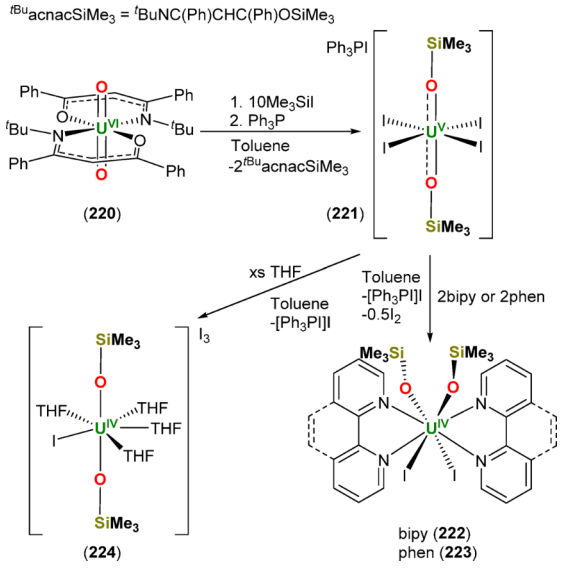

equivalents of ^{tBu}acnac ligand when treating **220** with excess Me_3SiI compared to only 1 equiv when ^{Ar}acnac is used (see Section 3, *vide supra*) has been attributed to the extra steric bulk imparted by the *tert*-butyl substituents, making ligand abstraction more facile. The formation of **221** is thought to proceed through the U^V intermediate, $[U^V(OSiMe_3)_2I_3]$, which is formed via $U^{VI} \rightarrow U^V$ reduction by I^- following Me_3Si^+ coordination to the uranyl oxo groups. The resulting I_2 reaction byproduct (0.5 equiv) then reacts with Ph_3P to provide $[Ph_3PI]I$, which is trapped by the proposed U^V intermediate. Due to the fact that only 0.5 equiv of I_2 is produced during this reaction, the maximum yield of **221** is 50%. When 2 equiv of either 4,4′-bipyridine (bipy) or 1,10-phenanthroline (phen) is added to a toluene solution of **221**, $[U^{IV}(OSiMe_3)_2I_2(bipy)_2]$ (**222**) or $[U^{IV}(OSiMe_3)_2I_2(phen)_2]$ (**223**) is obtained, respectively (Scheme 47). Alternatively, the addition of excess THF to a toluene solution of **221** provides $[U^{IV}(OSiMe_3)_2I(THF)_4][I_3]$ (**224**; Scheme 47). Compounds **222**−**224** are the product of $U^V \rightarrow U^{IV}$ reduction, which is thought to occur by I^- dissociation and oxidation to I_2. Complex **221** possesses U−O bond lengths of 1.990(6) and 1.976(8) Å, and complexes **222** and **224** possess U−O bond lengths that range from 2.065(6)−2.084(4) Å, which are representative of U^V and U^{IV} dioxo complexes, respectively. Complexes **221**−**224** are thermally unstable in solution, decomposing slowly to provide $(Me_3Si)_2O$ as a decomposition product.[57]

As was highlighted in Section 3, the macrocyclic Pacman ligand, H_4L^{Me}, or the mono(uranyl) Pacman complex **11-py** reacts with 2.5 equiv or 1.5 equiv of $[U^{VI}O_2\{N(SiMe_3)_2\}_2(py)_2]$ (**2-py**), respectively, to afford the doubly oxo-silylated bis(uranyl(V)) complex, $[\{U^VO(OSiMe_3)\}_2(L^{Me})]$ (**70**). Complex **70** may be further reduced with 2 equiv of K metal to afford $K_2[\{U^{IV}O(OSiMe_3)\}_2(L^{Me})]$ (**225**; Scheme 48), which was characterized by ^{1}H NMR, IR,

Scheme 48. Doubly Oxo-silylated $[\{U^VO(OSiMe_3)\}_2(L^{Me})]$ (70), Which May Be Obtained by Treating H_4L^{Me} with 2.5 equiv of $[U^{VI}O_2\{N(SiMe_3)_2\}_2(py)_2]$ (2-py), Reacts with 2 equiv of Potassium To Provide $K_2[\{U^{IV}O(OSiMe_3)_2\}_2(L^{Me})]$ (225). 225 Reacts with Either C_5H_5NO or 0.5 equiv of O_2 To Yield $[K(py)_3]_2[K(py)]_2[(U^VO_2)_2(L^{Me})]_2$ (19-py; see Section 2), and 70 May Be Regenerated by Treating 225 or 19 with I_2 or 2 equiv of Cl-SiMe$_3$, Respectively[38]

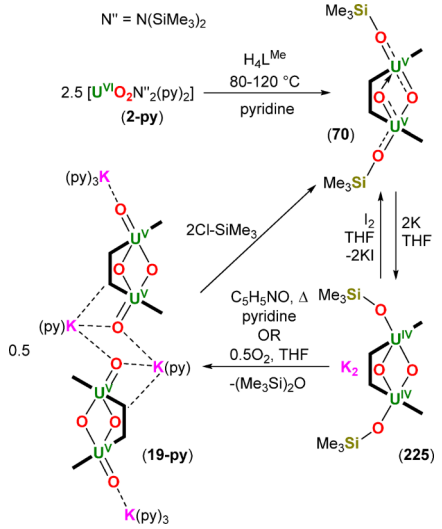

and UV/vis spectroscopies and elemental analysis. Complex **70** may be regenerated from **225** and I_2, producing KI as a reaction byproduct. Alternatively, **225** undergoes a double desilylation reaction with pyridine-*N*-oxide to afford $[K(py)_3]_2[K(py)]_2[(U^VO_2)_2(L^{Me})]_2$ (**19-py**) in pyridine or $\{K_2[(U^VO_2)_2(L^{Me})]\}_n$ (**19-THF**) in THF. Treating **19** with 2 equiv of Cl-SiMe$_3$ results in regeneration of **70** (Scheme 48). Complexes **19-py** and **19-THF** possess significantly more contracted U−O_{exo} bond lengths (1.851(5)−1.871(6) Å) relative to the U−O_{endo} bond lengths (2.077(5)−2.101(5) Å), indicating that they retain greater multiple bond character

DOI: 10.1021/acs.chemrev.9b00048
Chem. Rev. XXXX, XXX, XXX−XXX

and display appreciable air-sensitivity compared with the silyl-protected **70**.[38]

In addition to $U^{VI} \rightarrow U^{IV}$ reduction upon treating $[U^{VI}O_2Cl(L')]$ (**205**) with the inner-sphere reductant, $[Cp_2TiCl]_2$, as was highlighted in Section 5 (*vide supra*), complex **205** has been exploited to demonstrate the effects of axial and equatorial ligand manipulation on the reductive functionalization chemistry of the uranyl(VI) ion. Complex **205** reacts with 1 equiv of KNHAr (Ar = 2,6-^{i}Pr$_2$C$_6$H$_3$) to yield the U^V/U^V dimer $[U^VO_2(L')]_2$ (**226**; Scheme 49). The

Scheme 49. $U^{VI} \rightarrow U^V$ Reduction of $[U^{VI}O_2Cl(L')]$ (205) Using Either KNHAr (Ar = 2,6-^{i}Pr$_2$C$_6$H$_3$) or 2B(C$_6$F$_5$)$_3$/Hg to Provide $[U^VO_2(L')]_2$ (226) and $[U^V\{OB(C_6F_5)_3\}_2(L')]$ (228), respectively[a]

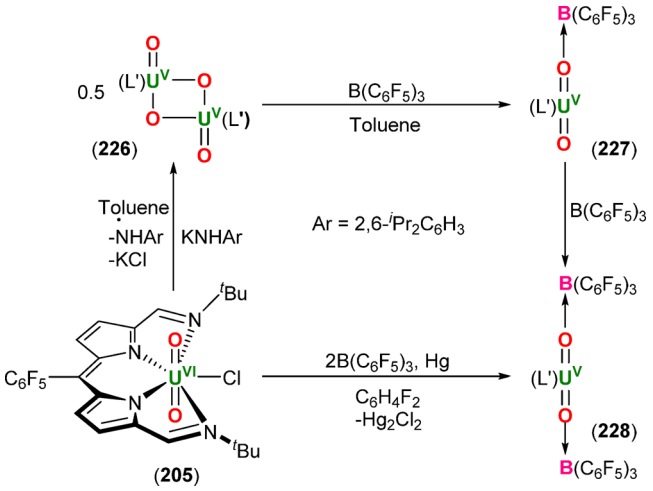

[a]**226** also reacts with 1 equiv of B(C$_6$F$_5$)$_3$ to afford $[U^VO\{OB(C_6F_5)_3\}(L')]$ (**227**).[58]

formation of **226** presumably proceeds through the unisolated anilido complex, $[U^{VI}O_2(NHAr)(L')]$, which then undergoes U−N bond homolysis. Complex **226** reacts with either 1 or 2 equiv of B(C$_6$F$_5$)$_3$ to afford singly or doubly oxo-functionalized $[U^VO\{OB(C_6F_5)_3\}(L')]$ (**227**) and $[U^V\{OB(C_6F_5)_3\}_2(L')]$ (**228**), respectively (Scheme 49). Complex **228** is also formed from the reaction of **205** with 2 equiv of B(C$_6$F$_5$)$_3$, resulting in loss of Cl$^\bullet$, but this reaction does not reach completion (even with heating in the presence of 8 equiv of B(C$_6$F$_5$)$_3$) unless elemental mercury is added, which enables the removal of the Cl$^\bullet$ byproduct in the form of solid Hg_2Cl_2 via reduction to Cl^- (Scheme 49). Complex **205** also reacts with Na[B{C$_6$H$_3$-3,5-(CF$_3$)$_2$}$_4$] to yield the cationic uranyl(VI) complex, $[U^{VI}O_2(L')][B\{C_6H_3\text{-}3,5\text{-}(CF_3)_2\}_4]$ (**229**), and with AgOTf to form $[U^{VI}O_2(OTf)(L')]$ (**230**).[58]

In this system, the sequential addition of borane to coordinate to the uranyl(V) ion shifts the $U^V \rightarrow U^{IV}$ reduction potential stepwise from −1.14 V vs Fc/Fc$^+$ for **226** to −0.78 V for **227** and then −0.49 V for **228**, enabling the use of very mild reducing agents to achieve $U^V \rightarrow U^{IV}$ reduction. As such, **228** is reduced by [FeCp*$_2$] (E_{red} = −0.56 V vs Fc/Fc$^+$) to yield the anionic uranium(IV) complex $[FeCp^*_2][U^{IV}\{OB(C_6F_5)_3\}_2(L')]$ (**231**), and also by H_2 (E_{red} = −0.54 V vs Fc/Fc$^+$) to provide $[U^{IV}\{OB(C_6F_5)_3\}\{OB(C_6F_5)_2\}(L')]$ (**232**). In this latter case, one of the B−C bonds of one of the oxo-coordinated B(C$_6$F$_5$)$_3$ groups is cleaved, producing C$_6$F$_5$H as a byproduct and converting the oxo-coordinated B-ligand from a neutral borane to an anionic boroxy ligand (Scheme 50); at a bond angle of 162.8(1)°, the O−U−O group is now

Scheme 50. $U^V \rightarrow U^{IV}$ Enabled by Uranyl(V) Oxo Group → Borane Coordination[a]

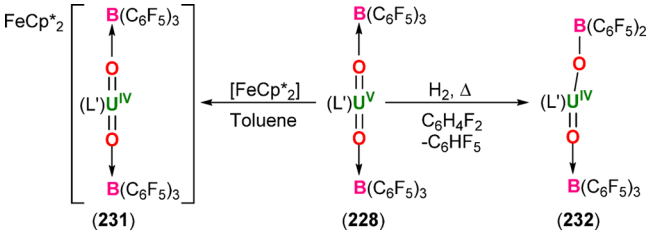

[a]$[U^V\{OB(C_6F_5)_3\}_2(L')]$ (**228**) reacts with [FeCp*$_2$] and H_2 to afford $[FeCp^*_2][U^{IV}\{OB(C_6F_5)_3\}_2(L')]$ (**231**) and $[U^{IV}\{OB(C_6F_5)_3\}\{OB(C_6F_5)_2\}(L')]$ (**232**), respectively.[58].

significantly more bent than other bis(silyloxide) complexes derived from uranyl reduction, indicating the loss of "yl" character.[58]

The reductive functionalization of uranyl(VI) may also be achieved through deployment of a suitable donor solvent in the absence of intricately designed and strictly equatorially coordinating ligands. As such, a new class of highly symmetrical, linear oxo-bridged mixed actinide/lanthanide complexes (Scheme 51) are accessible from uranyl reduction by low oxidation-state lanthanide and actinide halides.[95]

The reactions between $[U^{VI}O_2Cl_2(THF)_2]$ (**4-THF**) and 1.25 equiv of either $[Sm^{II}I_2(THF)_2]$ or $Dy^{II}I_2$ provide the mixed Ln/An complexes $[\{U^VO_2(py)_5\}_2(Ln^{III}I_4)]I$ (Ln = Sm

Scheme 51. Reductive Functionalization of $[U^{VI}O_2\{N(SiMe_3)_2\}_2(THF)_2]$ (2-THF) or $[U^{VI}O_2Cl_2(THF)_2]$ (4-THF) with Ln^{II} (Ln = Sm, Dy) or U^{III} Salts in Donor Solvents (pyridine or acetonitrile): (a) 1.25$[Ln^{II}I_2(THF)_2]$ (Ln = Sm, Dy), (b) 2$[Sm^{II}I_2(THF)_2]$, (c) 2$[U^{III}I_3(dioxane)_{1.5}]$, (d) 3$Dy^{II}I_2$.[95]

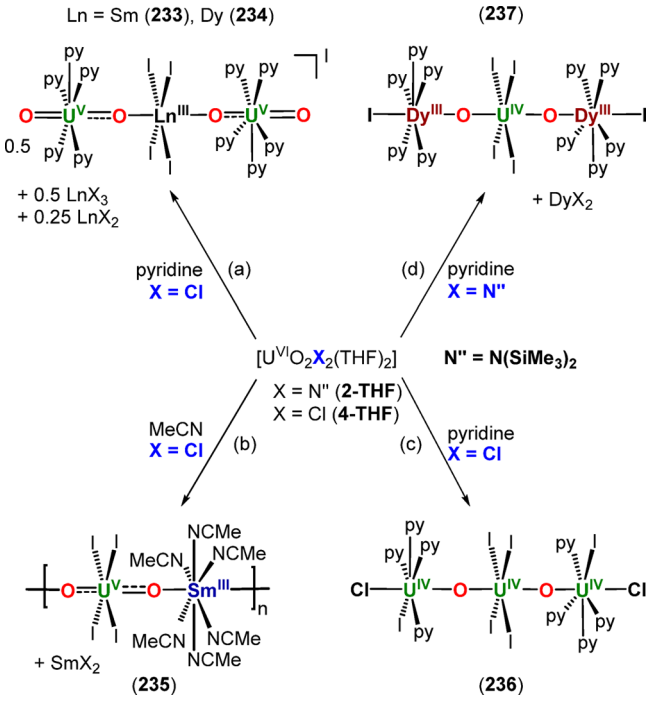

DOI: 10.1021/acs.chemrev.9b00048
Chem. Rev. XXXX, XXX, XXX−XXX

Chart 1. U−O Bond Length versus Uranium Oxidation State for Unfunctionalized and Functionalized Uranyl(VI), Uranyl(V), and Uranium(IV) Dioxo Complexes Reported in Tables 1−6: (a) Mean Values; (b)−(e) Ranges for the Different Formal Oxidation States from U(VI) to U(IV)

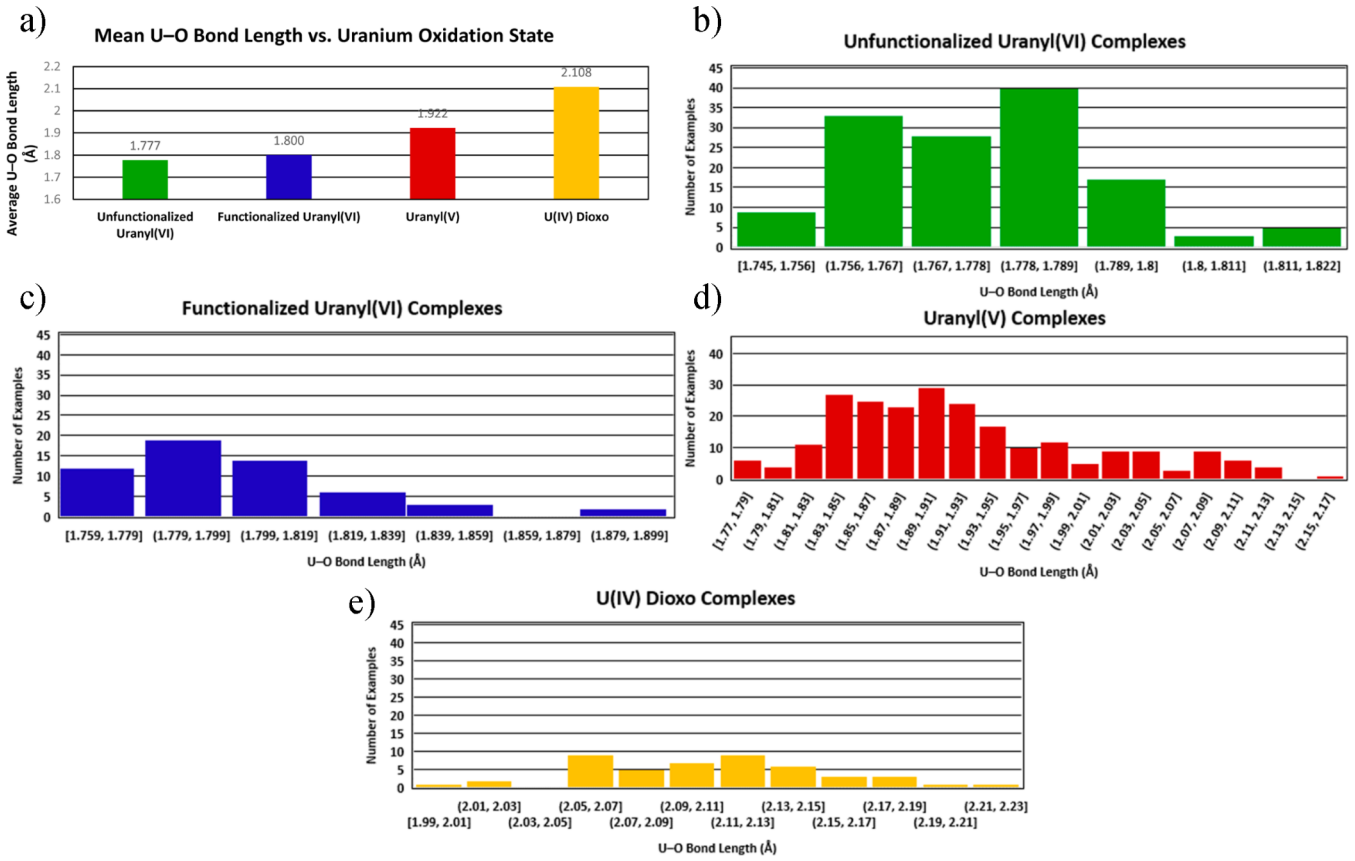

(**233**), Dy (**234**)), which display linear, oxo-bridged units made up of a $[Ln^{III}I_4]^-$ anion sandwiched between two $[U^VO_2]^+$ cations (Scheme 51a). Alternatively, **4-THF** reacts with 2 equiv of $[Sm^{II}I_2(THF)_2]$ in acetonitrile to provide the one-dimensional coordination polymer $[(U^VO_2I_4)\{Sm^{III}(NCMe)_6\}]_n$ (**235**; Scheme 51b) and with 2 equiv of $[U^{III}I_3(diox)_{1.5}]$ to yield the trimetallic $U^{IV}/U^{IV}/U^{IV}$ complex $[(U^{IV}O_2I_4)\{U^{IV}ICl(py)_4\}_2]$ (**236**; Scheme 51c). Complex **235** is composed of alternating anionic $[U^VO_2]^-$ and cationic Sm^{III} units, and **236** comprises a central $[U^{IV}O_2]^{2-}$ dianion bridged by two $[U^{IV}]^+$ cations. While treating **4-THF** with excess $Dy^{II}I_2$ only yielded **234**, treatment of $[U^{VI}O_2\{N(SiMe_3)_2\}_2(THF)_2]$ (**2-THF**) with 3 equiv of $Dy^{II}I_2$ provided access to $[(U^{IV}O_2I_4)\{Dy^{III}I(py)_5\}_2]$ (**237**), which similarly to **236**, possesses an anionic $[U^{IV}O_2I_4]^{2-}$ unit sandwiched between two Dy^{III} cations and is the product of $[U^{VI}O_2]^{2+} \rightarrow [U^{IV}O_2]$ reduction (Scheme 51d).[95]

The structural data (U−O and O−X bond lengths, O−U−O and U−O−X bond angles; X = oxo-functionalizing unit) determined by single crystal X-ray diffraction, and characteristic spectroscopic data (OUO vibrational stretching frequency) determined by FTIR or Raman spectroscopies for the reductively functionalized uranyl(V) and uranium(IV) dioxo complexes reported since 2010 and discussed in Section 6 (*vide supra*) are provided in Table 6, and their trends are discussed in more detail in Section 7 (*vide infra*).

7. STRUCTURAL AND SPECTROSCOPIC CHARACTERISTICS OF $[U^{VI}O_2]^{2+}$, $[U^VO_2]^+$, AND $[U^{IV}O_2]$ COMPLEXES

The structural data (U−O and O−X bond lengths, O−U−O and U−O−X bond angles; X = oxo-functionalizing unit) determined by single crystal X-ray diffraction, and characteristic spectroscopic data (OUO vibrational stretching frequency) determined by FTIR or Raman spectroscopies for uranyl(VI) and reductively functionalized uranyl(V) and U(IV) dioxo complexes reported since 2010 are provided in Tables 1−6. The U−O bond lengths in Tables 1−6 are also represented pictorially in Chart 1.

The $U-O_{yl}$ bond lengths and asymmetric OUO stretching frequency (when observable) are important aids in assignment of the formal oxidation state of the uranium center. The $U-O_{yl}$ bond lengths of uranyl(VI) complexes reported since 2010 range from 1.745(6)−1.82(1) Å for unfunctionalized uranyl(VI) complexes and 1.764(6)−1.885(4) Å for functionalized uranyl(VI) complexes. The $U-O_{yl}$ bond lengths of uranyl(V) and U(IV) dioxo complexes range from 1.77(1)−2.170(8) Å and 1.990(3)−2.219(2) Å, respectively. While for the most part there is a distinct difference in U−O bond lengths depending on the oxidation state of the uranium center, there is some overlap, particularly with respect to uranyl(V) compounds. We have found that uranyl(V) compounds that possess particularly elongated U−OR bonds (R = functionalizing unit of the former oxo ligand) also possess particularly short U−O bonds to the remaining oxo ligand, resulting in overlap in the ranges of expected U−O bond lengths for U(IV)

DOI: 10.1021/acs.chemrev.9b00048
Chem. Rev. XXXX, XXX, XXX−XXX

dioxo and uranyl(VI) compounds, respectively. As a result, the mean U−O bond length for each uranium oxidation state is plotted in Chart 1. The mean U−O bond lengths for unfunctionalized and functionalized uranyl(VI) complexes, uranyl(V) and U(IV) dioxo complexes, are 1.777, 1.800, 1.922, and 2.108 Å, respectively. However, we recognize that the mean values for the different U oxidation states are only a crude measure given that the compounds bear significantly different equatorially coordinating ligands and oxo ligand functionalizing units.

The asymmetric OUO stretching frequencies for uranyl(VI) complexes range from 860 to 964 cm^{-1} in the solid-state with stretching frequencies being reported as high as 973 cm^{-1} in solution, whereas those for uranyl(V) and U(IV) dioxo complexes range from 704 to 897 cm^{-1} (with one exception being $[\{U^{V}O_2Eu(py)_2(L^{Me})\}_2]$ (**106**), located at 564 cm^{-1}; see section 3) and 531−631 cm^{-1}, respectively. The latter range derives from only four examples in the literature, and tentative assignments are provided for one of those complexes. The O−U−O bond angle remains nearly linear for uranyl(VI) and reductively functionalized uranyl(V) and U(IV) dioxo complexes, ranging from 180−161.7(5)°, 180−169.3(1)° and 180−155.5(5)° for the +6, +5, and +4 oxidation states, respectively; three outliers exist for the U(IV) dioxo complexes, which are $[(py)(pinBO)U^{IV}OU^{IV}(OBpin)(py)(L^{A})]$ (**210**), $[(py)\{cat(py)BO\}U^{IV}OU^{IV}(OBcat)(py)(L^{A})]$ (**211**), and $[U^{IV}(OSiMe_3)_2I_2(bipy)_2]$ (**222**), which possess O−U−O angles of 96.51(7), 99.2(1), and 115.5(2)°, respectively (see sections 5 and 6 for discussion). In addition, the O−X bond lengths and U−O−X bond angles are dependent on the oxo-functionalizing unit, rendering these two structural parameters less useful for uranium oxidation state determination.

While Raman spectroscopy is an excellent technique to measure the symmetric OUO stretching frequency, many of the more complicated ligands now being used in molecular uranyl(V) and U(IV) dioxo complexes fluoresce or burn in the laser beam, so few data are available for isolated uranyl(V) complexes. Furthermore, data collection with air and moisture sensitive compounds while avoiding sample decomposition is difficult to achieve with these compounds. However, an outline for successful Raman data collection with respect to excitation wavelength and fluorescence/decomposition while maximizing signal intensity for the identification and relative abundance evaluation of uranyl(VI) species in solution was recently published.[96] This method takes into account approximate vibrational band locations and band widths using second derivative spectral analysis and could perhaps be extended to uranyl(V) and U(IV) dioxo complexes. In addition, authors tend to report the observed stretching frequencies obtained by IR and Raman spectroscopy for uranyl compounds rather than the associated calculated force constants within the OUO unit. We encourage the reporting of calculated force contants since this can provide additional information regarding the bonding within the uranyl ion.[42,97,98]

8. $[U^{VI}O_2]^{2+}$ PHOTOCHEMICAL REACTIVITY

Similarly to thermal pathways, photochemical reactivity studies of the uranyl(VI) ion invoke uranyl(V) intermediates, and when applied to photochemical transformations, including C−H bond activation, the resulting $[O{=}U^{V}{-}OH]^{2+}$ motif is H-functionalized. We therefore also discuss recent advances in the photochemistry of the uranyl(VI) ion.

In a transformation key to medicinal and agrochemical industries, the first photochemical, uranyl-mediated fluorination of sp^3 C−H bonds was recently reported.[99] Combining uranyl nitrate, $[U^{VI}O_2(NO_3)_2(OH_2)_2]\cdot 4H_2O$ (**238**) and a source of electrophilic fluorine (i.e., "F^{+}") with a visible light source (λ_{max} > 400 nm) in an optically transparent solvent (CH_3CN) under an argon atmosphere, it was demonstrated that the uranyl ion can catalyze the fluorination of saturated, unactivated C−H bonds in good yields (Scheme 52). It is

Scheme 52. C−H Bond Fluorination Using "F^{+}" Source[a]

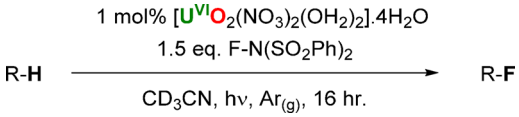

[a]R = cyclooctyl, C_8H_{15} (yield >95%); R = cyclohexyl, C_6H_{11} (yield = 42%); R = cyclopentyl, C_5H_9 (yield = 32%); R = tolyl, $C_6H_5CH_2$ (yield = trace).[99]

notable that (i) visible light is sufficient to drive the photocatalytic reaction, thus avoiding specialized UV sources, and (ii) catalyst turnover does not require dioxygen to regenerate U(VI), suggesting a greater scope of photoreactions with uranyl may be possible.[99]

The reaction proceeds through H-atom abstraction (HAA) and while no mechanism was directly discussed, it is clear that conversion is influenced through choice of uranyl coligand; using a blue LED strip, the nitrate (complex **238**) gives 52% conversion for the monofluorination of cyclooctane (i.e., fluorocyclooctane) whereas the acetate, $[UO_2(OAc)_2]\cdot 2H_2O$ (**235**), has ca. 8% conversion. Conversion increased to 95% with **238** using a high-intensity lamp.[99] Recent studies on conversion rates for a series of Ni^{III}−X HAT (hydrogen atom transfer) complexes with X = AcO^{-} or NO_3^{-} uncovered a 15× rate enhancement with X = NO_3^{-} over AcO^{-}, attributed to different electron deficiency on the *O*-ligand(s).[100]

Following this report, the chiral uranyl salen complex, $[U^{VI}O_2(HOEt)(L^{salen})]$ (**240**; L^{salen} = 2,2′-((1E,1′E)-((1R,2R)-cyclohexane-1,2-diylbis(azanylylidene))bis(methanylylidene))diphenol), was used to probe the α-cyanation of anilines with NaCN, CH_3COOH, and an oxidant and determined that relative to conversion with uranyl acetate (<1%), conversion is greatly enhanced (>80%, *in situ*; Scheme 53).[59] Though a mechanism is proposed (HAA followed by nucleophilic cyanide attack), the authors did not hypothesize why conversion is higher for the salen complex. It is likely that blocking four of the five normal equatorial uranyl binding sites reduces the deactivation (quenching) of the photoexcited state $*[U^{VI}O_2]^{2+}$ through nonradiative vibrational mechanisms that would be facilitated by water binding and dynamic exchange.[59]

Exposure of an anoxic pyridine solution of **238** to sunlight generated $[U^{VI}O_2(py)_2(NO_3)_2]_2O_2\cdot py$ (**241**) in 48% yield (based on [U]), which incorporates a bridging peroxide ligand and suggests that uranyl peroxides are formed from water and not dioxygen.[101] Larger uranyl-oxo clusters were obtained on exposure of **238** to light within the presence of C_6H_5COOK and pyridine, thus forming the mixed U(V)/U(VI) cluster $[U^{V}(U^{VI}O_2)_5(\mu\text{-}O)_5(C_6H_5COO)_5(py)]_7$ (**242**; Scheme 54).[60] By treating 0.5 equiv of the preformed $U^{V}O_2^{+}$ polymer $\{[U^{V}O_2(py)_5][KI_2(py_2)]\}_n$ (**128**) with C_6H_5COOK, the larger mixed U(IV)/U(V) $U^{IV}{}_{12}U^{V}{}_4O_{24}$ cluster $\{[K(py)_2]_2[K(py)]_2[U_{16}O_{24}(C_6H_5COO)_{24}(py)_2]\}$ (**243**) was crystallized,

DOI: 10.1021/acs.chemrev.9b00048
Chem. Rev. XXXX, XXX, XXX−XXX

Scheme 53. α-Cyanation of Anilines with $[U^{VI}O_2(HOEt)(L^{salen})]$ (240); R = H, CH_3, OCH_3, Cl, Br; R′ = H, CH_3[59]

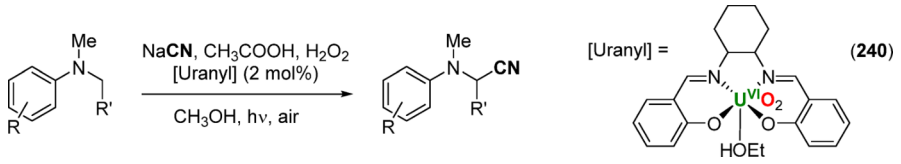

Scheme 54. Reactivity of Potassium Benzoate to Probe Likely Intermediates with U^V (top) (244) and with Light and $U^{VI}O_2^{2+}$ To Isolate a Mixed U(VI)/U(V) Cluster (bottom) (242).[60]

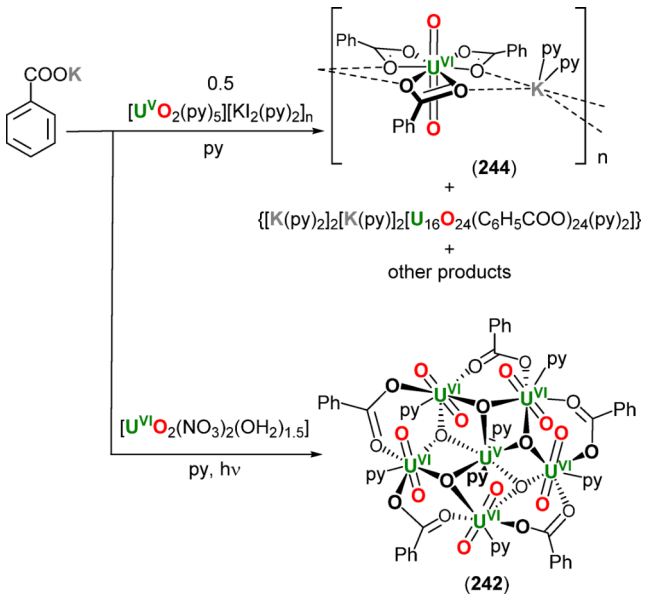

along with $\{[U^{VI}O_2(C_6H_5COO)_3][K(py)_2)]\}_n$ (**244**; Scheme 54) and other unidentified products.[60] Functionalized uranyl peroxides have been suggested as precursors for nuclear fuel fabrication,[102] while larger mixed-valence actinide oxo-clusters are postulated as relevant intermediates in environmental actinide speciation.[60]

A practical example of how uranyl may behave in the environment is exemplified in the degradation of the dye Rhodamine B, RhB, which is often used as a "model" organic pollutant.[103] Recent work has shown that when supported by salen or derivatized catecholate ligands, uranyl ions may assist in the photodegradation of herbicidal viologen-type pollutants. The complexes tested as photocatalysts for RhB destruction were either salicylidene-α-hydroxy acids ($[UO_2(L)(solv)]$ (solv = THF (**245**) or C_2H_5OH (**246**)), or geometric isomers suggested by the authors to result from the reaction between two asymmetric catecholamides and uranyl nitrate, "$[UO_2(L)]\cdot 2H_2O$" (**247**)); in both cases the uranyl-containing catalysts are poorly defined.[104,105] The extent of photocatalytic decomposition of RhB in aqueous solution by **245** and **246** over 3 h is found to be 90% and 70% vs 65−75% for **247**, respectively, with a first-order rate constant for the latter measured as approximately $-0.4\ s^{-1}$. Both reports invoke de-ethylation of RhB by a $*UO_2^{2+}$ electron transfer mechanism, with further oxidative degradation by superoxyl anions, $O_2^{\bullet-}$, peroxide radicals, or anion radicals, formed from water or dissolved O_2.[106] An analogous mechanism is postulated in the degradation of the antibiotic tetracycline hydrochloride using $[H_2\text{-bpp}][U^{VI}O_2(p\text{-nba})_3]_2$ (**248**) and $[H_2\text{-bipy}][(U^{VI}O_2)_4(\mu_3\text{-}O)_2(p\text{-nba})_6]$ (**249**) (bpp = 1,3-di(4-pyridyl)propane, *p*-Hnba = *p*-nitrobenzoic acid, bipy = 4,4′-bipyridine) as photocatalysts with H atom abstraction from the phenol group followed by oxidative degradation by reactive oxygen species (ROS) occurring.[107] Optimized UV−vis spectroscopic measurements on the aqueous suspensions show degradation of 70% (for **248**) and 75% (for **249**) over 5 h, with rate constants of $-0.2412\ s^{-1}$ and $-0.291\ s^{-1}$, respectively, illustrating that photoactive uranyl compounds may be viable routes to the sunlight-induced photodegradation of environmental organic pollutants, particularly in uranyl-contaminated water. Indeed, uranyl carbonates, which occur naturally in many uranium-bearing ores such as rutherfordine, $[U^{VI}O_2(CO_3)]$ (**250**),[108] have very recently been shown to be photoactive; the anion $[U^{VI}O_2(CO_3)_3]^{4-}$ (**251**) photooxidizes borohydrides to boric acid.[109]

A second developing application for uranyl photoreactivity is the *in vitro* study of biomolecules, for titrimetric metal detection from environmental samples and to elucidate

Scheme 55. Reactions of Recently Reported Uranyl(VI) Photocatalysts under Visible Light Irradiation with Selected Hydrocarbon Substrates: (A) the Oxidation of Substrates with Benzylic C−H Bonds with 238 or 251; (B) Formation of New C−C Bonds Using Cyclohexane and 238; (C) Oxidation of Cyclohexene Using Complex 252, Characterized by GC-MS (R Is Hydrocarbyl)[116−118]

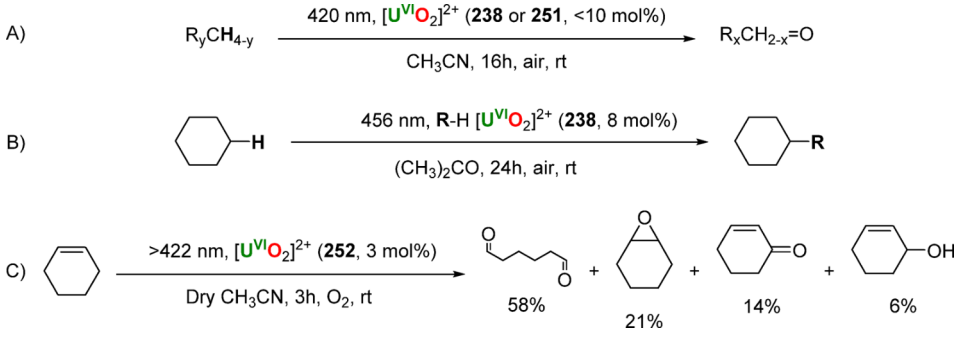

DOI: 10.1021/acs.chemrev.9b00048
Chem. Rev. XXXX, XXX, XXX−XXX

structure−property relationships in bio-oligomers. Oligomeric, metal-sensing "DNAzymes" (deoxyribozymes) are nucleotide sequences capable of metal-sensing, often possessing selectivity at the ppb level for metal ions. The extraction of uranium from seawater (ca. 3 ppb)[110] has been proposed using DNAzymes, and in a proof-of-concept study secondary protein structure vital to $[U^{VI}O_2]^{2+}$ selectivity in a uranyl-selective DNAzyme was identified through combining controlled, $[U^{VI}O_2]^{2+}$-mediated photocleavage and DNA footprinting.[111] Detection limits of 0.08 μg uranium per liter of seawater have recently been reported using a similar system.[112] The synthetic utility of $[U^{VI}O_2]^{2+}$-mediated photocleavage for protein purification and C-terminus peptide amidation (i.e., $-CONH_2$) has been demonstrated[113,114] and a HAA mechanism invoked. In accordance with pharmaceutically relevant amide formation being identified as a key challenge by the American Chemical Society,[115] the controlled cleavage of a peptide backbone with photoactivated uranyl represents a noteworthy alternative to traditional enzymatic or synthetic approaches.

During the course of writing this review, several new reports on uranyl photocatalysis have emerged. We reported the new uranyl-phenanthroline complex $[U^{VI}O_2(NO_3)_2(Ph_2phen)]$ (Ph_2phen = 4,7-diphenyl-1,10-phenanthroline, **251**) as a selective catalyst for the oxidation of benzylic C−H bonds and also C−C bond cleavage in a model of a lignin component; a large substrate scope study was reported, alongside comparisons of activity with the parent nitrate complex **238** ($[U^{VI}O_2(NO_3)_2(OH_2)_2]\cdot 4H_2O$).[116] Analogous H atom abstraction from cyclohexane and the subsequent radical addition to electrophilic alkenes was also demonstrated for **238**,[117] while the oxidation of cyclohexene with $[U^{VI}O_2(OPCyPh_2)_4][ClO_4]_2\cdot 2EtOH$ (**252**) to a range of products has been studied.[118] These reactions are illustrated in Scheme 55.

While demonstrating further the potential scope of uranyl photocatalysts in selective C−H bond activation, these reports also highlight that visible light is sufficient in a variety of cases to access the $*[U^{VI}O_2]^{2+}$ ion.

9. CONCLUSIONS AND OUTLOOK

The decade since the first formal reductive silylation of $[U^{VI}O_2]^{2+}$ was reported[40] has seen a rapid growth in uranyl oxo-group functionalization chemistry that now includes alumination, borylation, silylation, stannylation, alkylation, and metalation of the oxo groups by elements from all areas of the periodic table, from a proton to, pertinently, the transuranic neptunium. Such functionalization enables not only a controlled study of uranyl-oxo interactions with environmentally relevant cations but also a fundamental exploration of the chronically underexplored actinide-oxo motif.

Indeed, one of the academic, curiosity-driven research targets in uranyl chemistry is the synthesis of a *cis*-uranyl(VI) ion.[31,62,119] We envision that a potentially more effective route to *cis*-uranyl complexes may be through reductive functionalization to U(V) or U(IV) dioxo complexes followed by reoxidation; a decrease in U−O bond order upon reduction would enable the manipulation of the O−U−O bond angle.[119] It is expected that such compounds could provide information on the mechanisms of yl-oxo exchange processes that occur at high pH[120] and could also be more susceptible to new transformative reactivity pathways.

Ligand design has a profound effect on the reductive functionalization chemistry of the uranyl ion. For example, using a Pacman-shaped ligand that possesses a phenylene hinge between the top and bottom N_4-donor pockets enables access to one electron $U^{VI} \rightarrow U^{V}$ reductive functionalization, whereas two electron $U^{VI} \rightarrow U^{IV}$ is not observed. Alternatively, when a redox-active dipyrrin ligand or a Pacman ligand that possesses an anthracenyl-hinge and can incorporate two uranyl(VI) ions is used in uranyl chemistry, $U^{VI} \rightarrow U^{IV}$ reductive functionalization is observed, as opposed to a one electron $U^{VI} \rightarrow U^{V}$ process. While a wide variety of ligand designs that differ in both electron donor ability and steric properties have been used in uranyl chemistry to-date, a continued effort toward new ligand designs and their effects on the reactivity of the uranyl ion should be pursued. For example, redox-active ligands have only recently been used to support uranyl oxo chemistry, and so far with great effect. For the most part, *N*- and *O*-donor ligands have been targeted for coordination to the U center; a progression toward both neutral and anionic *P*- and *S*-donor ligands to stabilize lower oxidation state complexes or a combination of *N*/*O*- and *P*/*S*-donor groups within the same ligand to stabilize both high and low oxidation states may give rise to marked changes in the overall reactivity of the uranyl ion. Alternatively, the use of ambiphilic ligands that possess both Lewis acid and base functionality appears to be unexplored territory in uranyl chemistry and may provide an avenue for expanding on the functionalization chemistry accessed through coordination of the uranyl ion to unsupported Lewis acids such as tris(pentafluorophenyl)-borane.[58,69,92,93,121] Finally, the DIBAL-catalyzed route to selective mono-Group 1-metalated uranyl ions[73] could provide opportunities for other catalyzed uranyl functionalization reactions with *d*- and *f*-group metal cations. It could also offer a general low-cost, one-pot route to the selective Group-1 cation metalation of *d*-block metal oxo complexes.

CV experiments have provided the reduction potentials for a number of the complexes described, confirming that while the uranyl(VI) ion is not particularly difficult to reduce, the resulting products can often be difficult to isolate as kinetically inert complexes. Increased reporting of the reduction potentials for both $U^{VI}U^{V}$ and $U^{V}U^{IV}$ couples would be very useful for the community and would accelerate both the understanding and exploitation of these reduced states.

Raman spectroscopic monitoring of the change in the symmetric OUO stretching frequency upon reduction of uranyl complexes should be clearer than IR spectroscopic methods since Raman spectra are less cluttered by ligand-derived absorptions. Modern spectrometers give excellent data, and solution analyses are generally recommended to avoid excessive sample heating. Thus, suitable containment methods will undoubtedly need further development.

The utility of photochemical routes to new compounds and applications for uranyl-containing materials is also becoming more recognized, with reports of targeted C−H bond photoactivation catalyzed by uranyl in organic solvents, and the use of ligand design to impart unique reactivity not seen in the prototypical uranyl compounds such as $[UO_2(NO_3)_2(OH_2)_2]\cdot 4H_2O$ and $[UO_2(OAc)_2]\cdot 2H_2O$ in wholly-aqueous or semiaqueous systems. Multidentate salen or salen-type ligands that block equatorial uranyl coordination sites are excellent candidates for controlling or enhancing the photochemical reactivity of uranyl, and recent work demonstrates that calix[4]pyrroles may have potential for small molecule activation, via molecular photoswitching and activation of dioxygen.[122] Through the use of photochemically robust groups, it is conceptually possible to improve both the

DOI: 10.1021/acs.chemrev.9b00048
Chem. Rev. XXXX, XXX, XXX−XXX

quantum yield and conversion efficiency of photocatalytic reactions involving the uranyl(VI) ion. As visible light induced C−H bond cleavage and functionalization reactions are rapidly becoming commonplace in organic chemistry, further examples of uranyl-mediated, visible-light induced C−H bond cleavage reactions will undoubtedly be forthcoming over the next several years. Practically, we note also that photochemical reduction of $[U^{VI}O_2(NO_3)_2(OH_2)_2]\cdot 4H_2O$ to hydrated $[U^{IV}O_2]$ has previously been examined, and while not historically considered viable for industrial implementation in nuclear waste remediation,[123] recent applications, particularly environmental (uranium detection), biochemical (peptide photocleavage), and geologic ($[UO_2(CO_3)_3]^{4-}$ photoreactivity), continue to be explored and, we hope, applied.

As a final point, we note that previously almost all uranyl chemistry has been studied with the aim of understanding the fundamental electronic structure and reactivity of the cation and its behavior in the environment. Now, as a wide variety of new oxo chemistry is developed, there should be opportunities for these reactions, both stoichiometric and catalytic, to inform metal oxo chemistry being carried out in other areas of the periodic table.

AUTHOR INFORMATION

Corresponding Authors

*E-mail: jason.love@ed.ac.uk.
*E-mail: Polly.Arnold@ed.ac.uk.

ORCID

Jason B. Love: 0000-0002-2956-258X
Polly L. Arnold: 0000-0001-6410-5838

Notes

The authors declare no competing financial interest.

Biographies

Dr. Bradley E. Cowie obtained his Ph.D. in 2015 working under the supervision of Prof. David J. H. Emslie at McMaster University in Hamilton, Ontario, Canada. His Ph.D. research was focused on the synthesis of late transition metal complexes bearing Group 13 Lewis acid-containing ambiphilic ligands and their potential use for small molecule activation. In November 2015, he joined Professors Polly L. Arnold (FRS OBE) and Jason B. Love at the EaStCHEM School of Chemistry, University of Edinburgh, to explore new avenues for uranyl ion activation and reductive functionalization.

Jamie M. Purkis is currently pursuing his Ph.D. with Professors Polly L. Arnold (FRS OBE) and Jason B. Love, at the University of Edinburgh in the United Kingdom (UK), and Dr. Jonathan Austin, of the National Nuclear Laboratory, UK. His work focuses on developing coordination chemistry of new photoactive uranyl complexes toward the selective activation of C−H bonds in organic substrates. He obtained his Masters Degree in Chemistry at the University of Southampton, UK, in 2015 with Professor Gill Reid, studying macrocyclic complexes of Group 2 dications.

Dr. Jonathan Austin is a senior researcher in the Chemical and Process Modelling team at the National Nuclear Laboratory (NNL) in the United Kingdom (UK). Jonathan has a Ph.D. in quantum mechanics modeling of heavy elements, including uranyl complexes in aqueous solution, from the University of Manchester, UK. In 2009 Jonathan joined the Chemical and Process Modelling team at the NNL, working in the area of radioactively contaminated effluents, where he develops and applies models of plants used for the storage of spent nuclear fuel and for water treatment. Jonathan provides industrial supervision to a number of Ph.D. students funded by the Nuclear Decommissioning Authority (UK).

Professor Jason B. Love FRSC holds B.Sc. and Ph.D. degrees from the University of Salford, and he undertook postdoctoral positions at the Universities of Sussex, British Columbia, and Nottingham before being awarded a lectureship and Royal Society University Research Fellowship at the University of Sussex in 1999. He is currently Professor of Molecular Inorganic Chemistry at the University of Edinburgh and is the Head of Inorganic Chemistry. He has researched chemistry across the Periodic Table, focusing on small molecule redox catalysis in relation to energy and resource sustainability, ligand design strategies for *d*- and *f*-element chemistry, supramolecular catalysis, and metal recovery processes.

Professor Polly L. Arnold OBE FRS FRSE FRSC is the Crum Brown Chair of Chemistry at the University of Edinburgh. She holds degrees from Oxford and Sussex and was a Fulbright postdoctoral fellow at the Massachusetts Institute of Technology in the US prior to starting a lectureship in the UK in 1999. Her research is focused on exploratory synthetic chemistry of the *f*-block metals, in particular the actinides, and the development of homogeneous catalysis using the earth-abundant rare earths (www.homepages.ed.ac.uk/parnold). Polly also made "A Chemical Imbalance", a call to action for equality of opportunity for women and minorities in STEM, and was awarded an OBE in 2017 for services to chemistry and women in STEM (www.chemicalimbalance.ed.ac.uk).

ACKNOWLEDGMENTS

The authors acknowledge the EPSRC-UK grants EP/N022122/1 and EP/M010554/1, the European Commission Directorate General and Actinet JRC Userlab (ACTINET-I3-CP-CSA-JRP-232631), the Natural Sciences and Engineering Research Council of Canada for an NSERC Post-Doctoral Fellowship (BEC), and the UK National Nuclear Laboratory for funding (JMP). This project has received funding from the European Research Council (ERC) under the European Union's Horizon 2020 research and innovation programme (grant agreement No 740311).

ABBREVIATIONS

py	pyridine
Opy	pyridine-*N*-oxide
dme	1,2-dimethoxyethane
THF	tetrahydrofuran
DMSO	dimethyl sulfoxide
OEt_2	diethyl ether
OTf	$OS(O)_2CF_3$
TMEDA	$Me_2N(CH_2)_2NMe_2$
2,2′-bipy	2,2′-bipyridine
4,4′-bipy	4,4′-bipyridine
Cp	cyclopentadienyl
Cp*	1,2,3,4,5-pentamethylcyclopentadienyl
Mes/mesityl	2,4,6-trimethylphenyl
Me	methyl
Et	ethyl
^{i}Pr	*iso*-propyl
^{t}Bu	*tert*-butyl
^{i}Bu	*iso*-butyl
Ph	phenyl
DMAP	4-(dimethylamino)pyridine
$[CoCp^*_2]$	decamethylcobaltocene
pin	pinacolato
cat	catecholato

DOI: 10.1021/acs.chemrev.9b00048
Chem. Rev. XXXX, XXX, XXX−XXX

tolyl	*p*-C_6H_4Me
ferrocenyl	$[Fe(\eta^5\text{-}C_5H_5)(\eta^5\text{-}C_5H_4)]$
Fc	ferrocene, $[Fe(\eta^5\text{-}C_5H_5)_2]$
Fc^+	ferrocenium, $[Fe(\eta^5\text{-}C_5H_5)_2]^+$
NO_3^-	nitrate
AcO^-	acetate
CO_3^{2-}	carbonate
2.2.2-crypt	2.2.2-cryptand
-c-	crown, a crown ether
μ-	a bridging ligand between two or more metals
ε	molar absorptivity
mol	moles
L	liters
cm	centimeters
μg	micrograms
mM	millimolar
M	molar
Å	angstroms
°	degrees
ppb	parts per billion
N′′	$N(SiMe_3)_2$
$[HPy]^+$	pyridinium
uranyl(VI)	$[U^{VI}O_2]^{2+}$
uranyl(V)	$[U^{V}O_2]^{+}$
O_{exo}	exogenous oxo atom bound to the uranyl ion
O_{endo}	endogenous oxo atom bound to the uranyl ion
CCI	cation−cation interaction
ROS	reactive oxygen species
L^{Me}	a macrocyclic "Pacman" ligand; dimethylphenylene hinge between N_4-donor pockets, methyl substituents on *meso*-carbon atom of each N_4-donor pocket
L^{Et}	a macrocyclic "Pacman" ligand; dimethylphenylene hinge between N_4-donor pockets, ethyl substituents on *meso*-carbon atom of each N_4-donor pocket
L^{A}	a macrocyclic "Pacman" ligand; anthracenylene hinge between N_4-donor pockets, ethyl substituents on *meso*-carbon atom of each N_4-donor pocket
L^{m}	*meso*-bis(pentafluorophenyl)dipyriamethyrin
L′	a monoanionic, tetradentate dipyrrin ligand
L′′	a radical anion of L′
^{Ar}acnac	Ar*N*C(Ph)CHC(Ph)*O* (Ar = 3,5-^{t}Bu$_2$C$_6$H$_3$)
^{tBu}acnac	^{t}Bu*N*C(Ph)CHC(Ph)*O*
Ar_2nacnac	Ar*N*C(Me)CHC(Me)*N*Ar (Ar = 2,6-^{i}Pr$_2$C$_6$H$_3$)
^{Ar}acnacSiMe$_3$	ArNC(Ph)CHC(Ph)OSiMe$_3$ (Ar = 3,5-^{t}Bu$_2$C$_6$H$_3$)
NPh^F	-N(C_6F_5)$_2$
NPh^FPh	-N(C_6F_5)(C_6H_5)
NPh^F(2-py)	-N(C_6F_5)(C_5H_4N)
NAr^FPh	-N(3,5-{CF_3}$_2$-C_6H_3)(C_6H_5)
$DOPO^q$	2,4,6,8-tetra-*tert*-butyl-1-oxo-1*H*-phenoxazin-9-olate (q = monoanionic quinone form)
^{dipp}IQ	4,6-di-*tert*-butyl-2-{(2,6-diisopropylphenyl)-imino}quinone
^{dipp}ISQ	4,6-di-*tert*-butyl-2-{(2,6-diisopropylphenyl)-imino}semiquinone
^{dipp}AP	4,6-di-*tert*-butyl-2-{(2,6-diisopropylphenyl)-amido}phenolate
$^{Mes}PDI^{Me}$	2,6-((Mes)N═CMe)$_2C_5H_3N$
^{t}Bu-$^{Mes}PDI^{Me}$ =	2,6-((Mes)N═CMe)$_2$-*p*-C(CH$_3$)$_3$-C_5H_2N
^{H}N4	2,11-diaza[3,3](2,6)pyridinophane
^{Me}N4	*N*,*N*′-dimethyl-2,11-diaza[3,3](2,6)-pyridinophane
tmtaa	dibenzotetramethyl-tetraaz[14]annulene
L^{tBu}	2,6-bis[1-[(2-hydroxy-3,5-di-*tert*-butylphenyl)imino]ethyl]pyridine
L^{nap}	2,6-bis[1-[(2-hydroxynaphthyl)imino]-ethyl]pyridine
BPPA	bis(2-picolyl)(2-oxybenzyl)amine
Mesaldien	*N*,*N*′-(2-aminomethyl)diethylenebis-(salicylidene-imine)
H_2salan-^{t}Bu$_2$	*N*,*N*′-bis(2-hydroxybenzyl-3,5-di-*tert*-butyl)-1,2-dimethylaminomethane
salen	(2-$^-$O-C_6H_4-CH═NCH$_2$)$_2$
salfen	(2-$^-$O-3,5-(^{t}Bu)$_2$-CH═N)$_2$-($FeCp_2$)
TPA	tris(2-pyridylmethyl)amine
H_2dpaea	bis(pyridyl-6-methyl-2-carboxylate)-ethyl-amine
H_2salophen	*N*,*N*′-phenylene-bis(salicylideneimine)
H_2salophen-^{t}Bu$_2$	*N*,*N*′-phenylene-bis(3,5-di-*tert*-butylsalicylideneimine)
H_2acacen	*N*,*N*′-ethylene-bis(acetylacetoneimine)
BIPMH	HC(PPh_2NSiMe_3)$_2$
L^{salen}	2,2′-((1E,1′E)-((1*R*,2*R*)-cyclohexane-1,2-diylbis(azanylylidene))bis-(methanylylidene))diphenol
KL^{nacnac}	2-(4-tolyl)-1,3-bis(quinolyl)malondiiminate
H_3trensal	2,2′,2′′-tris(salicylideneimino)triethylamine
SCHS	[HC(PPh_2S)$_2$]$^-$
SCS	[C(PPh_2S)$_2$]$^{2-}$
$DPPFO_2$	[Fe{η^5-C_5H_4(Ph_2PO)}$_2$]
$dipy^R$	RC(C_4H_2NH)$_2$ (R = tolyl, mesityl, ferrocenyl, *p*-C_6H_4OMe)
MeIm	1-methylimidazole
dbm	*O*C(Ph)CHC(Ph)*O*
dppmo	$Ph_2P(O)CH_2P(O)PPh_2$
TEMPO	(2,2,6,6-tetramethylpiperidin-1-yl)oxidanyl
bpp	1,3-di(4-pyridyl)-propane
p-Hnba	*p*-nitrobenzoic acid
phen	1,10-phenanthroline
DIBAL	diisobutylaluminum hydride
HEPES	4-(2-hydroxyethyl)-1-piperazineethanesulfonic acid
NMR	nuclear magnetic resonance
IR	infrared
PFGSTE	Pulsed-Field Gradient Stimulated Echo
DFT	density functional theory
UV−vis−NIR	ultraviolet−visible−near-infrared
CV	cyclic voltammetry
HAA	H atom abstraction

REFERENCES

(1) Denning, R. G. Electronic Structure and Bonding in Actinyl Ions and their Analogs. *J. Phys. Chem. A* **2007**, *111*, 4125−4143.

(2) Lovley, D. R.; Phillips, E. J. P.; Gorby, Y. A.; Landa, E. R. Microbial Reduction of Uranium. *Nature* **1991**, *350*, 413−416.

(3) Renshaw, J. C.; Butchins, L. J. C.; Livens, F. R.; May, I.; Charnock, J. M.; Lloyd, J. R. Bioreduction of Uranium: Environmental Implications of a Pentavalent Intermediate. *Environ. Sci. Technol.* **2005**, *39*, 5657−5660.

DOI: 10.1021/acs.chemrev.9b00048
Chem. Rev. XXXX, XXX, XXX−XXX

(4) Morris, D. E. Redox Energetics and Kinetics of Uranyl Coordination Complexes in Aqueous Solution. *Inorg. Chem.* **2002**, *41*, 3542−3547.
(5) Steele, H.; Taylor, R. J. A. Theoretical Study of the Inner-Sphere Disproportionation Reaction Mechanism of the Pentavalent Actinyl Ions. *Inorg. Chem.* **2007**, *46*, 6311−6318.
(6) OECDNEA. *IAEA "Management of Depleted Uranium"*, 2001.
(7) Moon, H. S.; McGuinness, L.; Kukkadapu, R. K.; Peacock, A. D.; Komlos, J.; Kerkhof, L. J.; Long, P. E.; Jaffé, P. R. Microbial Reduction of Uranium Under Iron- and Sulfate-Reducing Conditions: Effect of Amended Goethite on Microbial Community Composition and Dynamics. *Water Res.* **2010**, *44*, 4015−4028.
(8) Jones, D. L.; Andrews, M. B.; Swinburne, A. N.; Botchway, S. W.; Ward, A. D.; Lloyd, J. R.; Natrajan, L. S. Fluorescence Spectroscopy and Microscopy as Tools for Monitoring Redox Transformations of Uranium in Biological Systems. *Chem. Sci.* **2015**, *6*, 5133−5138.
(9) Li, Y.; Su, J.; Mitchell, E.; Zhang, G.; Li, J. Photocatalysis with Visible-Light-Active Uranyl Complexes. *Sci. China: Chem.* **2013**, *56*, 1671−1681.
(10) Fortier, S.; Hayton, T. W. Oxo Ligand Functionalization in the Uranyl Ion (UO_2^{2+}). *Coord. Chem. Rev.* **2010**, *254*, 197−214.
(11) Fonseca, S. M.; Burrows, H. D.; Miguel, M. G.; Sarakha, M.; Bolte, M. Photooxidation of Cellulose Acetate and Cellobiose by the Uranyl Ion. *Photochem. Photobiol. Sci.* **2004**, *3*, 317−321.
(12) Wang, W.-D.; Bakac, A.; Espenson, J. H. Uranium(VI)-Catalyzed Photooxidation of Hydrocarbons with Molecular Oxygen. *Inorg. Chem.* **1995**, *34*, 6034−6039.
(13) Hill, R. J.; Kemp, T. J.; Allen, D. M.; Cox, A. Absorption Spectrum, Lifetime and Photoreactivity Towards Alcohols of the Excited State of the Aqueous Uranyl ion (UO_2^{2+}). *J. Chem. Soc., Faraday Trans. 1* **1974**, *70*, 847−857.
(14) Park, Y.-Y.; Tomiyasu, H. Photochemistry of the Uranyl Ion with Alkenes in Acetone—Water Mixtures. *J. Photochem. Photobiol., A* **1992**, *64*, 25−33.
(15) Sarakha, M.; Bolte, M.; Burrows, H. D. The Photo-Oxidation of 2,6-Dimethylphenol and Monophenylphenols by Uranyl Ion in Aqueous Solution. *J. Photochem. Photobiol., A* **1997**, *107*, 101−106.
(16) Mao, Y.; Bakac, A. Uranyl-Sensitized Photochemical Oxidation of Naphthalene by Molecular Oxygen. Role of Electron Transfer. *J. Phys. Chem. A* **1997**, *101*, 7929−7933.
(17) McCleskey, T. M.; Burns, C. J.; Tumas, W. Uranyl Photochemistry with Alkenes: Distinguishing Between H-Atom Abstraction and Electron Transfer. *Inorg. Chem.* **1999**, *38*, 5924−5925.
(18) Sarakha, M.; Bolte, M.; Burrows, H. D. Electron-Transfer Oxidation of Chlorophenols by Uranyl Ion Excited State in Aqueous Solution. Steady-State and Nanosecond Flash Photolysis Studies. *J. Phys. Chem. A* **2000**, *104*, 3142−3149.
(19) Burrows, H. D.; Cardoso, A. C.; Formosinho, S. J.; Gil, A. M. P. C.; Miguel, M. D. G. M.; Barata, B.; Moura, J. J. G. The Photochemical Reaction Between Uranyl Nitrate and Azulene. *J. Photochem. Photobiol. A: Chem.* **1992**, *68*, 279−287.
(20) Vidya, K.; Kamble, V. S.; Selvam, P.; Gupta, N. M. Uranyl-Anchored MCM-41 as a Highly Efficient Photocatalyst for the Complete Oxidation of Methanol Under Sunlight. *Appl. Catal., B* **2004**, *54*, 145−154.
(21) Natrajan, L. S. Developments in the Photophysics and Photochemistry of Actinide Ions and Their Coordination Compounds. *Coord. Chem. Rev.* **2012**, *256*, 1583−1603.
(22) Baker, R. J. New Reactivity of the Uranyl(VI) Ion. *Chem. - Eur. J.* **2012**, *18*, 16258−16271.
(23) Arnold, P. L.; Love, J. B.; Patel, D. Pentavalent Uranyl Complexes. *Coord. Chem. Rev.* **2009**, *253*, 1973−1978.
(24) Graves, C. R.; Kiplinger, J. L. Pentavalent Uranium Chemistry-Synthetic Pursuit of a Rare Oxidation State. *Chem. Commun.* **2009**, 3831−3853.
(25) Gong, Y.; de Jong, W. A.; Gibson, J. K. Gas Phase Uranyl Activation: Formation of a Uranium Nitrosyl Complex from Uranyl Azide. *J. Am. Chem. Soc.* **2015**, *137*, 5911−5915.
(26) Abergel, R. J.; de Jong, W. A.; Deblonde, G. J.-P.; Dau, P. D.; Captain, I.; Eaton, T. M.; Jian, J.; van Stipdonk, M. J.; Martens, J.; Berden, G.; Oomens, J.; Gibson, J. K. Cleaving Off Uranyl Oxygens through Chelation: A Mechanistic Study in the Gas Phase. *Inorg. Chem.* **2017**, *56*, 12930−12937.
(27) *Computational Methods in Lanthanide and Actinide Chemistry*; John Wiley & Sons, Ltd: West Sussex, United Kingdom, 2015.
(28) Kaltsoyannis, N. Transuranic Computational Chemistry. *Chem. - Eur. J.* **2018**, *24*, 2815−2825.
(29) Jones, G. M.; Arnold, P. L.; Love, J. B. Oxo−Group 14 Element-Bond Formation in Binuclear Uranium(V) Pacman Complexes. *Chem. - Eur. J.* **2013**, *19*, 10287−10294.
(30) Seaman, L. A.; Hrobárik, P.; Schettini, M. F.; Fortier, S.; Kaupp, M.; Hayton, T. W. A Rare Uranyl(VI)-Alkyl Ate Complex $[Li(DME)_{1.5}]_2[UO_2(CH_2SiMe_3)_4]$ and Its Comparison with a Homoleptic Uranium(VI)-Hexaalkyl. *Angew. Chem., Int. Ed.* **2013**, *52*, 3259−3263.
(31) Pedrick, E. A.; Assefa, M. K.; Wakefield, M. E.; Wu, G.; Hayton, T. W. Uranyl Coordination by the 14-Membered Macrocycle Dibenzotetramethyltetraaza[14]annulene. *Inorg. Chem.* **2017**, *56*, 6638−6644.
(32) Assefa, M. K.; Pedrick, E. A.; Wakefield, M. E.; Wu, G.; Hayton, T. W. Oxidation of the 14-Membered Macrocycle Dibenzotetramethyltetraaza[14]annulene upon Ligation to the Uranyl Ion. *Inorg. Chem.* **2018**, *57*, 8317−8234.
(33) Seaman, L. A.; Pedrick, E. A.; Wu, G.; Hayton, T. W. Promoting Oxo Functionalization in the Uranyl Ion by Ligation to Ketimides. *J. Organomet. Chem.* **2018**, *857*, 34−37.
(34) Pattenaude, S. A.; Coughlin, E. J.; Collins, T. S.; Zeller, M.; Bart, S. C. Expanding the Library of Uranyl Amide Derivatives: New Complexes Featuring the *tert*-Butyldimethylsilylamide Ligand. *Inorg. Chem.* **2018**, *57*, 4543−4549.
(35) Arnold, P. L.; Pécharman, A.-F.; Hollis, E.; Yahia, A.; Maron, L.; Parsons, S.; Love, J. B. Uranyl Oxo Activation and Functionalization by Metal Cation Coordination. *Nat. Chem.* **2010**, *2*, 1056−1061.
(36) Schettini, M. F.; Wu, G.; Hayton, T. W. Synthesis and Reactivity of a Uranyl-Imidazolyl Complex. *Chem. Commun.* **2012**, *48*, 1484−1486.
(37) Lewis, A. J.; Yin, H.; Carroll, P. J.; Schelter, E. J. Uranyl-Oxo Coordination Directed by Non-Covalent Interactions. *Dalton Trans* **2014**, *43*, 10844−10851.
(38) Jones, G. M.; Arnold, P. L.; Love, J. B. Controlled Deprotection and Reorganization of Uranyl Oxo Groups in a Binuclear Macrocyclic Environment. *Angew. Chem., Int. Ed.* **2012**, *51*, 12584−12587.
(39) Arnold, P. L.; Patel, D.; Pécharman, A.-F.; Wilson, C.; Love, J. B. Equatorial Ligand Substitution by Hydroxide in Uranyl Pacman Complexes of a Schiff-Base Pyrrole Macrocycle. *Dalton Trans* **2010**, *39*, 3501−3508.
(40) Arnold, P. L.; Patel, D.; Wilson, C.; Love, J. B. Reduction and Selective Oxo-Group Silylation of the Uranyl Dication. *Nature* **2008**, *451*, 315−318.
(41) Coughlin, E. J.; Qiao, Y.; Lapsheva, E.; Zeller, M.; Schelter, E. J.; Bart, S. C. Uranyl Functionalization Mediated by Redox-Active Ligands: Generation of O-C Bonds via Acylation. *J. Am. Chem. Soc.* **2019**, *141*, 1016−1026.
(42) Cobb, P. J.; Moulding, D. J.; Ortu, F.; Randall, S.; Wooles, A. J.; Natrajan, L. S.; Liddle, S. T. Uranyl-tri-*bis*(silyl)amide Alkali Metal Contact and Separated Ion Pair Complexes. *Inorg. Chem.* **2018**, *57*, 6571−6583.
(43) Burns, C. J.; Clark, D. L.; Donohoe, R. J.; Duval, P. B.; Scott, B. L.; Tait, C. D. A Trigonal Bipyramidal Uranyl Amido Complex: Synthesis and Structural Characterization of $[Na(THF)_2][UO_2(N(SiMe_3)_2)_3]$. *Inorg. Chem.* **2000**, *39*, 5464−5468.
(44) Bell, N. L.; Arnold, P. L.; Love, J. B. Controlling Uranyl Oxo Group Interactions to Group 14 Elements using Polypyrrolic Schiff-Base Macrocyclic Ligands. *Dalton Trans* **2016**, *45*, 15902−15909.

DOI: 10.1021/acs.chemrev.9b00048
Chem. Rev. XXXX, XXX, XXX−XXX

(45) Arnold, P. L.; Jones, G. M.; Odoh, S. O.; Schreckenbach, G.; Magnani, N.; Love, J. B. Strongly Coupled Binuclear Uranium-Oxo Complexes from Uranyl Oxo Rearrangement and Reductive Silylation. *Nat. Chem.* **2012**, *4*, 221−227.
(46) Brown, J. L.; Wu, G.; Hayton, T. W. Oxo Ligand Silylation in a Uranyl β-Ketoiminate Complex. *J. Am. Chem. Soc.* **2010**, *132*, 7248−7249.
(47) Arnold, P. L.; Dutkiewicz, M. S.; Zegke, M.; Walter, O.; Apostolidis, C.; Hollis, E.; Pécharman, A.-F.; Magnani, N.; Griveau, J.-C.; Colineau, E.; Caciuffo, R.; Zhang, X.; Schreckenbach, G.; Love, J. B. Subtle Interactions and Electron Transfer Between U^{III}, Np^{III}, or Pu^{III} and Uranyl Mediated by the Oxo Group. *Angew. Chem., Int. Ed.* **2016**, *55*, 12797−12801.
(48) Faizova, R.; Scopelliti, R.; Chauvin, A.-S.; Mazzanti, M. Synthesis and Characterization of a Water Stable Uranyl(V) Complex. *J. Am. Chem. Soc.* **2018**, *140*, 13554−13557.
(49) Tourneux, J.-C.; Berthet, J.-C.; Cantat, T.; Thuéry, P.; Mézailles, N.; Ephritikhine, M. Exploring the Uranyl Organometallic Chemistry: From Single to Double Uranium-Carbon Bonds. *J. Am. Chem. Soc.* **2011**, *133*, 6162−6165.
(50) Mougel, V.; Pécaut, J.; Mazzanti, M. New Polynuclear U(IV)-U(V) Complexes from U(IV) Mediated Uranyl(V) Disproportionation. *Chem. Commun.* **2012**, *48*, 868−870.
(51) Chatelain, L.; Mougel, V.; Pécaut, J.; Mazzanti, M. Magnetic Communication and Reactivity of a Stable Homometallic Cation-Cation Trimer of Pentavalent Uranyl. *Chem. Sci.* **2012**, *3*, 1075−1079.
(52) Camp, C.; Chatelain, L.; Mougel, V.; Pécaut, J.; Mazzanti, M. Ferrocene-Based Tetradentate Schiff Bases as Supporting Ligands in Uranium Chemistry. *Inorg. Chem.* **2015**, *54*, 5774−5783.
(53) Mougel, V.; Biswas, B.; Pécaut, J.; Mazzanti, M. New Insights into the Acid Mediated Disproportionation of Pentavalent Uranyl. *Chem. Commun.* **2010**, *46*, 8648−8650.
(54) Kiernicki, J. J.; Cladis, D. P.; Fanwick, P. E.; Zeller, M.; Bart, S. C. Synthesis, Characterization, and Stoichiometric U−O Bond Scission in Uranyl Species Supported by Pyridine(diimine) Ligand Radicals. *J. Am. Chem. Soc.* **2015**, *137*, 11115−11125.
(55) Pankhurst, J. R.; Bell, N. L.; Zegke, M.; Platts, L. N.; Lamfsus, C. A.; Maron, L.; Natrajan, L. S.; Sproules, S.; Arnold, P. L.; Love, J. B. Inner-Sphere vs. Outer-Sphere Reduction of Uranyl Supported by a Redox-Active, Donor-Expanded Dipyrrin. *Chem. Sci.* **2017**, *8*, 108−116.
(56) Arnold, P. L.; Jones, G. M.; Pan, Q.-J.; Schreckenbach, G.; Love, J. B. Co-Linear, Double-Uranyl Coordination by an Expanded Schiff-Base Polypyrrole Macrocycle. *Dalton Trans* **2012**, *41*, 6595−6597.
(57) Brown, J. L.; Mokhtarzadeh, C. C.; Lever, J. M.; Wu, G.; Hayton, T. W. Facile Reduction of a Uranyl(VI) β-Ketoiminate Complex to U(IV) Upon Oxo Silylation. *Inorg. Chem.* **2011**, *50*, 5105−5112.
(58) Bell, N. L.; Shaw, B.; Arnold, P. L.; Love, J. B. Uranyl to Uranium(IV) Conversion through Manipulation of Axial and Equatorial Ligands. *J. Am. Chem. Soc.* **2018**, *140*, 3378−3384.
(59) Azam, M.; Al-Resayes, S. I.; Trzesowska-Kruszynska, A.; Kruszynski, R.; Kumar, P.; Jain, S. L. Seven-Coordinated Chiral Uranyl(VI) Salen Complex as Effective Catalyst for C−H Bond Activation of Dialkylanilines Under Visible Light. *Polyhedron* **2017**, *124*, 177−183.
(60) Chatelain, L.; White, S.; Scopelliti, R.; Mazzanti, M. Isolation of a Star-Shaped Uranium(V/VI) Cluster from the Anaerobic Photochemical Reduction of Uranyl(VI). *Angew. Chem., Int. Ed.* **2016**, *55*, 14325−14329.
(61) Pattenaude, S. A.; Kuehner, C. S.; Dorfner, W. L.; Schelter, E. J.; Fanwick, P. E.; Bart, S. C. Spectroscopic and Structural Elucidation of Uranium Dioxophenoxazine Complexes. *Inorg. Chem.* **2015**, *54*, 6520−6527.
(62) Pedrick, E. A.; Schultz, J. W.; Wu, G.; Mirica, L. M.; Hayton, T. W. Perturbation of the O-U-O Angle in Uranyl by Coordination to a 12-Membered Macrocycle. *Inorg. Chem.* **2016**, *55*, 5693−5701.
(63) Hardy, E. E.; Wyss, K. M.; Eddy, M. A.; Gorden, A. E. V. An Example of Unusual Pyridine Donor Schiff Base Uranyl (UO_2^{2+}) Complexes. *Chem. Commun.* **2017**, *53*, 5718−5720.
(64) Brewster, J. T., II; He, Q.; Anguera, G.; Moore, M. D.; Ke, X.-S.; Lynch, V. M.; Sessler, J. L. Synthesis and Characterization of a Dipyriamethyrin-Uranyl Complex. *Chem. Commun.* **2017**, *53*, 4981−4984.
(65) Lu, E.; Cooper, O. J.; McMaster, J.; Tuna, F.; McInnes, E. J. L.; Lewis, W.; Blake, A. J.; Liddle, S. T. Synthesis, Characterization, and Reactivity of a Uranium(VI) Carbene Imido Oxo Complex. *Angew. Chem., Int. Ed.* **2014**, *53*, 6696−6700.
(66) Faizova, R.; White, S.; Scopelliti, R.; Mazzanti, M. The Effect of Iron Binding on Uranyl(V) Stability. *Chem. Sci.* **2018**, *9*, 7520−7527.
(67) Kannan, S.; Deb, S. B.; Drew, M. G. B. Synthesis, Characterization and Molecular Structure of 1,1'Bis-(Diphenylphosphino Ferrocene) Dioxide Complex of the *cis*-Uranyl Dichloride. *J. Organomet. Chem.* **2012**, *701*, 93−95.
(68) Bolotaulo, D.; Metta-Magaña, A.; Fortier, S. F-Element Metalated Dipyrrins: Synthesis and Characterization of a Family of Uranyl Bis(Dipyrrinate) Complexes. *Dalton Trans* **2017**, *46*, 3284−3294.
(69) Pedrick, E. A.; Wu, G.; Kaltsoyannis, N.; Hayton, T. W. Reductive Silylation of a Uranyl Dibenzoylmethanate Complex: An Example of Controlled Uranyl Oxo Ligand Cleavage. *Chem. Sci.* **2014**, *5*, 3204−3213.
(70) Pedrick, E. A.; Wu, G.; Hayton, T. W. Reductive Silylation of the Uranyl Ion with Ph_3SiOTf. *Inorg. Chem.* **2014**, *53*, 12237−12239.
(71) Arnold, P. L.; Pécharman, A.-F.; Love, J. B. Oxo Group Protonation and Silylation of Pentavalent Uranyl Pacman Complexes. *Angew. Chem., Int. Ed.* **2011**, *50*, 9456−9458.
(72) Arnold, P. L.; Pécharman, A.-F.; Lord, R. M.; Jones, G. M.; Hollis, E.; Nichol, G. S.; Maron, L.; Fang, J.; Davin, T.; Love, J. B. Control of Oxo-Group Functionalization and Reduction of the Uranyl Ion. *Inorg. Chem.* **2015**, *54*, 3702−3710.
(73) Zegke, M.; Nichol, G. S.; Arnold, P. L.; Love, J. B. Catalytic One-Electron Reduction of Uranyl(VI) to Group 1 Uranyl(V) Complexes via Al(III) Coordination. *Chem. Commun.* **2015**, *51*, 5876−5879.
(74) Arnold, P. L.; Hollis, E.; Nichol, G. S.; Love, J. B.; Griveau, J.-C.; Caciuffo, R.; Magnani, N.; Maron, L.; Castro, L.; Yahia, A.; Odoh, S. O.; Schreckenbach, G. Oxo-Functionalization and Reduction of the Uranyl Ion through Lanthanide-Element Bond Homolysis: Synthetic, Structural, and Bonding Analysis of a Series of Singly Reduced Uranyl−Rare Earth $5f^1$-$4f^n$ Complexes. *J. Am. Chem. Soc.* **2013**, *135*, 3841−3854.
(75) Arnold, P. L.; Hollis, E.; White, F. J.; Magnani, N.; Caciuffo, R.; Love, J. B. Single-Electron Uranyl Reduction by a Rare-Earth Cation. *Angew. Chem., Int. Ed.* **2011**, *50*, 887−890.
(76) Sarsfield, M. J.; Steele, H.; Helliwell, M.; Teat, S. J. Uranyl Bis-Iminophosphorane Complexes with In- and Out-Of-Plane Equatorial Coordination. *Dalton Trans* **2003**, 3443−3449.
(77) Mills, D. P.; Cooper, O. J.; Tuna, F.; McInnes, E. J. L.; Davies, E. S.; McMaster, J.; Moro, F.; Lewis, W.; Blake, A. J.; Liddle, S. T. Synthesis of a Uranium(VI)-Carbene: Reductive Formation of Uranyl(V)-Methanides, Oxidative Preparation of a $[R_2C{=}U{=}O]^{2+}$ Analogue of the $[O{=}U{=}O]^{2+}$ Uranyl Ion (R = $Ph_2PNSiMe_3$), and Comparison of the Nature of U^{IV}=C, U^{V}=C, and U^{VI}=C Double Bonds. *J. Am. Chem. Soc.* **2012**, *134*, 10047−10054.
(78) Mougel, V.; Horeglad, P.; Nocton, G.; Pécaut, J.; Mazzanti, M. Cation-Cation Complexes of Pentavalent Uranyl: From Disproportionation Intermediates to Stable Clusters. *Chem. - Eur. J.* **2010**, *16*, 14365−14377.
(79) Natrajan, L.; Burdet, F.; Pécaut, J.; Mazzanti, M. Synthesis and Structure of a Stable Pentavalent-Uranyl Coordination Polymer. *J. Am. Chem. Soc.* **2006**, *128*, 7152−7153.
(80) Berthet, J.-C.; Siffredi, G.; Thuéry, P.; Ephritikhine, M. Easy Access to Stable Pentavalent Uranyl Complexes. *Chem. Commun.* **2006**, 3184−3186.

DOI: 10.1021/acs.chemrev.9b00048
Chem. Rev. XXXX, XXX, XXX−XXX

(81) Nocton, G.; Horeglad, P.; Vetere, V.; Pécaut, J.; Dubois, L.; Maldivi, P.; Edelstein, N. M.; Mazzanti, M. Synthesis, Structure, and Bonding of Stable Complexes of Pentavalent Uranyl. *J. Am. Chem. Soc.* **2010**, *132*, 495−508.
(82) Mougel, V.; Chatelain, L.; Pécaut, J.; Caciuffo, R.; Colineau, E.; Griveau, J.-C.; Mazzanti, M. Uranium and Manganese Assembled in a Wheel-Shaped Nanoscale Single-Molecule Magnet with High Spin-Reversal Barrier. *Nat. Chem.* **2012**, *4*, 1011−1017.
(83) Chatelain, L.; Pécaut, J.; Tuna, F.; Mazzanti, M. Hetermoetallic Fe_2^{II}-U^{V} and Ni_2^{II}-U^{V} Exchange-Coupled Single-Molecule Magnets: Effect of the 3d Ion on the Magnetic Properties. *Chem. - Eur. J.* **2015**, *21*, 18038−18042.
(84) Chatelain, L.; Walsh, J. P. S.; Pécaut, J.; Tuna, F.; Mazzanti, M. Self-Assembly of a 3d−5f Trinuclear Single-Molecule Magnet from a Pentavalent Uranyl Complex. *Angew. Chem., Int. Ed.* **2014**, *53*, 13434−13438.
(85) Chatelain, L.; Tuna, F.; Pecaut, J.; Mazzanti, M. Synthesis and SMM Behaviour of Trinuclear *versus* Dinuclear 3d-5f Uranyl(V)-Cobalt(II) Cation-Cation Complexes. *Dalton Trans* **2017**, *46*, 5498−5502.
(86) Mougel, V.; Catelain, L.; Hermle, J.; Caciuffo, R.; Colineau, E.; Tuna, F.; Magnani, N.; de Geyer, A.; Pécaut, J.; Mazzanti, M. A Uranium-Based UO_2^{+}-Mn^{2+} Single-Chain Magnet Assembled Through Cation-Cation Interactions. *Angew. Chem., Int. Ed.* **2014**, *53*, 819−823.
(87) Chatelain, L.; Tuna, F.; Pécaut, J.; Mazzanti, M. A Zig-Zag Uranyl(V)-Mn(II) Single Chain Magnet with a High Relaxation Barrier. *Chem. Commun.* **2015**, *51*, 11309−11312.
(88) Kiernicki, J. J.; Harwood, J. S.; Fanwick, P. E.; Bart, S. C. Reductive Silylation of Cp*UO_2(^{Mes}PDI^{Me}) Promoted by Lewis Bases. *Dalton Trans* **2016**, *45*, 3111−3119.
(89) Kiernicki, J. J.; Zeller, M.; Bart, S. C. Facile Reductive Silylation of UO_2^{2+} to Uranium(IV) Chloride. *Angew. Chem., Int. Ed.* **2017**, *56*, 1097−1100.
(90) Pedrick, E. A.; Wu, G.; Hayton, T. W. Oxo Ligand Substitution in a Cationic Uranyl Complex: Synergistic Interaction of an Electrophile and a Reductant. *Inorg. Chem.* **2015**, *54*, 7038−7044.
(91) Cowie, B. E.; Nichol, G. S.; Love, J. B.; Arnold, P. L. Double Uranium Oxo Cations Derived from Uranyl by Borane or Silane Reduction. *Chem. Commun.* **2018**, *54*, 3839−3842.
(92) Schnaars, D. D.; Wu, G.; Hayton, T. W. Reduction of Pentavalent Uranyl to U(IV) Facilitated by Oxo Functionalization. *J. Am. Chem. Soc.* **2009**, *131*, 17532−17533.
(93) Schnaars, D. D.; Wu, G.; Hayton, T. W. Borane-Mediated Silylation of a Metal−Oxo Ligand. *Inorg. Chem.* **2011**, *50*, 4695−4697.
(94) Schnaars, D. D.; Wu, G.; Hayton, T. W. Silylation of the Uranyl Ion Using $B(C_6F_5)_3$-Activated Et_3SiH. *Inorg. Chem.* **2011**, *50*, 9642−9649.
(95) Arnold, P. L.; Cowie, B. E.; Suvova, M.; Zegke, M.; Magnani, N.; Colineau, E.; Griveau, J.-C.; Caciuffo, R.; Love, J. B. Axially Symmetric U−O−Ln- and U−O−U-Containing Molecules from the Control of Uranyl Reduction with Simple f-Block Halides. *Angew. Chem., Int. Ed.* **2017**, *56*, 10775−10779.
(96) Lu, G.; Forbes, T. Z.; Haes, A. J. Evaluating Best Practices in Raman Spectral Analysis for Uranium Speciation and Relative Abundance in Aqueous Solutions. *Anal. Chem.* **2016**, *88*, 773−780.
(97) Schnaars, D. D.; Wilson, R. E. Structural and Vibrational Properties of U(VI)$O_2Cl_4^{2-}$ and Pu(IV)$O_2Cl_4^{2-}$ Complexes. *Inorg. Chem.* **2013**, *52*, 14138−14147.
(98) Bullock, J. I. Raman and Infrared Spectroscopic Studies of the Uranyl Ion: the Symmetric Stretching Frequency, Force Constants, and Bond Lengths. *J. Chem. Soc. A* **1969**, 781−784.
(99) West, J. G.; Bedell, T. A.; Sorensen, E. J. The Uranyl Cation as a Visible-Light Photocatalyst for C(sp^3)−H Fluorination. *Angew. Chem., Int. Ed.* **2016**, *55*, 8923−8927.
(100) Pirovano, P.; Farquhar, E. R.; Swart, M.; McDonald, A. R. Tuning the Reactivity of Terminal Nickel(III)−Oxygen Adducts for C−H Bond Activation. *J. Am. Chem. Soc.* **2016**, *138*, 14362−14370.
(101) McGrail, B. T.; Pianowski, L. S.; Burns, P. C. Photochemical Water Oxidation and Origin of Nonaqueous Uranyl Peroxide Complexes. *J. Am. Chem. Soc.* **2014**, *136*, 4797−4800.
(102) Blanchard, F.; Ellart, M.; Rivenet, M.; Vigier, N.; Hablot, I.; Morel, B.; Grandjean, S.; Abraham, F. Neodymium Uranyl Peroxide Synthesis by Ion Exchange on Ammonium Uranyl Peroxide Nanoclusters. *Chem. Commun.* **2016**, *52*, 3947−3950.
(103) Hassanpour, M.; Safardoust-Hojjaghan, H.; Salavatir-Niasari, M. Degradation of Methylene Blue and Rhodamine B as Water Pollutants via Green Synthesized Co_3O_4/ZnO Nanocomposite. *J. Mol. Liq.* **2017**, *229*, 293−299.
(104) Zhang, Q.; Jin, B.; Peng, R.; Wang, X.; Shi, Z.; Liu, Q.; Lei, S.; Liang, H. Investigation on the Synthesis and Photocatalytic Property of Uranyl Complexes of the β-Diketonates Biscatecholamide Ligand. *Int. J. Photoenerg.* **2017**, 8041647.
(105) Chrisman, M. A.; Baldwin, M. J. Photochemistry of Uranyl Complexes with the Salicylidene-α-Hydroxy Acid Chelates, X-Sal-AHA. *Polyhedron* **2018**, *141*, 271−275.
(106) Yu, Z.-T.; Liao, Z.-L.; Jiang, Y.-S.; Li, G.-H.; Chen, J.-S. Water-Insoluble Ag−U−Organic Assemblies with Photocatalytic Activity. *Chem.—Eur. J.* **2005**, *11*, 2642−2650.
(107) Ren, Y.-N.; Xu, W.; Zhou, L.-X.; Zheng, Y.-Q. Two New Uranyl Complexes as Visible Light Driven Photocatalysts for Degradation of Tetracycline. *Polyhedron* **2018**, *139*, 63−72.
(108) Bonales, L. J.; Colmenero, F.; Cobos, J.; Timón, V. Spectroscopic Raman Characterization of Rutherfordine: a Combined DFT and Experimental Study. *Phys. Chem. Chem. Phys.* **2016**, *18*, 16575−16584.
(109) Takao, K.; Tsushima, S. The Oxidation of Borohydrides by Photoexcited $[UO_2(CO_3)_3]^{4-}$. *Dalton Trans* **2018**, *47*, 5149−5152.
(110) Abney, C. W.; Mayes, R. T.; Saito, T.; Dai, S. Materials for the Recovery of Uranium from Seawater. *Chem. Rev.* **2017**, *117*, 13935−14013.
(111) Cepeda-Plaza, M.; Null, E. L.; Yi, L. Metal Ion as Both a Cofactor and a Probe of Metal-Binding Sites in a Uranyl-Specific DNAzyme: a Uranyl Photocleavage Study. *Nucleic Acids Res.* **2013**, *41*, 9361−9370.
(112) Huang, C.; Fan, X.; Yuan, Q.; Zhang, X.; Hou, X.; Wu, P. Colorimetric Determination of Uranyl (UO_2^{2+}) in Seawater via DNAzyme-Modulated Photosensitization. *Talanta* **2018**, *185*, 258−263.
(113) Zhang, Q.; Jørgensen, T. J. D.; Nielsen, P. E.; Møllegaard, N. E. A Phosphorylation Tag for Uranyl Mediated Protein Purification and Photo Assisted Tag Removal. *PLoS One* **2014**, *9*, e91138.
(114) Elnegaard, R. L. B.; Møllegaard, N. E.; Qiang, Z.; Kjeldsen, F.; Jørgensen, T. J. D. Uranyl Photocleavage of Phosphopeptides Yields Truncated C-Terminally Amidated Peptide Products. *ChemBioChem.* **2017**, *18*, 1117−1122.
(115) Constable, D. J. C.; Dunn, P. J.; Hayler, J. D.; Humphrey, G. R.; Leazer, J. L.; Linderman, R. J.; Lorenz, K.; Manley, J.; Pearlman, B. A.; Wells, A.; Zaks, A.; Zhang, T. Y. Key Green Chemistry Research Areas—A Perspective from Pharmaceutical Manufacturers. *Green Chem.* **2007**, *9*, 411−420.
(116) Arnold, P. L.; Purkis, J. M.; Rutkauskaite, R.; Kovacs, D.; Love, J. B.; Austin, J. Controlled Photocatalytic Hydrocarbon Oxidation by Uranyl Complexes. *ChemCatChem* **2019**, in press, DOI: 10.1002/cctc.201900037.
(117) Capaldo, L.; Merli, D.; Fagnoni, M.; Ravelli, D. Visible Light Uranyl Photocatalysis: Direct C-H to C-C Bond Conversion. *ACS Catal.* **2019**, *9*, 3054−3058.
(118) Mashita, T.; Tsushima, S.; Takao, K. Photocatalytic Oxygenation of Cyclohexene Initiated by Excitation of $[UO_2(OPCyPh_2)_4]^{2+}$ under Visible Light. *ACS Omega* **2019**, *4*, 7194−7199.
(119) Hayton, T. W. Understanding the Origins of O_{yl}-U-O_{yl} Bending in the Uranyl (UO_2^{2+}) Ion. *Dalton Trans* **2018**, *47*, 1003−1009.
(120) Szabó, Z.; Grenthe, I. On the Mechanism of Oxygen Exchange Between Uranyl(VI) Oxygen and Water in Strongly Alkaline Solution

DOI: 10.1021/acs.chemrev.9b00048
Chem. Rev. XXXX, XXX, XXX−XXX

as Studied by ^{17}O NMR Magnetization Transfer. *Inorg. Chem.* **2010**, *49*, 4928−4933.
(121) Hayton, T. W.; Wu, G. Exploring the Effects of Reduction or Lewis Acid Coordination on the U=O Bond of the Uranyl Moiety. *Inorg. Chem.* **2009**, *48*, 3065−3072.
(122) Lee, J.; Brewster, J. T.; Song, B.; Lynch, V. M.; Hwang, I.; Xiaopeng, L.; Sessler, J. L. Uranyl Dication Mediated Photoswitching of a Calix[4]Pyrrole-Based Metal Coordination Cage. *Chem. Commun.* **2018**, *54*, 9422−9425.
(123) Boxall, C.; Le Gurun, G.; Taylor, R. J.; Xiao, S. In *Environmental Photochemistry Part II*; Boule, P., Bahnemann, D. W., Robertson, P. K. J., Eds.; Springer Berlin Heidelberg: Berlin, Heidelberg, 2005, DOI: 10.1007/b138191.

DOI: 10.1021/acs.chemrev.9b00048
Chem. Rev. XXXX, XXX, XXX−XXX